Winter 2005

Regulation of SPARC Gene Expression by the Activator Protein 1 Transcription Factor

Joseph William Briggs
Old Dominion University

REGULATION OF SPARC GENE EXPRESSION BY THE ACTIVATOR PROTEIN 1 TRANSCRIPTION FACTOR

by

Joseph William Briggs
B.S. August 1996, Old Dominion University

A Dissertation Submitted to the Faculty of
Old Dominion University in Partial Fulfillment of the
Requirement for the Degree of

DOCTOR OF PHILOSOPHY

BIOMEDICAL SCIENCES

OLD DOMINION UNIVERSITY

December 2005

Approved by:

Timothy J. Bos (Director)

Ann E. Campbell (Member)

Julie A. Kerry (Member)

Kenneth D. Somers (Member)

ABSTRACT

REGULATION OF SPARC GENE EXPRESSION BY THE ACTIVATOR PROTEIN 1 TRANSCRIPTION FACTOR

Joseph William Briggs
Old Dominion University, 2005
Chair: Dr. Timothy J. Bos

Overexpression of the c-Jun proto-oncogene in MCF7 breast cancer cells results in a variety of phenotypic changes related to malignant progression including a shift to estrogen independent growth, increased cell motility and invasion. Concurrent with these phenotypic changes are alterations to cellular gene expression patterns. One gene that becomes highly upregulated is SPARC (secreted protein acidic and rich in cysteine). Increased SPARC expression is associated with malignant progression in a variety of different cancers, although little is known regarding the mechanisms of SPARC gene regulation. Therefore, the objectives of this study were: 1.) to determine the mechanisms by which c-Jun regulates SPARC gene expression, and 2.) to determine the contribution of SPARC to c-Jun induced phenotype in a MCF7 breast cancer model system.

In order to determine the role of SPARC in c-Jun mediated oncogenic progression, we over-expressed SPARC in MCF7 cells and blocked its expression in the c-Jun/MCF7 cell line. We found that antisense mediated suppression of SPARC dramatically inhibits both cell motility and invasion in this c-Jun/MCF7 model. In contrast, stable overexpression of SPARC in the parental MCF7 cell line was not sufficient to stimulate cell motility or invasion suggesting that SPARC cooperates with other c-Jun target genes to establish a pro-invasive phentoytpe.

In order to determine the mechanism(s) of c-Jun induced SPARC gene activation, we started by analyzing DNA binding and transactivation using the human SPARC promoter. The activity of the full-length SPARC promoter (-1409/+28) was 15-30 fold higher in c-Jun over-expressing cells compared to vector control cells. Promoter deletion analysis revealed that a region between –120 and –70 conferred c-Jun responsiveness. This region does not contain an AP-1 binding site, but does contain a GC rich element which is recognized *in vitro* and *in vivo* by Sp1. Importantly, chromatin immunoprecipitation analysis demonstrated that c-Jun is physically associated with the SPARC proximal promoter region during gene activation.

Further analysis of the SPARC promoter sequence, including the c-Jun responsive region, revealed the presence of multiple CpG sequences. Methylation of cytosine residues in a CpG context has been shown to inhibit gene expression. Therefore, we examined the contribution of DNA methylation to SPARC gene regulation. Analysis of MCF7 cells, in which SPARC expression is undetectable, revealed methylation of the SPARC promoter at both distal and proximal sites. Inhibition of DNA methyltransferase activity in these cells resulted in a dose dependent increase in SPARC mRNA levels suggesting that SPARC may be transcriptionally repressed via DNA methylation in MCF7 cells. Interestingly, overexpression of c-Jun cells resulted in a localized demethylation of the SPARC promoter near the transcription start site correlating with an increase in SPARC mRNA and protein levels. Transfection of an *in vitro* methylated SPARC promoter/reporter plasmid into c-Jun/MCF7 cells resulted in a dramatic decrease in promoter activity suggesting an important functional role for SPARC promoter methylation in regulating c-Jun responsiveness.

Additional characterization of the SPARC promoter revealed changes in post-translational modification of histone H3 and H4 known to be associated with chromatin remodeling and gene activation. Specifically, chromatin immunoprecipitation analysis demonstrated hyperacetylation of histones as well as enrichment of methylated histone H3 at lysine 4 in response to c-Jun.

In conclusion, our results support a model where c-Jun acts as a molecular switch directing site-specific epigenetic changes leading to SPARC gene activation. Moreover, we have identified SPARC as an important c-Jun target gene which contributes to phenotypic progression in an MCF7 model system.

This dissertation is dedicated to family and friends that supported me and made this research possible.

ACKNOWLEDGMENTS

I would like to thank my committee for their help and guidance over the last six years. I would like to express my gratitude to Dr. Ann Campbell for giving me an opportunity to conduct research in her laboratory during my first laboratory rotation. Her mentorship and commitment to teaching were a tremendous help to me. I am indebted to Dr. Julie Kerry for her expert advice and unparalleled enthusiasm during the course of my graduate studies. I would like to thank Dr. Ken Somers for teaching me how to think about the "big picture" during my studies. I would especially like to thank the Chairman of my committee, Dr. Timothy Bos, for his unwavering commitment throughout this process. His guidance and training have given me the confidence and ability to "just do it".

I would like to thank Dr. Michael Birrer (National Cancer Institute) for the kind gift of the MCF7 and c-Jun/MCF7 cell lines used in these studies. I would also like to thank Dr. Marc Castellazzi (INSERM, France) for providing the SPARC promoter/luciferase reporter plasmids used in these studies. In addition, I would like to thank Dr. Julie Kerry (Eastern Virginia Medical School) for providing the recombinant adenovirus system used in these studies.

I would also like to acknowledge and thank the members of the Bos lab including Melissa Johnston, Janet Rinehart-Kim, Lisa Bolin, Christian Reyes and Marissa Tribby. Their support was instrumental in helping me accomplish my goals. I am thankful to Jackie Slater, Dr. Laura Hanson and Dr. Victoria Cavanaugh of the Campbell lab for years of insightful discussion and friendship. I would like to thank Toni Dorn and Dr.

William Wasilenko for their commitment to the students of the Biomedical Sciences program.

I am grateful to the faculty, staff and administration at the Center for Pediatric Research. Specifically, I would like to thank Laurie Jackson for introducing me to life in the laboratory. I would also like to thank Dr. Doug Mitchell for his mentorship during my time at the Center for Pediatric Research.

I would also like to thank the faculty at Old Dominion University including Nancy Wade, Dr. Lytton Musselman and Dr. Renee Olander for their support and encouragement during my undergraduate and graduate studies.

Finally, I am eternally grateful to my high school Engineering teacher, Mr. Gene Dew, for encouraging me to continue my education.

TABLE OF CONTENTS

Page

Page

LIST OF FIGURES

Figure Page

Figure Page

LIST OF ABBREVIATIONS

AP-1	Activator protein-1
bp	Base pair
BSA	Bovine serum albumin
BZIP	Basic region leucine zipper
CBP	Cyclic adenosine monophosphate binding protein
ChIP	Chromatin immunoprecipitation
CMV	Cytomegalovirus
CpG	Cytosine-phosphate-guanine
CPE	Cytopathic effect
cpm	Counts per minute
dIdC	deoxyinosine deoxycytosine
DNA	Dexoyribonucleic acid
DNMT	DNA methyltransferase
dNTP	deoxynucleotide triphosphate
DTT	Dithiothreitol
EDTA	Ethylene diaminetetracetic acid
ER	Estrogen receptor
HAT	Histone acetylase
HEPES	N-2-hydroxyethylpiperazine-N'-2-ethanesolfonic acid
HEK293	Human embryonic kidney-293 cells
HMT	Histone methyltransferase

Hr	Hour
HRP	Horse radish peroxidase
IP	Immunoprecipitation
IUPAC	International Union of Pure and Applied Chemistry
kDa	Kilodalton
M	Molar
mA	Milliamp
mg	Milligram
μg	Microgram
ml	Millilitre
μl	Microlitre
μm	Micrometer
μM	Micromolar
mM	Millimolar
mm	Millimeter
MBD	Methyl binding domain
Min	Minute
MMLV	Moloney Murine Leukemia Virus
MMP	Matrix metalloprotease
MOI	Multiplicity of infection
MTT	3-[4,5-dimethylthiazol-2-yl]-2,5-diphenyl tetrasodium bromide
ng	Nanogram
nm	Nanometer

PCR	Polymerase chain reaction
Pfu	Plaque forming unit
PBS	Phosphate buffered saline
PMA	Phorbol 12-myristate 13-acetate
PMSF	Phenylmethylsulfonylfluoride
RISC	RNA induced silencing complex
RNA	Ribonucleic acid
RNAi	Ribonucleic acid interference
RT-PCR	Reverse transcriptase-polymerase chain reaction
SDS-PAGE	Sodium dodecyl sulfate-polyacrylamide gel electrophoresis
Sec	Second
siRNA	Small interfering RNA
SPARC	Secreted protein acidic and rich in cysteine
TBP	TATA binding protein
TIMP	Tissue inhibitor of metalloproteases
TSA	Trichostatin A

CHAPTER I

INTRODUCTION

A. Breast Cancer Biology and Epidemiology

Breast cancer is a major health problem in the United States and worldwide. It is estimated that 211,240 new cases of invasive breast cancer will be diagnosed in 2005 and that 40,410 women in the United States will die from this disease this year (1). Breast cancer is the third most common cause of death in women 40-55 years of age and the incidence of disease increases with age. More than 94% of new cases and 96% of deaths attributed to breast cancer occur in women ages 40 and older (1). Success in treating the disease relies, in large part, on early diagnosis and appropriate therapeutic intervention prior to spread of the disease. The five-year survival rate for patients diagnosed with only localized tumor involvement is 97% (1). This number drops to 78% when there is regional spread of the disease (1). Patients diagnosed late in disease progression, in which the tumor has spread to secondary organ systems, have only a 23% five-year survival rate (1).

B. The Etiology of Breast Cancer

It is widely accepted that breast cancer, like other neoplasms, is the result of genetic alterations which lead to aberrant cell growth (2-5). Greater than 90% of breast cancers arise from cells of epithelial origin (6). Breast malignancies are categorized based on the type of tissue from which they arise. The two most common types are

---

This dissertation follows the format of the journal *Cancer Research*.

ductal (tissue connecting the milk glands and nipple) carcinomas and lobular (milk producing glandular tissue) carcinomas. Tumors can further be classified based on cell genotype and phenotype. Mutations in the breast cancer associated genes *BRCA1* and *BRCA2* are associated with familial forms of breast cancer (3, 7). However, these cases comprise only a small portion of the total number of breast cancer cases diagnosed each year (8, 9). More frequently, the underlying cause of sporadic breast tumors is not known. Other genetic alterations which have been shown to occur in the more frequent, sporadic cases of breast cancer include: gene mutations, gene amplifications, gene deletions and/or genetic rearrangements (10-13). For example, mutation of the *p53* tumor suppressor gene has been demonstrated in approximately 25% of breast tumors (14, 15). In addition, amplification of the *MYC* proto-oncogene occurs in 15-20% of breast cancers (16, 17). Finally, amplification of the *HER2/neu* gene has been shown in 25-30% of breast neoplasms (17-19).

In addition to gene copy number differences, altered gene expression is a common occurrence in breast cancer. A study comparing the gene expression profiles of normal mammary epithelial cells to invasive breast cancer cells revealed differences in gene expression patterns between the two cell populations (20). It is believed that some of these differentially regulated genes are involved in breast cancer progression from a benign to a malignant state. Differential expression of genes such as estrogen receptor alpha, *HER2/neu* and the proto-oncogene *JUN* are well documented (21-26). These observations have led to the understanding that the cellular gene expression profile ultimately determines cell phenotype. This knowledge has been used to develop new treatment regimes for breast cancer and to identify biomarkers for use as prognostic

indicators. For example, estrogen receptor positive tumors respond to the growth inhibitory effects of the anti-estrogen, tamoxifen (27). Likewise, the growth of breast tumors with elevated levels of the *HER2/neu* gene product is inhibited by the monoclonal antibody trastuzumab (28).

Our current understanding of breast cancer progression is that it is a multi-step process consisting of the initiating oncogenic event(s) followed by promotion of tumor cell growth and finally, disease progression (2, 29). These step-wise alterations have been characterized histopathologically and phenotypically as 1.) normal mammary epithelial cell 2.) benign hyperplasia 3.) carcinoma *in situ* 4.) locally invasive and 5.) metastatic carcinoma. The conversion from benign to malignant neoplasia is characterized by an invasive cellular phenotype where cells become motile and degrade the local extracellular matrix and basement membrane (30-34). These phenotypes are not characteristic of normal epithelial cells, but rather cells of mesenchymal origin. This phenomenon has been described as "epithelial-to-mesenchymal transition" (35). This is considered an important event in the "evolution" of a tumor cell because it represents a time when the phenotype has been sufficiently altered resulting in pathology. This pathology involves disruption of the normal tissue architecture, disruption of the basement membrane, trauma, and inflammation. A subset of locally invasive cells may disseminate into the lymphatics and vasculature of the breast. An even smaller portion of the cells which enter the circulation (<0.01%) result in the formation of metastatic foci (36). Metastasis is defined as establishment of the tumor in a secondary organ system, discontinuous from the primary lesion (1). This event is important because the majority of morbidity and mortality associated with breast cancer is the result of metastatic

disease. However, the cellular events required for malignant progression remain a mystery.

In order to better understand the molecular mechanisms of breast cancer progression it would be of use to identify genes which play a functional role in the disease process. As a result there has been an effort to identify and validate functional genes as opposed to bystander genes. Along these same lines, it is of interest to better understand how expression of these genes is regulated in non-invasive versus invasive tumor cells.

A number of studies have demonstrated that the proto-oncogene *JUN* may play an important role in oncogenesis and tumor progression. For example, overexpression of c–Jun has been shown to induce cell transformation in primary chicken embryo fibroblasts and, in cooperation with oncogenic Ras, to transform primary rat cells (37-43). Importantly, c-Jun expression is increased in primary and metastatic breast tumor samples when compared to normal breast epithelial cells (25, 44, 45). Patients with c-Jun positive breast tumors are also less responsive to tamoxifen therapy and have shorter survival rates (45). In support of these observations, there is an inverse correlation between c-Jun expression and estrogen receptor status (44-46). Interestingly, to date, there have been no reports of *JUN* gene amplification or mutation. However, several studies have demonstrated an increase in c-Jun expression and/or c-Jun DNA binding and related transcriptional activity (25, 47-49). The current paradigm is that c-Jun acts at the level of transcriptional transactivation to "turn-on" and/or "turn-off" a subset of genes involved in regulating cell phenotype.

In addition to c-Jun, other members of the AP-1 transcription factor family have been implicated in breast cancer. For example, increased expression of c-Fos correlates with failure to respond to endocrine therapy and poor survival (45). In addition, Fra-1 expression is high in invasive breast cancer cell lines and its expression correlates with estrogen receptor negative breast tumors (44, 50, 51). Interestingly, we and others, have shown that *FRA1* is a c-Jun target gene (50, 51). In contrast, JunB expression is decreased in the invasive breast cancer cell line MDA-MB-231 compared to less invasive cell lines (20). Increased FosB expression correlates with well differentiated, estrogen receptor positive tumors (44). Finally, a comparison of gene expression patterns from 13 different breast cancer cell lines revealed dramatically elevated expression of both c-Jun and Fra-1, primarily in the highly invasive lines (20).

C. Properties and Functions of the Transcription Factor c-Jun

The Jun oncoprotein was originally identified as the Avian Sarcoma Virus 17 gene product responsible for viral induced cell transformation (52). Subsequent studies demonstrated the existence of a cellular counterpart to viral Jun, and was termed c-Jun (53). c-Jun belongs to the superfamily of bZIP (basic region leucine zipper) proteins which are known as transcriptional regulators (54, 55). Within the bZIP family c-Jun is the proto-type for the activator protein-1 (AP-1) transcription factor family (53). The *JUN* gene is evolutionarily conserved in organisms from *Drosophila* to humans. In humans, *JUN* is a single copy gene located on chromosome 1p31-32. *JUN* encodes a 39kDa protein which is required for normal embryonic development. This is supported by observations that *JUN* -/- (null) mice exhibit embryonic lethality (56, 57).

c-Jun has been shown to contain distinct modular domains involved in transactivation, dimerization and DNA binding (Fig. 1) (53, 54, 58). Under normal physiological conditions, c-Jun expression follows immediate-early kinetics in response to mitogenic stimuli as well as stress activated cell signaling (55, 59, 60). In addition, c–Jun is rapidly induced in cells following treatment with the tumor promoting agent, phorbol ester (55, 59-61). This activation of c-Jun expression has been shown to occur as a result of protein kinase C signaling events (55, 59-61). In NIH3T3 cells, c-jun mRNA levels increase as early as 30 minutes following serum stimulation and return to basal levels after approximately two hours (62). The half-life of the c-jun message is regulated by the presence of AU rich mRNA destabilizing elements in the 3' untranslated region (63). Furthermore, c-Jun protein undergoes rapid turnover mediated by a proteolytic signal PEST amino acid sequence (64, 65). However, during pathological conditions, such as tumorigenesis, c-Jun expression and/or steady-state levels has been shown to be increased (25, 45, 66, 67).

The c-Jun protein is capable of forming dimers with members of the Jun (c-Jun, Jun B, Jun D), Fos (c-Fos, Fra 1, Fra 2, Fos B), ATF/CREB (ATF2, ATF3), and Maf/Nr1 families through a common leucine zipper motif (54, 68-73). This prerequisite dimerization affects DNA binding affinity and site recognition as well as transactivation potential (54, 71-73). For example, Jun/Fos heterodimers form stronger interactions than Jun/Jun homodimers and *in vitro* synthesized Jun proteins exhibit lower affinity binding to AP-1 sequences than if mixed with c-Fos (74-76). As a result, it is widely accepted that the relative abundance of AP-1 proteins determines the identity of AP-1 dimer combinations and the cellular profile of genes they regulate.

A

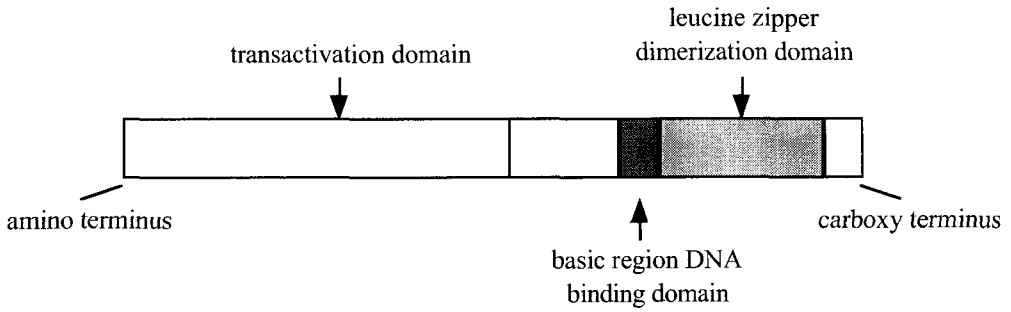

B

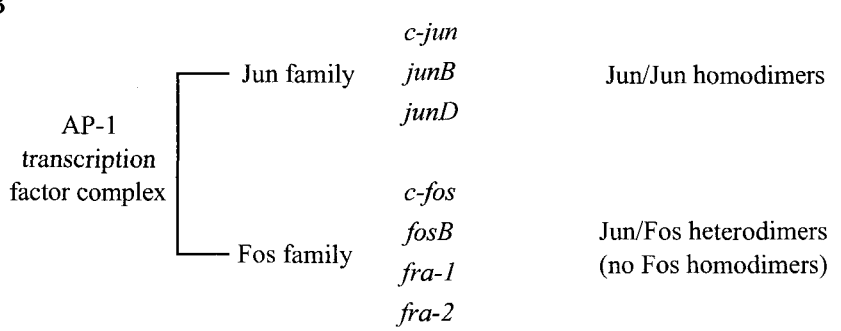

Fig. 1. c-Jun and the AP-1 transcription factor family members. *A*, Schematic representation of the c-Jun protein modular domain architecture. *B*, Summary of Jun and Fos gene family members.

In the direct model of AP-1 regulated gene expression, AP-1 dimeric complexes recognize and bind the consensus DNA sequence TGAC/GTCA in the promoters and enhancers of target genes (72-74, 77, 78). The specificity of DNA binding is determined by positively charged amino acids in the basic region, adjacent to the leucine zipper dimerization domain (69). However, AP-1 is fairly promiscuous and recognizes numerous non-canonical variations of this site as well as variations of the eight base pair consensus binding site for the ATF/CREB proteins, TGACGTCA (79-81). For instance, c-Jun/ATF2 will bind to the AP-1 site in the urokinase plasminogen activator promoter with the sequence TGAAGTCA with high affinity (82). In contrast, c-Jun/c-Fos heterodimers do not bind well to this sequence and c-Jun homodimers do not bind at all (82). The AP-1 like site in the proenkephalin enhancer, TGCGTCA, binds well to JunD but not to JunB homodimers (83). We have demonstrated similar qualitative sequence specificity differences for variations of AP-1 and CREB target sequences between v-Jun and c-Jun isolated from chicken embryo fibroblasts (80). The existence of both high and low affinity AP-1 binding sites has important gene regulatory implications. Specifically, target gene regulation by AP-1 proteins depends not only on binding site context but also on the levels of specific AP-1 dimers expressed at any given time. Taken together, these studies demonstrate the capability for unique gene target regulation based on the compositional properties of AP-1 dimers. It is these gene regulatory patterns, which ultimately influence the biological phenotype.

In addition to these direct mechanisms of transcriptional control, c-Jun/AP-1 can also influence gene regulation through indirect mechanisms by interacting with other sequence specific transcription factors (84-91). For example, c-Jun has been shown to

interact with the Sp1 transcription factor to regulate expression of the $p21^{WAF1/Cip1}$ and *12(S)-lipoxygenase* genes (92, 93). In these examples, c-Jun mediated transcriptional activation was shown to be independent of binding to an AP-1 DNA element (92, 93). c–Jun has also been shown to interact with the retinoblastoma (RB) protein resulting in synergistic activation of the DNA methyltransferase gene, *DNMT1*. However, in this example a consensus AP-1 site in the *DNMT1* promoter was required for c-Jun mediated transactivation (94). Additionally, c-Jun has been shown to utilize non-canonical AP-1 sites such as one present in the multi-drug resistance gene, *MDR1*, as a means of regulating gene transcription (95). Mutation of the *MDR1* AP-1 like site from TCAGTCA to a consensus site (TGAGTCA) resulted in increased promoter activity in MCF7 cells transiently transfected with c-Jun (95).

But how does c-Jun promote transcription activation? The current paradigm is that c-Jun binds DNA in a sequence specific manner and interacts with components of the basal transcription machinery and co-activators to stabilize the transcription pre-initiation complex (PIC). In support of this, c-Jun has interacts with TAF1 and TFIIB (96-98). Furthermore, c-Jun mediated transcription is dependent on transcription associated factors (TAFs) *in vitro* (97). Interaction with co-activators such as CBP (cyclic AMP responsive element binding protein) leads to chromatin remodeling due to CBP's intrinsic histone acetyltransferase activity (99, 100). As a result, it is believed that these events lead to increased chromatin accessibility and long term potentiation of transcription by directing chromatin modification at a target locus.

D. The MCF7 Breast Cancer Model System

In order to study the role of c-Jun in breast cancer progression, our laboratory has previously shown that c-Jun enhances tumorigenicity of the human mammary carcinoma cell line, MCF7 (46). These changes include a shift to estrogen independent growth, increased *in vitro* cell motility and invasion and increased tumor formation in ovariectomized athymic (nude) mice (Fig. 2) (46). These changes are specific to c-Jun as demonstrated by comparing MCF7 stable cell lines overexpressing c-Jun or the related *JUN* family member, JunD. JunD/MCF7 cells fail to exhibit phenotypic changes consistent with malignant progression (Appendix A, Fig. 38). In addition, nuclear extracts isolated from c-Jun/MCF7 cells demonstrate increased AP-1 DNA binding activity compared to JunD/MCF7 or empty vector control/MCF7 stable cell lines (Appendix A, Fig. 39). Consistent with this observation, we found that overexpression of c-Jun induces a number of changes in gene expression including upregulation of the mesenchymal cell marker, vimentin, and downregulation of estrogen receptor alpha (Fig. 2) (46, 51). In addition, analysis of the AP-1 expression profile in c-Jun/MCF7 cells, compared to JunD/MCF7 and vector control/MCF7 cells, reveals changes consistent with those observed in clinical tumors (44). These changes include upregulation of Fra-1 and FosB and downregulation of JunB (Fig. 3). Taken together, these studies establish that the c-Jun/MCF7 cell culture model provides a useful tool in which to study mechanisms involved in breast cancer development and progression.

A

List of c-Jun Target Genes in MCF7 Breast Cancer Cells

Upregulated	Downregulated
1.) Cytokeratin 7	1.) GADD 153
2.) EMMPRIN	2.) $p21^{WAF1/Cip1}$
3.) Fibronectin	3.) Cytokeratin 19
4.) Metallothionein III	4.) TRIP6
5.) MMIF	5.) Estrogen receptor alpha
6.) $p16^{INK4a}$	
7.) PAI-1	
8.) SPARC	
9.) TIMP-1	
10.) Vimentin	

B

Summary of c-Jun Induced Phenotypic Changes in MCF7 Cells

phenotype	empty vector control/MCF7 stable cell lines	c-Jun/MCF7 stable cell lines
cell morphology	tight junctions, adherent	large, less adherent, less compact growth
responsiveness to estrogen	yes	no
growth doubling time	faster, except in estrogen depleted medium	slower
tumorigenicity in nude mice	0/18	13/18
cell motility and chemotaxis	weak	strong
Matrigel™ invasion	weak	strong

Fig. 2. Summary of c-Jun induced changes in gene expression and phenotype in MCF7 cells. *A*, A list of genes up or down regulated in response to constitutive overexpression of c-Jun in MCF7 cells. *B*, A summary of phenotypic changes in c-Jun/MCF7 cells compared to empty vector control/MCF7 stable cell lines.

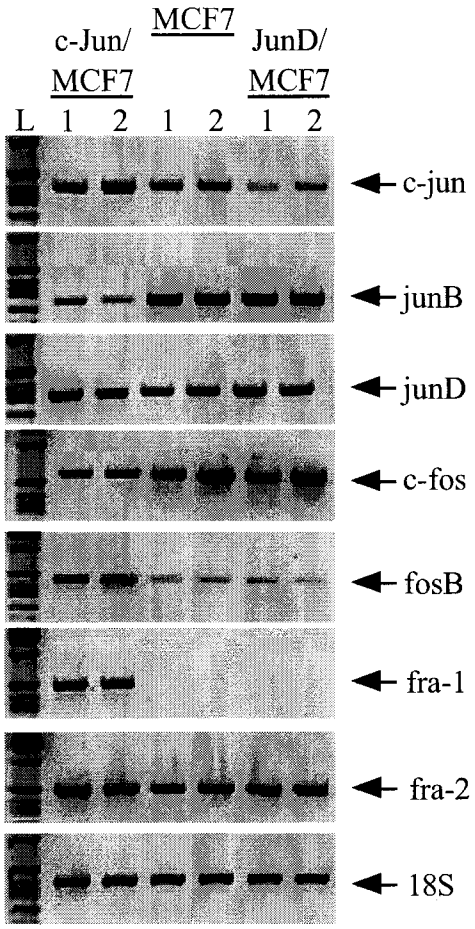

Fig. 3. Expression profile of *JUN* and *FOS* family genes in MCF7, JunD/MCF7 and c-Jun/MCF7 stable cell lines. Semi-quantitative RT-PCR analysis of endogenous AP-1 mRNA levels in the presence or absence of c-Jun or JunD overexpression in MCF7 cells. The numbers (1) and (2) denote individual stable cell lines tested. 18S serves as an invariantly expressed internal control gene. (L) denotes DNA molecular weight marker.

E. Properties and Functions of SPARC

One of the genes most highly upregulated by c-Jun in MCF7 breast cancer cells is SPARC (secreted protein acidic and rich in cysteine) (51). An analysis of SPARC expression by semi-quantitative RT-PCR demonstrated a >100 fold increase in steady state mRNA levels (Fig. 4). SPARC, also known as osteonectin and BM-40, belongs to the matricellular family of proteins which are involved in mediating interactions between the cell and extracellular matrix (101-107). The SPARC gene is evolutionarily conserved from *C. elegans* to humans and was originally identified as a glycoprotein constituent of bovine bone (108-110). Structural and functional analysis demonstrated the existence of several modular domains including: 1.) an amino-terminal acidic domain which has been shown to bind calcium 2.) a follastatin-like domain containing a copper binding region and promotes angiogenesis 3.) a carboxy terminal E-F hand domain which consists of a second calcium binding region (111). Additional studies have demonstrated the potential for differential N-linked glycosylation patterns depending on the cell type analyzed (112). In platelets, SPARC contains mainly complex type sugars, whereas in bone, SPARC contains primarily high mannose type (112). The functional significance of this differential glycosylation is unknown.

Expression of SPARC has been demonstrated in a wide range of tissues and is increased in epithelial cells during the processes of tissue remodeling and tumorigenesis (107, 108, 113, 114). SPARC is secreted from cells and binds to proteins such as collagen, thrombospondin, platelet derived growth factor (PDGF) receptor and vascular endothelial growth factor (VEGF) receptor (115-117). The normal physiological role for SPARC has been demonstrated during the processes of wound healing, morphogenesis

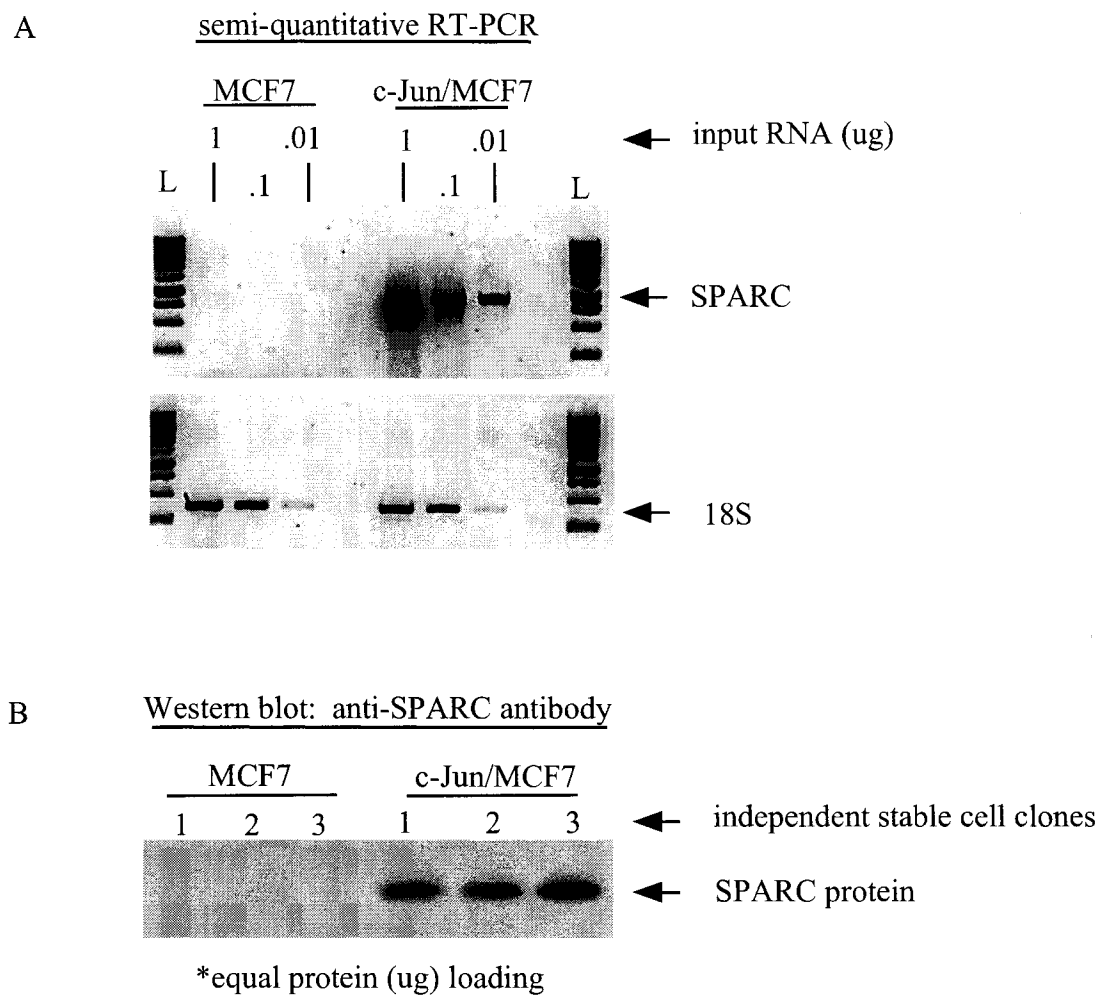

Fig. 4. Analysis of SPARC expression in MCF7 and c-Jun/MCF7 cells. *A,* RT-PCR analysis demonstrating steady state levels of SPARC RNA expression using 18S as an internal control. *B,* Western blot showing expression of the 43kDa glycosylated form of SPARC protein. Equal amounts of total protein (50μg) were loaded in each lane.

and bone formation (102). SPARC inhibits cell adhesion resulting in perturbed cell-to-cell contacts (101, 102). These observations are likely a result of decreased focal adhesion contacts during conditions when SPARC is highly expressed (103, 118, 119). In addition, overexpression of SPARC has been shown to inhibit cell cycle progression by initiating G_1 arrest in some cell types (102).

A multitude of studies have been conducted in which differences in SPARC gene expression correlate with tumor formation and/or progression. For example, SPARC mRNA and protein levels are increased in metastatic prostate cancer cells when compared to primary tumor cells (120). In addition, in well-differentiated brain astrocytoma tumors SPARC expression is increased (121). Furthermore, increased expression of SPARC has been demonstrated in bladder cancer and hepatocellular carcinoma and is associated with poor prognosis and late stage disease (122, 123). A clinical study of patients with melanoma demonstrated that SPARC expression was elevated in primary and metastatic forms of the disease (124, 125). Importantly, specific inhibition of SPARC in malignant melanoma cells abolished *in vivo* tumorigenicity in a mouse model (126). Immunohistochemical analysis of invasive meningioma and breast tumor samples revealed an increase in SPARC protein when compared to benign tissue (127, 128). Interestingly, increased SPARC expression has been observed in conjunction with increased c-Jun and Fra-1 expression in a panel of invasive breast cancer cell lines (20). Taken together, these studies suggest that increased SPARC may play a role in tumor cell progression.

F. Regulation of SPARC Gene Expression

While there is an abundance of evidence emphasizing the importance of SPARC expression in numerous cancer model systems, we know very little with regards to basic mechanisms of SPARC gene regulation. The human SPARC promoter was originally isolated and shown to be active in transient transfection assays in HT1080 human fibrosarcoma cells and HeLa cervical carcinoma cells when inserted upstream of a luciferase reporter gene (129). Initial experiments characterizing the chicken SPARC promoter established Jun responsiveness in chicken embryo fibroblasts (130). Interestingly, in these cells, endogenous chicken SPARC is normally expressed, but becomes downregulated in response to v-Jun expression. This v-Jun mediated repression of SPARC was shown to contribute to transformation of chicken embryo fibroblasts *in vitro* and fibrosarcoma formation *in vivo* (42). Conversely, we have shown that overexpression of c-Jun in MCF7 breast cancer cells results in SPARC gene activation, increased cell motility and invasion (46, 131). This interesting paradox regarding SPARC expression and regulation by v-Jun and c-Jun likely reflects cell type specific and/or species specific differences, but nonetheless, emphasizes the relationship between c-Jun expression and SPARC gene regulation.

G. Hypothesis and Specific Aims

Increased c-Jun/AP-1 expression is associated with breast cancer progression to a more invasive, hormone independent phenotype. However, the mechanisms by which c–Jun contributes to tumor progression remain unclear. Because c-Jun is a transcription factor, it is widely accepted that deregulated expression of c-Jun target genes plays a role

in this process. One intriguing c-Jun target gene shown to be upregulated in our MCF7 model system was SPARC. Increased SPARC expression is associated with tumorigenesis and malignant progression in a variety of cancers. Therefore, the objectives of this dissertation were to: 1.) determine the mechanisms by which c-Jun regulates SPARC gene expression, and 2.) determine the contribution of SPARC to c-Jun induced phenotype in a MCF7 breast cancer model system. Characterization of the events is critical in order to better understand the process of c-Jun mediated gene regulation during phenotypic progression. Our hypothesis was that c-Jun binds to SPARC gene regulatory regions leading to an increase in SPARC expression and a concomitant change to a pro-invasive cell phenotype. To test our hypothesis we proposed the following three specific aims:

Aim 1. To determine the effects of SPARC gene expression on MCF7 cell phenotype.

Aim 2. To map the c-Jun responsive region(s) of the human SPARC gene promoter.

Aim 3. To analyze epigenetic modifications associated with SPARC gene expression.

CHAPTER II

MATERIALS AND METHODS

Cells used in these studies

The c-Jun/MCF7 stable cell lines and empty vector control/MCF7 cell lines were a generous gift from Dr. Mike Birrer (National Institutes of Health/National Cancer Institute). Cell lines were maintained in a humidified chamber at 37°C and 5% carbon dioxide in Improved Minimal Essential Medium with zinc option (Mediatech Incorporated, Herndon, VA) supplemented with 10% fetal bovine serum and 1% penicillin/streptomycin.

Large scale preparation of plasmid DNA

Large scale preparation of plasmid DNA was done using the Qiagen High-Speed Midiprep Kit (Qiagen Corporation, Valencia, CA) according to manufacturer's instructions.

Cloning of the human SPARC protein coding region

Total RNA was isolated from c-Jun/MCF7 cells using TRIZOL® reagent (Invitrogen Corporation) according to manufacturer's recommendations. 100ng of total RNA was reverse transcribed using Moloney Murine Leukemia Virus reverse transcriptase (Promega Corporation) and random hexamers. The human SPARC protein coding region was amplified from the cDNA synthesis reaction using the Advantage™ 2 PCR kit (Clontech Corporation) using the following primers: SPARC cloning primer 1=

5' gtcagaagcttatgagggcctggatcttctttctcc 3', SPARC cloning primer 2= 5' gtcagatcgattggatttagatcacaagatccttgtcg 3'. SPARC cloning primer 1 has a HindIII site incorporated at the 5' end to facilitate subsequent cloning while SPARC cloning primer 2 has a ClaI site at its 5' end. Thermocycling conditions for SPARC amplification were as follows: step 1, 95°C for 2 minutes, step 2, 95°C for 30 seconds, step 3, 68°C for 30 seconds, step 4, 68°C for 1 minute, repeat steps 2-4, 29 times. The resultant PCR product is expected to be 944 base pairs consisting of 912 bases corresponding to the human SPARC coding region. PCR products were resolved by electrophoresis on a 1% low melting point agarose/1X TBE gel stained with GelStar® reagent (Cambrex Corporation, East Rutherford, NJ) at a final concentration of 1X for visualization. The SPARC amplicon was purified using the Qiaquick Gel Extraction Kit (Qiagen Corporation, Valencia, CA) following manufacturer's recommendations. This purified RT-PCR product was digested with HindIII and ClaI restriction enzymes and ligated to a similarly digested pGEM-7Zf+ plasmid (Promega Corporation, Madison, WI). Following transformation into DH5 alpha, electrocompetent *E. coli* cells, a positive clone containing an insert of the correct size was selected for sequence verification. DNA sequencing was conducted using an ALF automated DNA sequencer (Amersham/Pharmacia Biotech). Human SPARC oligonucleotide primers and sequence comparisons were based on GenBank accession number NM_003118.

Generation of SPARC/MCF7 and JunD/MCF7 stable cell lines

SPARC/MCF7 and JunD/MCF7 stable cell lines were made utilizing the pLPCX retroviral vector system (Clontech Corporation, Palo Alto, CA) according to

manufacturer's recommendations. Briefly, the human SPARC protein coding region was subcloned from the pGEM7-Zf+ HindIII/ClaI site into the HindIII/ClaI site of pLPCX retroviral vector (Clontech Corporation, Palo Alto, CA). The rat JunD protein coding region (kind gift from Dr. Rodrigo Bravo, Bristol-Myers Squibb, Trenton, New Jersey) was subcloned from HindIII/NotI into a HindIII/NotI digested LPCX vector. Purified plasmid DNA containing the appropriate expression cassettes for SPARC and JunD were transfected into the RetroPack^{TM} PT67 packaging cell line in order to produce infectious retrovirus. This cell line is derived from the murine fibroblast NIH3T3 cell line. Retroviruses produced from these cells contain the dualtropic 10A1 viral envelope protein thereby allowing for retroviral entry into target cells via the cell surface receptor(s) RAM1 (Pit2) and/or GALV (Pit1) (132, 133). PT67 cells were plated at a density of 5 X 10^5 cells/100mm plate. 24 hours later, cells were transfected with 12μg DNA/100mm plate using FuGENE 6 reagent (Boehringer Mannheim) according to manufacturer's recommendations (DNA:FuGENE ratio= 2:1). After 48 hours PT67 cells were placed under antibiotic selection using 2.5μg/ml of puromycin. Clonal populations of antibiotic resistant cells were allowed to grow together until confluent. Growth media containing virus was harvested and filtered through a 0.45μm cellulose acetate filter for subsequent infection of target cells. MCF7 cells were infected by incubating cells in the presence of viral supernatant and 10μg/ml of polybrene. Cells were incubated with virus for 6 hours then refed with Improved Minimal Essential Media with zinc option (Mediatech Incorporated, Herndon, VA) containing 10% fetal bovine serum and 1% penicillin/streptomycin. Forty-eight hours after infection, cells were placed under antibiotic selection using 2.0μg/ml of puromycin. After approximately 3 weeks

individual antibiotic resistant cell clones were isolated using sterile glass cloning rings (8mm diameter X 6mm height). To accomplish this, tissue culture dishes containing cell colonies were gently washed two times with 37°C phosphate buffered saline. Next, one end of a cloning ring was coated with sterile petroleum jelly and placed over an individual cell colony using sterilized forceps. A 50µl aliquot of trypsin/EDTA was added to the inside of each cloning ring to facilitate removal of the cell colony and to disperse cells. The trypsinized cells were then transferred to a single well of a 12-well tissue culture dish using a pipette. Stable cell clones were maintained in Improved Minimal Essential Medium with zinc option (Mediatech Incorporated, Herndon, VA) containing 10% fetal bovine serum, 1% penicillin/streptomycin and 2.0µg/ml of puromycin. Individual stable cell lines were then assayed SPARC or JunD protein expression as described below.

Western blot analysis

Monolayer cultures of cells were washed twice using 1X phosphate buffered saline and collected in 1.5mls phosphate buffered saline for each 100mm plate. Cells were then centrifuged at 16,000 X *g* at 4°C for 2 minutes. The resulting cell pellet was resuspended in 0.25M Tris, pH 7.8 followed by a series of three freeze/thaw cycles to facilitate cell lysis. The samples were then centrifuged at 16,000 X *g* at 4°C for 5 minutes. The supernatant was transferred to a new microfuge tube and protein was quantitated using the Bradford method (134). 50-100µg of protein was mixed with sample loading buffer (100mM Tris, pH 6.8, 2% sodium dodecylsulphate, 5% beta-mercaptoethanol, 15% glycerol and 0.025% bromophenol blue). Samples were denatured

by heating for 3 minutes in a boiling water bath and then analyzed on a 10% sodium dodecylsulfate-polyacrylamide gel electrophoresed in 1X Tris/glycine running buffer. Protein was transferred from the gel to a nitrocellulose membrane using a semi-dry electroblot apparatus (200mA for 15 minutes then 360mA for 20 minutes). Nitrocellulose membranes were washed twice in deionized water followed by a one minute incubation in 100% isopropanol. Membranes were then blocked using 5% non-fat milk/1X Tris buffered saline for one hour at room temperature with constant rocking. Next, samples were incubated for one hour at room temperature with a anti-SPARC mouse monoclonal primary antibody (OST1 clone, Biodesign International, Saco, ME) diluted 1:1,000 in 5% non-fat milk/1X Tris buffered saline. Membranes were washed three times in 1X Tris buffered saline/0.1% Tween-20 to remove unbound primary antibody. Samples were subsequently incubated for one hour at room temperature with anti-mouse horseradish peroxidase conjugated secondary antibody (Santa Cruz Biotechnology, Santa Cruz, CA) diluted 1:5,000 in 5% non-fat milk/1X Tris buffered saline. Protein was visualized by enhanced chemiluminescence (Amersham Biosciences, Upsala, Sweden) and detected on film. Protein molecular weight was estimated using Rainbow marker (Amersham Biosciences, Upsala, Sweden) or MagicMark™ (Invitrogen Corporation, Carlsbad, CA) as protein mass standards.

Construction of antisense SPARC adenovirus

Replication incompetent adenoviruses were constructed using the Adeno-X™ Expression System (Clontech Corporation, Palo Alto, CA) according to manufacturer's recommendations. Briefly, the human SPARC coding region was subcloned from the

HindIII/XhoI sites of PGEM7-Zf+ and inserted into the HindIII/XhoI sites of the plasmid pcDNA3.1/Zeo (Invitrogen Corporation, Carlsbad, CA). pcDNA3.1/Zeo/SPARC was subsequently digested with AflII/ApaI restriction enzymes to subclone the SPARC coding region in the antisense orientation into a AflII/ApaI digested pShuttle vector (Clontech Corporation, Palo Alto, CA). pShuttle/SPARC and pShuttle/LacZ plasmids were digested with the restriction enzymes, I-Ceu-I and PI-SceI and ligated into similarly digested Adeno-X™ viral genomes resulting in adenovirus-SPARC antisense and adenovirus-LacZ viral genomic DNA. Following digestion using SwaI restriction enzyme, adenovirus-SPARC antisense and adenovirus-LacZ plasmids were transformed into DH5 alpha electrocompetent *E. coli.* Subsequently, adenoviral plasmid DNA was purified using the NucleoBond® Plasmid Maxi Kit (Clontech Corporation, Palo Alto, CA) according to manufacturer's instructions. Purified plasmid DNA was digested with *Pac*I restriction enzyme prior to transfection into the HEK293 packaging cell line. HEK293 cells were seeded at a density of 3 X 10^6 cells/100mm tissue culture dish 24 hours prior to transfection. Cell were grown in a humidified chamber at 37°C and 5% carbon dioxide in Dulbecco's Modification of Eagle's Medium with 10% fetal bovine serum and 1% penicillin/streptomycin 24 hours prior to transfection. Cells were transfected with purified plasmid DNA using FuGENE 6 reagent (Roche Diagnostics, Indianapolis, IN) according to manufacturers recommendations (2:1 FuGENE volume:DNA mass). Cells were harvested 7-14 days post-transfection when cytopathic effect (CPE) was evident throughout the plate. The cells were then pelleted by centrifugation and resuspended in phosphate buffered saline. Virus was freed from cells by freezing and thawing cell pellets three times with vortexing after each thaw. This

supernatant containing virus was used to re-infect HEK293 cells in order to increase the viral titer. For infection, cells were seeded at a density of 1 X 10^6 cells/35mm tissue culture dish. Twenty-four hours later, cell growth medium was removed and 1.0ml of virus suspended in Dulbecco's phosphate buffered saline (with calcium) was added to each 35mm dish. Infections were conducted for 4 hours in a humidified chamber at 37°C and 5% carbon dioxide. Following the 4 hour incubation, complete growth medium was added and cells were refed with fresh medium the next day.

Following a single round of viral amplification, viral titer was determined using the Adeno-X™ Rapid Titer Kit (Clontech Corporation, Palo Alto, CA) following manufacturer's instructions. Briefly, infected HEK293 cells were fixed in methanol and rinsed two times with 1X phosphate buffered saline. Samples were then incubated with an anti-hexon, adenovirus specific, primary antibody. The primary antibody was then washed away and a horse radish peroxidase conjugated secondary antibody was added. Diaminobenzidine was added to the reaction to facilitate colorimetric detection. Individual cells producing virus were readily detectable using conventional light microscopy.

The amount of infectious viral particles following a single round of amplification was typically 1-5 X 10^8 plaque forming units (pfu)/ml (see Appendix A, Fig. 40). In order to determine the optimal multiplicity of infection (MOI) for c-Jun/MCF7 cells, a series of infections were conducted over a broad range of MOI using adenovirus-LacZ as a means of determining the number of infected cells (see Appendix A, Fig. 41). Adenovirus-LacZ infected c-Jun/MCF7 cells were stained using the beta-galactosidase staining kit (Invitrogen Corporation, Carlsbad, CA) according to manufacturer's

instructions. An optimal MOI of between 5-10 was determined to infect the majority of cells without being cytotoxic. This MOI was used to infect c-Jun/MCF7 cells with antisense SPARC adenovirus in order to suppress endogenous SPARC expression. A time course following infection was conducted in order to determine the optimal time following infection in which endogenous SPARC expression was suppressed to the greatest extent. These conditions were used for all subsequent experiments.

In vitro cell motility and invasion assays

For invasion assays, a solution of collagen type IV was made in 0.01M acetic acid in order to coat modified Boyden chamber membranes. Membranes were soaked overnight at 4°C followed by coating with Matrigel™ (BD Biosciences, Franklin Lakes, NJ). Cells were suspended in serum-free Improved Minimal Essential Media with zinc option supplemented with 0.1% bovine serum albumin. NIH3T3 cell culture supernatant was used as the chemoattractant added to the lower wells of a modified Boyden chamber apparatus. Cells were incubated for 4-5 hours followed by staining with Diff-Quick® (American Scientific Products, Chicago, IL) according to manufacturer's instructions. The number of cells that had migrated in response to the chemoattractant was determined by counting cells from three fields of view at 40X magnification. Motility assays were conducted using the same procedure except membranes were only coated with gelatin.

Cell proliferation assays

The rate of cell proliferation was determined using the CellTiter 96® Non-Radioactive Cell Proliferation Assay Kit (Promega Corporation, Madison, WI) according

to manufacturer's instructions. This kit is a colorimetric assay based on the conversion of MTT (3-[4,5-dimethylthiazol-2-yl]-2,5-diphenyl) tetrasodium bromide to formazan via the succinate-tetrazolium reductase system in viable cells (135). Cells were seeded at a density of 5,000 cells/well in a 96-well plate and serum starved for 24 hours prior to beginning the assay. The medium was then replaced with Improved Minimal Essential Medium with zinc option containing 10% fetal bovine serum and 1% penicillin/streptomycin. Four replicate plates were set up so that cell proliferation rates could be measured at 24, 48, 72 and 96 hours. Each cell line/condition was assayed in seven replicate wells for each time point. In addition, wells containing only media were set up in order to serve as background controls. At the indicated time points, 15µl of MTT assay dye was added to each well followed by a 4 hour incubation at 37°C and 5% carbon dioxide. Next, 100µl of stop solution was added for solublization of the formazan reaction product. Samples were subsequently incubated for 1 hour then mixed by pipetting up and down. Bubbles were removed by aspiration and the sample absorbance was recorded at 570nm using a microtiter plate reader. Each experiment was conducted in triplicate. Mean absorbance values and standard deviation were calculated for each cell line and time point. Linear regression analysis was conducted in order to determine proliferation rates. The proliferation rate of empty vector control/MCF7 cells was set at 100% and the values of c-Jun/MCF7 and SPARC/MCF7 cells were expressed as percent of empty vector control/MCF7 cells.

Generation of c-Jun/MCF7 stable cell lines expressing SPARC siRNAs

The pSilencer 3.1-H1-hygromycin plasmid based system (Ambion Incorporated, Austin, TX) was used for expression of siRNA sequences designed against the human SPARC mRNA. Four siRNA sequences were designed using guidelines available at www.ambion.com. Briefly, the human SPARC mRNA sequence was analyzed for adenine-adenine dinucleotide repeats. The 19 nucleotides immediately 5' of adenine-adenine repeats were recorded. Sequences that were 50-60% guanine and cytosine (G/C) residues, without runs of three or more consecutive G/Cs, were given priority scores. Of the sequences meeting these criteria, four sequences were selected that were predicted to target different regions of the SPARC mRNA. Oligonucleotides were commercially synthesized with 5' phosphate modification and polyacrylamide gel purified (Integrated DNA Technologies Incorporated, Coralville, IA). Lyophilized oligonucleotides were resuspended at a concentration of 1μg/μl in nuclease-free water. 2μg of paired sense and antisense oligonucleotides were mixed in 46μl of oligonucleotide annealing buffer (Ambion Incorporated, Austin, TX) to facilitate complementary base pairing and formation of duplex DNA. Annealing of oligonucleotides was accomplished by heating to 90°C for 3 minutes followed by cooling in a heat block to 37°C. The duplexes were then diluted 1:10 in nuclease-free water and 1μl was used in a ligation reaction. The oligonucleotides were designed to have BamHI/HindIII overhangs after annealing to facilitate ligation into a BamHI/HindIII digested pSilencer 3.1-H1-hygromycin plasmid. The following oligonucleotides were used:

SPARC +161 (sense):

5' phos-gatcccgtttgatgatggtgcagaggttcaagagacctctgcaccatcatcaaatttttggaaa 3'

SPARC +161 (antisense):

5' phos-agcttttccaaaaaatttgatgatggtgcagaggtctcttgaacctctgcaccatcatcaaacgg 3'

SPARC +328 (sense):

5' phos-gatcccggtgtgcagcaatgacaacttcaagagagttgtcattgctgcacacctttttttggaaa 3'

SPARC +328 (antisense):

5' phos-agcttttccaaaaaaggtgtgcagcaatgacaactctcttgaagttgtcattgctgcacaccgg 3'

SPARC +418 (sense):

5' phos-gatcccgctccacctggactacatcttcaagagagatgtagtccaggtggagctttttttggaaa 3'

SPARC +418 (antisense):

5' phos-agcttttccaaaaaagctccacctggactacatctctcttgaagatgtagtccaggtggacggg 3'

SPARC +604 (sense):

5' phos-gatcccgtgagaagcgcctggaggcattcaagagatgcctccaggcgcttctcatttttttggaaa 3'

SPARC +604 (antisense):

5' phos-agcttttccaaaaaatgagaagcgcctggaggcatctcttgaatgcctccaggcgcttctcacgg 3'

To generate stable cell lines expressing the individual siRNA transcripts, c–Jun/MCF7 cells were plated at a density of 2.5 X 10^6 cells/100mm plate and grown in Improved Minimal Essential Medium with zinc option, 10% fetal bovine serum and 1% penicillin/streptomycin. Cells were transfected 24 hours later using 27μg of individual SPARC siRNA/pSilencer 3.1-H1-hygromycin expression plasmids. FuGENE 6 transfection reagent (Roche Diagnostics, East Rutherfod, NJ) was used to deliver plasmid DNA (FuGENE:DNA ratio = 2:1). Twenty-four hours after transfection, cells were refed with fresh, complete media containing 200μg/ml hygromycin (Clontech Corporation, Palo Alto, CA) in order to select stable cell populations. Cell cultures were subsequently

refed every other day with fresh media containing hygromycin. After approximately three weeks, cell populations from the same plate (expressing the same individual siRNA) were trypsinized, pooled and maintained as a single culture. SPARC protein expression was determined by Western blot analysis as previously described in this section. Expression of c-Jun protein was determined by Western blot analysis using a rabbit polyclonal c-Jun specific antibody, c-Jun/AP-1 (Ab-1) (Oncogene Science, Cambridge, MA) at a 1:5,000 dilution.

SPARC promoter/luciferase reporter plasmids

The SPARC promoter constructs corresponding to nucleotides -1409/+28 and–120/+28 in pGL2-Basic (Promega Corporation, Madison, WI) were a kind gift from Dr. Marc Castellazzi and have been described elsewhere (129). To generate the SPARC promoter 5' deletion construct corresponding to positions –70/+28 we used polymerase chain reaction to amplify this region from the SPARC promoter –1409/+28-pGL2-Basic parental plasmid. The following primers were used: primer 1= -70/+28 5' acggggtggaggggagatgacccag 3', primer 2= pGL2-Basic primer 5' ctttatgtttttggcgtcttcca 3'. 2ng of plasmid DNA was used as a template and mixed with the following PCR master mix components: 4µl dNTPs (2.5mM each), 10X Advantage^{TM} 2 reaction buffer (Clontech Corporation), 150ng of each primer, 0.5µl Advantage2-HF enzyme mix containing Taq polymerase and a proofreading enzyme (Clontech Corporation, Palo Alto, CA). Themocycling conditions were as follows: step 1, 95°C for 2 minutes, step 2, 95°C for 30 seconds, step 3, 65°C for 30 seconds, step 4, 68°C for 30 seconds, repeat steps 2-4 for a total of 25 cycles. PCR products were analyzed on a 1% low melt agarose gel and

visualized by staining with ethidium bromide and gel purified using the Qiaquick Gel Extraction Kit (Qiagen Corporation, Valencia, CA). Two-step PCR was used to generate point mutations within the SPARC promoter AP-1 like site at –1051/-1045. The pGL2-Basic forward primer 5' tgtatcttatggtactgtaactg 3', designated A1, corresponds to a region of the pGL2-Basic plasmid which is upstream of the plasmid SmaI site. The pGL2-Basic reverse primer 5' ctttatgtttttggcgtcttcca 3', designated B1, corresponds to a region immediately downstream of the plasmid HindIII site. The internal primers used to introduce point mutations to the –1051/-1045 AP-1 like site are as follows: -1051/-1045 mutated to consensus= primer (C1) 5' gcctgggcgacagagtgagtcag 3' and primer (D1) 5' gttttgagacagagtctgactcactc 3', -1051/-1045 more mutated= primer (E1) 5' gcctgggcgacagagcgaatgag 3' and primer (F1) 5' gttttgagacagagtctcattcgctc 3'.

PCR was performed using the following primer combinations: A1/D1, A1/F1, B1/C1, B1/E1. The PCR master mix for each of these reactions contained the following components: 4µl dNTPs (2.5mM each), 10X Advantage^{TM} 2 reaction buffer (Clontech Corporation, Palo Alto, CA), 150ng of each primer, 0.5µl Advantage^{TM} 2 enzyme mix containing Taq polymerase and a proofreading enzyme (Clontech Corporation, Palo Alto, CA). Themocycling conditions were as follows: step 1, 95°C for 2 minutes, step 2, 95°C for 30 seconds, step 3, 63°C for 30 seconds, step 4, 68°C for 60 seconds, repeat steps 2-4 for a total of 25 cycles. Products were purified on a 1% low-melt agarose gel and gel purified using the Qiaquick Gel Extraction Kit (Qiagen Corporation, Valencia, CA). A portion of the purified PCR products containing the corresponding mutations were mixed into a second PCR reaction to produce the full-length mutated product. PCR products generated with the following primer combinations were mixed and used as the template

for subsequent PCR reactions: A1/D1 and B1/C1 containing the mutation to a consensus context, A1/F1 and B1/E1 containing the mutations to a more mutated context. Amplification of full-length mutant promoter fragments was done using primers A1 and B1 under the following thermocycling conditions: step 1, 95°C for 2 minutes, step 2, 95°C for 30 seconds, step 3, 63°C for 30 seconds, step 4, 68°C for 90 seconds, repeat steps 2-4 for a total of 25 cycles. These full-length mutated PCR products were gel purified using the Qiaquick Gel Extraction Kit (Qiagen Corporation, Valencia, CA) according to manufacturer's instructions. Purified PCR amplicons were treated with DNA polymerase I large (Klenow) fragment followed by digestion with HindIII restriction enzyme. The mutant promoter fragments were subsequently cloned into a SmaI/HindIII digested pGL2-Basic vector. Mutations were confirmed by DNA sequencing.

Luciferase assays

Cells were seeded in 6-well tissue culture plates (area=35mm^2/well) at a density of 3 x 10^5 cells/well approximately 24 hours prior to transfection. 3μg of the indicated plasmid DNA was added to 6μl of FuGENE 6 (Roche Diagnostics, East Rutherfod, NJ) reagent pre-mixed with serum-free Improved Minimal Essential Media and added dropwise to each well. After 48 hours, cells were washed twice with 1X phosphate buffered saline (PBS). Following the final PBS wash, 150μl of Reporter Lysis Buffer (Promega Corporation, Madison, WI) was added to cells and incubated for 10 minutes. These samples were frozen at –80°C for at least 1 hour to facilitate cell lysis and then collected for analysis. Luciferase assays were done following manufacturers

recommendations and quantitated using a luminometer (Turner Designs Incorporated, Sunnyvale, CA) with the following parameters: delay= 2 seconds, integration= 15 seconds, replicates= 3. Relative luciferase values were normalized to protein concentration per volume assayed (assay amounts were 20μl unless the luciferase activity was outside of the linear range of detection in which case protein samples were diluted accordingly in 1X lysis buffer). Protein quantitation was conducted using the Bradford method (134).

Nuclear extract preparation

Nuclear extracts were prepared according to a modification of the procedure established by Dignam (136). Monolayer cell cultures were washed two times with phosphate buffered saline and collected in a buffer consisting of 10mM HEPES pH 7.9, 1.5mM magnesium chloride, 10mM potassium chloride, 0.5% NP-40, 2μg/ml aprotinin, 0.5μg/ml leupeptin, 1μg/ml pepstatin, 1mM PMSF, 0.5mM DTT. Cells were incubated on ice for 10 minutes followed by centrifugation at 16,000 X *g* at 4°C. The nuclear pellet was resuspended in 20mM HEPES pH 7.9, 25% glycerol, 0.42M sodium chloride, 1.5mM magnesium chloride, 0.2mM EDTA, 1μg/ml aprotinin, 0.5μg/ml leupeptin, 1μg/ml pepstatin, 1mM PMSF, 0.5mM DTT. The pellet was incubated for 30 minutes on ice with gentle mixing at 5 minute intervals. This mixture was then centrifuged at 16,000 X *g* for 30 minutes at 4°C. The supernatant was collected and dialyzed against a buffer consisting of 20mM HEPES pH 7.9, 20% glycerol, 0.1M potassium chloride, 0.2mM EDTA, 1mM PMSF, 0.5mM DTT for 4 hours at 4°C. The dialysis buffer was changed once during the 4 hour incubation. Samples were snap-frozen using a dry ice-ethanol

bath and stored in 30µl aliquots at –80°C. Protein concentration was determined using the Bradford method (134).

Gel Shifts, antibody supershifts and competitions

Empty vector control/MCF7, c-Jun/MCF7 and JunD/MCF7 nuclear extracts were prepared as previously described in this section. ^{32}P labeled gel shift probes were prepared using partially overlapping, complementary oligonucleotide primers as indicated. Oligonucleotide primer pairs were annealed by heating to 90° C for 3 minutes followed by cooling to room temperature on the bench top. DNA polymerase I large (Klenow) fragment was used to fill-in single stranded regions with alpha-^{32}P dNTP (alpha-^{32}P dATP or alpha-^{32}P dTTP depending on probe) and non-radiolabeled dNTPs. Radiolabeled gel shift probes were subsequently extracted once with an equal volume of phenol and purified from unincorporated radiolabel using a Chromaspin-10 TE chromatography column (Clontech Corporation, Palo Alto, CA). The specific activity of radiolabeled probes was quantitated using a liquid scintillation counter and expressed as counts per minute (cpm) as indicated in individual figure legends. A 2X gel shift reaction buffer for AP-1 binding consisted of 20mM HEPES, 35% glycerol, 0.2mM EDTA, 40mM sodium chloride, 8mM magnesium chloride, 5mM DTT (made fresh), 4mM spermidine, 1µg poly-dIdC and 0.1% NP-40. AP-1 DNA binding competitors were generated in the same way as ^{32}P radiolabeled probes except a full complement of non-radiolabeled dNTPs were used in the labeling reaction. Cold competitors were added in the indicated amounts for 20 minutes prior to incubation with the appropriate ^{32}P labeled probe. Gel shifts using antibodies to either compete or supershift DNA bound proteins

were done by pre-incubating the nuclear extracts for 20 minutes with 2μg of anti- c-Jun antibody directed against the DNA binding domain (Santa Cruz Biotechnology, Santa Cruz, CA), 2μg of anti Fra-1 antibody R-20 clone (Santa Cruz Biotechnology, Santa Cruz, CA), 2μg of anti-Sp1 antibody PEP-1 (Santa Cruz Biotechnology, Santa Cruz, CA), 2μg of anti-p130 antibody N-17 (Santa Cruz Biotechnology, Santa Cruz, CA) or 2μg of anti-p16 antibody N-20 (Santa Cruz Biotechnology, Santa Cruz, CA). 1μg poly-dIdC was added to each reaction to inhibit non-specific protein/DNA interactions. Reactions were analyzed on 6% non-denaturing polyacrylamide gels electrophoresed in 1% TBE running buffer at room temperature. Gels were pre-run for 20 minutes at 20mA constant current with 10μl of 2X gel shift reaction buffer loaded in each well. Gel shift reactions were then loaded onto the gel and electrophoresis was continued for approximately 2 hours at 30mA constant current. Gels were then transferred to filter paper and dried at 80°C for 2 hours followed by autoradiography for detection of protein/DNA complexes.

To analyze DNA binding of protein complexes with Sp family binding specificity the gel shift reactions were done as indicated above with the following modifications. Reactions were electrophoresed on a 5% non-denaturing polyacrylamide gel in 0.5% TBE running buffer at room temperature unless otherwise noted. Sp1 consensus and mutant competitors (kind gift from Dr. Julie Kerry, Eastern Virginia Medical School) were added to nuclear extracts and DNA binding buffer 20 minutes prior to incubation with the indicated probe. The binding buffer used was as follows: 20mM HEPES, 35% glycerol, 0.2mM EDTA, 40mM sodium chloride, 8mM magnesium chloride, 5mM DTT

(made fresh), 4mM spermidine, 1μg poly-dIdC/reaction and 0.1% NP-40. The following gel shift probes were used in these studies:

PG32-1 consensus AP-1 probe:

Forward primer: 5' acccggggatcctctagaatgactcatcgg 3'

Reverse primer: 5' cttgcatgcctgcaggatccgatgagtcat 3'

SPARC promoter AP-1 like site at –1051/-1045 mutated to consensus:

Forward primer: 5' gcctgggcgacagagtgagtcag 3'

Reverse primer: 5' gttttgagacagagtctgactcactc 3'

SPARC promoter AP-1 like site at –1051/-1045 mutated to wild type:

Forward primer: 5' gcctgggcgacagagtgagtgag 3'

Reverse primer: 5' gttttgagacagagtctcactcactc 3'

SPARC promoter AP-1 like site at –1051/-1045 mutated to more mutated:

Forward primer: 5' gcctgggcgacagagcgaatgag 3'

Reverse primer: 5' gttttgagacagagtctcattcgctc 3'

Heterologous competitor for AP-1 gel shift reactions:

Forward primer: 5' ttgacgtcaataatgacg 3'

Reverse primer: 5' tatgggaacatacgtcat 3'

Sp1 consensus gel shift competitor probe:

Forward primer: 5' tcatacaacgtagggcgggattgttgagaa 3'

Reverse primer: 5' tgttctcaacaatcccgccctacgttgtat 3'

Sp1 mutant gel shift competitor probe:

Forward primer: 5' tcatacaacgtagagtactattgttgagaa 3'

Reverse primer: 5' tgttctcaacaatagtactctacgttgtat 3'

SPARC promoter –120/-83 gel shift probe:

Forward primer: 5' gggagaaggaggaggccgggggaag 3'

Reverse primer: 5' ctcctgtctcctccttcccccgg 3'

RNA isolation

Total cellular RNA was isolated using TRIZOL® reagent (Invitrogen Corporation, Carlsbad, CA) according to the manufacturers protocol. Cells were washed two times in phosphate buffered saline followed by the addition of TRIZOL® reagent (2.5mls for 100mm plate, 1ml for 60mm plate). Samples were collected using a sterile plastic scraper and aliquoted into nuclease-free microfuge tubes. Samples were then vortexed for 15 seconds and incubated at room temperature for 5 minutes. Chloroform was then added and samples were shaken by hand vigorously for 30 seconds followed by incubation for 5 minutes at room temperature. Samples were subsequently centrifuged at 10,000 X *g* at 4°C for 10 minutes. Following centrifugation, the upper (aqueous) phase was carefully aliquoted into a new nuclease-free microfuge tube using a nuclease-free, aerosol barrier pipette tip. An equal volume of 100% isopropanol was then added and the sample was vortexed briefly followed by a 10 minute incubation at room temperature. The sample was then centrifuged at 10,000 X *g* for 15 minutes at 4°C to collect the RNA precipitate. Following centrifugation, the supernatant was carefully removed from the RNA pellet and discarded. Ice-cold 70% ethanol was gently added to the pellet followed by a final centrifugation at 10,000 X *g* for 7 minutes. The ethanol was then removed and the pellet was air dried. The RNA pellet was resuspended in an appropriate volume of

nuclease-free water. An aliquot of the purified RNA was quantitated by spectophotometry at 260nm.

Semi-quantitative reverse transcriptase-polymerase chain reaction (RT-PCR)

100ng of total RNA was incubated in the presence of 20pmol of random hexamers (Applied Biosystems, Foster City, CA) at 70°C for 2 minutes followed by snap-cooling at 4°C. The reverse transcription master mix was then added to the RNA/primer mixture. The reverse transcriptase master mix consisted of 5µl of a 5X Moloney Murine Leukemia Virus reverse transcriptase (MMLV-RT) reaction buffer (Promega Corporation, Madison, WI), 20 units of recombinant Rnasin (Promega Corporation, Madison, WI), 4µl of dNTP mix (2.5mM each), 200 units of Moloney Murine Leukemia Virus reverse transcriptase (Promega Corporation, Madison, WI) and nuclease-free water (Promega Corporation, Madison, WI). The reverse transcription reaction was then incubated at 42°C for 1 hour followed by heating at 94°C for 5 minutes to halt cDNA synthesis. The samples were then cooled to 4°C until further use.

A 1.5µl aliquot of the reverse transcription reaction was used to amplify a portion of the 18S ribosomal subunit gene transcript using the following oligonucleotide primers: 18S sense primer= 5' tgactctagataacctcggg 3', 18S antisense primer= 5' cccaagatccaactacgagc 3'. The PCR reaction mixture consisted of the following: 1.5µl of template cDNA, 5µl of 10X PCR buffer (Clontech Corporation, Palo Alto, CA), 4µl dNTP mix (2.5mM each), 150ng of sense and antisense 18S primers, 0.5µl of Titanium™ Taq DNA polymerase (Clontech Corporation, Palo Alto, CA) and nuclease-free water for a 50µl total reaction volume. Polymerase chain reaction for 18S was conducted using a

Biometra T-Gradient Thermocycler as follows: step one, 95°C for 1 minute, step two, 95°C for 30 seconds, step three, 55°C for 30 seconds, step four, 68°C for 45 seconds. Steps 2-4 were repeated for a total of 13 cycles which corresponded to mid-log phase amplification using 100ng of input, total cellular RNA. The expected amplification product is 403 base pairs. The method for determining the mid-log phase of amplification is described later in this section.

A 2μl aliquot of the reverse transcription reaction was used to amplify a portion of SPARC utilizing a gene specific primer pair that would span intron regions. The primers used for SPARC RT-PCR were as follows: SPARC sense primer= 5' gtcagaagcttatgagggcctggatcttctttctcc 3', SPARC antisense primer= 5' gtcagatcgattggatttagatcacaagatccttgtcg 3'. The PCR reaction mixture consisted of the following: 2μl of template cDNA, 5μl of 10X PCR buffer (Clontech Corporation, Palo Alto, CA), 4μl dNTP mix (2.5mM each), 150ng of sense and antisense SPARC primers, 0.5μl of Titanium™ Taq DNA polymerase (Clontech Corporation, Palo Alto, CA) and nuclease-free water for a 50μl total reaction volume. Polymerase chain reaction for SPARC was conducted using a Biometra T-Gradient Thermocycler as follows: step one, 95°C for 1 minute, step two, 95°C for 30 seconds, step 3, 68°C for 30 seconds, step 4, 68°C for 1 minute. Steps 2-4 were repeated for a total of 30 cycles which corresponded to mid-log phase amplification using 100ng of input, total cellular RNA. The expected amplicon size is 944 base pairs. The method for determining the mid-log phase of amplification is described later in this section.

For visualization of RT-PCR amplicons, reaction products were electrophoresed on a 1.5% agarose gel stained with GelStar® reagent (Cambrex Corporation, East

Rutherford, NJ). Following ultraviolet transillumination at 312nm, images were captured using a Kodak DC40 digital camera equipped with an ethidium bromide lens filter and PCR amplicon signals quantitated using Kodak 1D Image Analysis software package.

In order to utilize 18S as an endogenous control for standardization purposes it was necessary to identify when 18S amplification was in mid-log phase to allow for appropriate quantitation. This was done by conducting multiple, parallel 18S PCR reactions over a range of cycle numbers and input RNA concentrations utilizing aliquots from the same cDNA mixtures as the template. For SPARC (and other indicated genes), mid-log phase amplification was conducted by testing samples over a range of different cycle numbers and varying input RNA concentration as well. Following quantitation using Kodak 1D Image Analysis software (Kodak Corporation), the values were plotted as relative intensity vs. cycle number as well as relative intensity vs. input RNA amount. The cycle number which correlated to mid-log phase amplification using 100ng of input total RNA was used for all subsequent experiments for standardization of SPARC expression between the two cell types. Input RNA was adjusted to ten-fold higher (1.0μg) and ten-fold lower (10ng) in the reverse transcription reaction to ensure linear amplification over a one-log change in RNA concentration in either direction.

The primers used for RT-PCR analysis of AP-1 family gene expression were as follows:

fra-1 sense= (position 410-427, GenBank accession number X16707)=

5' AGGAAGGAACTGACCGAC 3'

fra-1 antisense= (position 889-906, GenBank accession number X16707)=

5' GAAGGGGAGGAGACATTG 3'

fosB sense= (position 3137-3155, GenBank accession number NM_006732)=

5' GCTATTTATCCCTTTCCTG 3'

fosB antisense= (position 3579-3597, GenBank accession number NM_006732)=

5' TGCTCACACTCTCACACTC 3'

c-jun sense= (position 2036-2065, GenBank accession number J04111)=

5' GCATGAGGAACCGCATCGCTGCCTCCAAGT 3'

c-jun antisense= (position 2416-2445, GenBank accession number J04111)=

5' GCGACCAAGTCC TTCCCACTCGTGCACACT 3'

junB sense= (position 1469-1496, GenBank accession number NM_002229)=

5' CCAGTCCTTCCACCTCGACGTTTACAAG 3'

junB antisense= (position 1696-1725, GenBank accession number NM_002229)=

5' GACTAAGTGCGTGTTTCTTTTTCCACAGTAC 3'

junD sense= (position 1273-1293, GenBank accession number X51346)=

5' CAGCCTCAAACCCTGCCTTTC 3'

junD antisense= (position 1571-1590, GenBank accession number X51346)=

5' AACAGAAAACCGGGCGAACC 3'

c-fos sense= (position 1170-1187, GenBank accession number NM_005252.2)=

5' TCTTCCTTCGTCTTCACC 3'

c-fos antisense= (position 1727-1746, GenBank accession number NM_005252.2)=

5' AATCAGAACACACTATTGCC 3'

fra-2 sense= (position 570-587, GenBank accession number BC022791)=

5' AGGAGGAGAGATGAGCAG 3'

fra-2 antisense= (position 1070-1087, GenBank accession number BC022791)=

5' GGATAGGTGAAGACGAGG 3'

Conditions used for semi-quantitative RT-PCR analysis of AP-1 family members were the same as for SPARC except that a 66°C annealing temperature was used for each primer pair during PCR. Mid-log phase amplification conditions were determined for each AP-1 family member using the same technique described previously in this section for SPARC and 18S. The number of PCR amplification cycles required for mid-log phase amplification using 100ng of total RNA as input for reverse transcription were as follows: fra-1= 29 cycles, fosB= 36 cycles, c-jun= 30 cycles, junB= 34 cycles, junD= 32 cycles, c-fos= 36 cycles, fra-2= 30 cycles.

Chromatin immunoprecipitation (ChIP) analysis

Cells were seeded in duplicate 150mm tissue culture plates at a density of 3 X 10^6 cells per plate. Approximately 48 hours later, cells from one plate were counted in order to normalize for differences in cell number. To the second plate, a 37% stock of formaldehyde was added directly to the tissue culture medium to achieve a final concentration of 1%. The plate was gently rocked to facilitate mixing and then the plates were incubated at 37°C for 10 minutes. The tissue culture media was removed and the cells were washed 3 times in ice-cold phosphate buffered saline plus protease inhibitors (aprotinin 1μg/ml, leupeptin 1μg/ml, PMSF 1mM final concentration). For ChIP analysis of acetylated histones, the histone deacetylase inhibitor, trichostatin A, was added to wash buffers at a final concentration of 100ng/ml. Cells were collected by gentle scraping using a rubber policeman. The cell suspension was centrifuged at 1,500 X *g* for 5 minutes at 4°C in order to pellet cells. The supernatant was discarded and the cell pellet

was resuspended in 200µl of cell lysis buffer (1% SDS, 10mM EDTA, 50mM Tris-HCl, pH 8.1, aprotinin 1µg/ml, leupeptin 1µg/ml, PMSF 1mM) for every 1 X 10^6 cells (estimated by cell counts). Samples were then incubated at room temperature for 10 minutes to allow for membrane dissociation. An aliquot equal to 8 X 10^6 cells was subjected to sonication. A Fisherbrand 60 watt sonic dismembrator with a 1/8" diameter tip was used for all sonication (Fisher Scientific Corporation, Pittsburgh, PA). Sonication consisted of eight, 6 watt pulses, each lasting 12 seconds. Samples were kept on ice during the entire sonication procedure and a 1 minute incubation on ice was done in between each pulse to prevent sample heating. Under these conditions, DNA was sheared to an average size of 500-1,000 base pairs. Following sonication, samples were centrifuged for at 10,000 X *g* for 5 minutes at 4°C. The supernatant, containing soluble chromatin, was collected and distributed into 200µl aliquots for each immunoprecipitation. A 100µl aliquot was saved and designated as input chromatin not subjected to immunoprecipitation. This sample was saved until the crosslink reversal step. Chromatin aliquots subjected to immunoprecipitation were diluted in 1700µl of ice-cold ChIP dilution buffer (0.01% SDS, 1.1% Triton X-100, 1.2mM EDTA, 16.7mM Tris-HCl, pH 8.1, 167mM sodium chloride, 1µg/ml aprotinin, 1µg/ml leupeptin, 1mM PMSF). Samples were then pre-cleared using 80µl of salmon sperm DNA/protein A agarose (stock=1.5ml packed beads with 600µg sonicated salmon sperm DNA, 500µg BSA 1.5mg recombinant protein A, 50% slurry up to 3mls suspended in TE with 0.05% sodium azide). For pre-clearing, samples were incubated at 4°C for 1 hour with constant rotation. Next, samples were centrifuged for 1 minute at 100 X *g* in a tabletop microfuge in order to pellet beads. Supernatants were aliquoted into new, nuclease-free microfuge

tubes followed by the addition of 10μg of antibody. The following antibodies were used in chromatin immunoprecipitation analysis: anti-tetraacetylated (K5, K8, K12, K16) histone H4 (Upstate Biotechnology, Charlottesville, VA) catalog #06-866, anti-diacetylated (K9, K14) histone H3 (Upstate Biotechnology, Charlottesville, VA) catalog #06-599, anti-dimethyl histone H3 lysine 4 (Upstate Biotechnology, Charlottesville, VA) catalog #07-030, anti-trimethyl histone H3 lysine 9 (Abcam Ltd., Cambridge, United Kingdom) catalog #ab8898, anti-Fra-1 R-20 clone (Santa Cruz Biotechnology, Santa Cruz, CA) catalog #sc-605, anti-c-Jun H79 clone (Santa Cruz Biotechnology, Santa Cruz, CA) catalog #sc-1694, anti-Neu C-18 clone catalog #sc-284 (Santa Cruz Biotechnology, Santa Cruz, CA), anti-Sp1 PEP 2 clone (Santa Cruz Biotechnology, Santa Cruz, CA) catalog #sc-59.

Samples were immunoprecipitated overnight at 4°C with constant rotation. The next day, antibody/protein/DNA complexes were isolated by adding 60μl of protein A agarose/sheared salmon sperm DNA to the samples followed by incubation for 2 hours at 4°C with constant rotation. Samples were then centrifuged at 100 X *g* for 1 minute in a tabletop microfuge. The supernatant was discarded and then the samples washed one time for 5 minutes at 4°C with constant rotation using 1ml of ice-cold low salt wash buffer (0.1% SDS, 1% Triton X-100, 2mM EDTA, 20mM Tris-HCl, pH 8.1, 150mM sodium chloride). Samples were then centrifuged at 100 X *g* for 1 minute in a tabletop microfuge to collect complexes. Supernatants were discarded and samples were subjected to a second wash for 5 minutes at 4°C with constant rotation using 1ml of ice-cold high salt wash buffer (0.1% SDS, 1% Triton X-100, 2mM EDTA, 20mM Tris-HCl, pH 8.1, 500mM sodium chloride). Samples were then centrifuged at 100 X *g* for 1

minute in a tabletop microfuge to collect complexes. Supernatants were discarded and samples washed a third time for 5 minutes at 4°C with constant rotation using 1ml of ice-cold lithium chloride wash buffer (0.25M lithium chloride, 1% NP-40, 1% sodium deoxycholate, 1mM EDTA, 10mM Tris-HCl, pH 8.1). Samples were then centrifuged at 100 X *g* for 1 minute in a tabletop microfuge to collect complexes. Supernatants were discarded and samples washed a fourth time for 5 minutes at 4°C with constant rotation using 1ml of ice-cold Tris/EDTA buffer (10mM Tris-HCl, 1mM EDTA, pH 8.0). Samples were centrifuged at 100 X *g* for 1 minute in a tabletop microfuge to collect complexes and washed a final time using 1ml of ice-cold Tris/EDTA buffer. Following this final wash, immunoprecipitated protein/DNA complexes were eluted off of the protein A agarose beads by vortexing samples with 250µl of 1% sodium dodecylsulfate/0.1M sodium bicarbonate followed by a 15 minute incubation at room temperature with constant rotation. Samples were centrifuged at 100 X *g* in a tabletop microfuge and the supernatant transferred into a new nuclease-free tube. The elution process was repeated a second time and eluted supernatants (500µl) combined. Input chromatin samples were thawed and diluted by adding 400µl of nuclease-free water. In order to reverse protein/DNA crosslinks, all samples received 20µl of 5M sodium chloride followed by incubation for at least 4 hours at 65°C. DNA was subsequently purified by extracting samples with an equal volume of phenol and then an equal volume of chloroform. DNA was precipitated by adding 2.5 volumes of ice-cold 100% ethanol and 20µg of glycogen. Samples were incubated for at least 5 hours at -20°C. Samples were then centrifuged at 16,000 X *g* for 30 minutes at 4°C in order to pellet DNA. Pellets

were washed once with 70% ethanol then air-dried. DNA was resuspended in 50µl of nuclease-free water for subsequent PCR analysis.

Chromatin immunoprecipitation PCR analysis of the SPARC proximal promoter region was conducted using the following two oligonucleotide primers: primer 1= 5' cagccctggcactctgtgagtcggt 3' corresponding to nucleotide position -257/-233 of the human SPARC promoter and primer 2= 5' ggcagtctgaaggaccgcgggaatggagg 3', corresponding to nucleotide position +27/-4 of the human SPARC promoter. PCR reactions consisted of 5µl of 10X Titanium™ Taq buffer (Clontech Corporation, Palo Alto, CA), 4µl of a dNTP mix (2.5mM each dATP, dTTP, dCTP, dGTP), 200ng each of primer 1 and primer 2, 0.5µl of Titanium™ Taq DNA polymerase (Clontech Corporation, Palo Alto, CA), and nuclease-free water in a reaction volume of 48µl. 2µl of immunoprecipitated DNA was added as the template for ChIP PCR. In addition, several dilutions of input DNA (non-immunoprecipitated sample) were analyzed by PCR under the same conditions in order to demonstrate that the reactions were conducted under non-saturating, semi-quantitative conditions. PCR was conducted using a Biometra T-Gradient Thermocycler as follows: step 1, 95°C for 3 minutes, step 2, 95°C for 1 minute, step 3, 68°C for 45 seconds, step 4, 68°C for 45 seconds. Steps 2-4 were repeated an additional 29-35 times depending on empirical determination of optimal cycle number for each sample so that reactions were analyzed within the linear range of PCR amplification. Reactions were subsequently cooled to 4°C and 15µl of each reaction was analyzed by agarose gel electrophoresis. 0.8% agarose gels in 1X TBE were prepared and stained with 1X GelStar® reagent (Cambrex Corporation, East Rutherford, NJ) in order to visualize PCR amplification products by ultraviolet transillumination at 312nm. Gel

images were captured using a Kodak DC40 digital camera equipped with an ethidium bromide filter. Images were analyzed by densitometry using Kodak 1D Digital Science imaging software in order to quantitate PCR amplicon signal intensities. For quantitation, pixel intensity values for individual immunoprecipitated samples signal intensity compared with input DNA signal on the same gel from the same batch of chromatin preparation. This was represented as fold enrichment relative to input DNA signal. Comparisons between cell lines were done by calculating differences in fold enrichment for each antibody. At least two independent chromatin preparations were analyzed for each immunoprecipitation.

In vitro methylation of plasmid DNA

Twenty units of recombinant HpaII methylase (New England Biolabs, Ipswich, MA) were used to methylate 10μg of SPARC promoter/pGL2-Basic luciferase reporter plasmid DNA in a reaction containing 1X HpaII methylase reaction buffer (New England Biolabs, Ipswich, MA), 80μM *S*-adenosyl methionine (New England Biolabs, Ipswich, MA) and nuclease-free water in a total reaction volume of 100μl. Samples were incubated at 37°C for 16 hours. After 4 hours, reactions were supplemented with fresh *S*-adenosyl methionine. The enzyme was then heat inactivated by incubating samples at 70°C for 10 minutes. DNA was then purified using Qiaquick Gel Extraction Kit (Qiagen Corporation, Valencia, CA) according to manufacturers instructions and eluted in nuclease-free water. Two, 500ng aliquots (estimated from input) of purified HpaII methylated DNA were subsequently digested using HpaII or MspI restriction enzymes to

determine the completeness of *in vitro* methylation. Two independent HpaII methylated plasmid preparations were tested.

In vitro methylation of gel shift probes

A gel shift probe spanning the region from –120/-83 of the human SPARC promoter was synthesized as described elsewhere in this section. Following probe quantitation, an equal amount of probe (as determined by liquid scintillation counting) was subjected to *in vitro* methylation using recombinant HpaII methylase (New England Biolabs, Ipswich, MA). A second aliquot of the probe was "mock" methylated in a reaction lacking HpaII methylase. Following methylation reactions, gel shift probes were phenol extracted once and purified using a Chromaspin-10 TE chromatography column (Clontech Corporation, Palo Alto, CA). Samples were re-quantitated by scintillation counting to determine cpm/μl of purified probe. Equal aliquots (25,000cpm/reaction) of mock and HpaII methylated gel shift probes were digested with 20 units of HpaII or MspI restriction enzymes in order to determine the efficiency of *in vitro* probe methylation. The ^{32}P labeled gel shift probes from these restriction enzyme digestion reactions were extracted once with an equal volume of phenol and purified using a Chromaspin-10 TE chromatography column (Clontech Corporation, Palo Alto, CA). Digested mock methylated and HpaII methylated probes were resolved on a non-denaturing polyacrylamide gel as described previously in this Chapter. The completeness of methylation was determined by comparing the molecular weight of the mock methylated probe and HpaII methylated probe digested with HpaII restriction enzyme. At least two independent preparations of HpaII methylated gel shift probes were assayed.

HpaII/MspI mapping of SPARC promoter methylation

Purified genomic DNA was separated into three separate 1μg aliquots. One aliquot was incubated with restriction enzyme digestion reaction mix without enzyme (designated as uncut). A second aliquot was digested with the restriction enzyme HpaII. A third aliquot was digested with the restriction enzyme MspI. Samples were digested at 37°C for 4 hours. Samples were then incubated for 10 minutes at 70°C to heat inactivate the enzymes. Reactions were diluted to 10ng/μl in nuclease-free water. A 2.5μl aliquot from each reaction was subjected to PCR using the following primer pairs:

SPARC promoter HpaII/MspI site #1:

Forward primer: 5' gaagccaaggcattcggattgcccaag 3'

Reverse primer: 5' gttttgagacagagtctcactcactc 3'

SPARC promoter HpaII/MspI site #2:

Forward primer: 5' gcctgggcgacagagtgagtga 3'

Reverse primer: 5' ggctgctgcctaaaccgactcac 3'

SPARC promoter HpaII/MspI site #3:

Forward primer: 5' catatataacaggagtgacccaag 3'

Reverse primer: 5' gctgtcctgaccaaacgtcccaacc 3'

SPARC promoter HpaII/MspI site #4:

Forward primer: 5' ggttgggacgtttggtcaggacagc 3'

Reverse primer: 5' gggcgtctgaaggaccgcgggaatgtggagg 3'

Primers were designed to flank individual HpaII/MspI restriction enzyme digestion sites. Polymerase chain reaction for SPARC was conducted using a Biometra T-Gradient thermocycler as follows: step one, 95°C for 3 minutes, step two, 95°C for 45

seconds, step 3, 68°C for 30 seconds, step 4, 68°C for 1 minute. Steps 2-4 were repeated for a total of 30 cycles. PCR reaction products were separated by agarose gel electrophoresis and visualized by GelStar® nucleic acid stain (Cambrex Corporation, East Rutherford, NJ) via ultraviolet transilluminatation at 312nm. A PCR reaction in which template was omitted was run with each sample set as a negative control. The expected PCR amplicon sizes for SPARC promoter HpaII/MspI site #1= 252 base pairs, SPARC promoter HpaII/MspI site #2= 847 base pairs, SPARC promoter HpaII/MspI site #3= 711 base pairs, SPARC promoter HpaII/MspI site #4= 180 base pairs.

5-aza-2'deoxycytidine and trichostatin A treatment of cells

A 5mM stock of 5-aza-2'deoxycytidine (Sigma-Aldrich Corporation, St. Louis, MO) was made fresh daily in sterile water and then filter sterilized using a 0.22μm syringe filter. Cells received fresh drug once daily for the indicated times and concentrations. A trichostatin A (Wako Chemicals USA, Incorporated, Richmond, VA) stock solution was prepared in 100% ethanol and stored at –20°C. When used in combination with 5-aza-2'deoxycytidine, trichostatin A was added at the end of the time course (the last 12-14 hours) at a final concentration of 100ng/ml. When trichostatin A was used alone, cells were incubated for 60 hours before the drug was added. As a negative control for trichostatin A experiments, parallel samples were treated with the same volume of 100% ethanol vehicle.

Genomic DNA isolation

Genomic DNA was isolated from MCF7 vector control cells and c-Jun/MCF7 cells using a Qiagen Genomic DNA Isolation Kit (Qiagen Corporation, Valencia, CA). Cells were seeded at a density of 1 X 10^6 cells/100mm tissue culture plate and harvested 48 hours later. Cells were washed twice with ice-cold phosphate buffered saline then collected using a plastic scraper. Samples were aliquoted into a 15ml conical tube and centrifuged at 1,500 X *g* for 10 minutes at 4°C. The cell pellet was resuspended in 500µl of ice-cold phosphate buffered saline. 500µl of ice-cold buffer C1 and 1.5mls of ice-cold distilled water was added to the sample to facilitate cell membrane lysis. Samples were mixed by inversion and incubated on ice for 10 minutes. Next, samples were centrifuged at 1,300 X *g* for 15 minutes at 4°C. The supernatant was discarded and 250µl of ice-cold buffer C1 was added followed by vortexing and centrifugation at 1,300 X *g* for 15 minutes at 4°C to remove cell debris. The supernatant was discarded followed by the addition of 1ml of buffer G2. Samples were vortexed vigorously for 30 seconds followed by the addition of 25µl of Qiagen protease or Qiagen proteinase K. Samples were then incubated at 50°C for 1 hour. During this time a Qiagen genomic DNA purification column 20/G was equilibrated using 1ml of buffer QBT. Samples were vortexed prior to adding to the purification column. Columns were then washed three times with 1ml of buffer QC. Genomic DNA was eluted from column using 1ml of buffer QT pre-warmed to 50°C. Elution was repeated a second time. DNA was precipitated by adding 1.4mls of 100% isopropanol at room temperature to the sample followed by vortexing. Samples were aliquoted equally into two, 2.0ml nuclease-free tubes and centrifuged at 16,000 X *g* at 4°C for 15 minutes in a refrigerated table-top microfuge. Each DNA pellet was

washed with 1ml of 70% ice-cold ethanol, vortexed and centrifuged at 16,000 X *g* for 10 minutes at 4°C. The supernatant was removed and DNA pellets were allowed to air-dry before resuspending samples in 50µl Tris-EDTA, pH 8.0. Samples were incubated overnight at 50°C and then quantitated by ultraviolet spectophotometry at a 260nm wavelength.

Cytosine methylation analysis using sodium bisulfite modification of genomic DNA

2µg of purified genomic was modified using the EZ DNA Methylation Kit™ (Zymo Research Corporation, Orange, CA) following the manufacturer's instructions. 1–2µg of high quality, purified genomic (free of RNA and protein) DNA was used for each bisulfite modification reaction. PCR primers used for bisulfite modified DNA amplification were designed using the MethPrimer program (http://www.ucsf.edu/urogene/methprimer/) (137). The primers used to amplify a 398 base pair region of the *SPARC* 5' promoter region (bisulfite modified) were as follows: primer 1= 5' tagttatagattgaatttttgtatttttt 3', primer 2= 5' attttattttaaaacaaaatctcactcactcta 3'. The primers used to amplify a 366 base pair region of the *SPARC* 3' promoter region (bisulfite modified) were as follows: primer 1= 5' ggttagaagattaagatatttgggtttg 3', primer 2= 5' caaaaaaccactcaaaactctaaactaa 3'. PCR reactions consisted of 5µl of 10X Titanium Taq buffer (Clontech Corporation, Palo Alto, CA), 4µl of a dNTP mix (2.5mM each dATP, dTTP, dCTP, dGTP), 200ng each of primer 1 and primer 2, 0.5µl of Titanium™ Taq DNA polymerase (Clontech Corporation, Palo Alto, CA), and nuclease-free water to a reaction volume of 48µl. 2µl of bisulfite modified genomic DNA was used as the template for PCR. Polymerase chain reaction was conducted using a Biometra T-

Gradient thermocycler as follows: step 1, 95°C for 3 minutes, step 2, 95°C for 45 seconds, step 3, 60°C for 45 seconds, step 4, 68°C for 1 minute. Steps 2-4 were repeated an additional 32 times. Reactions were subsequently cooled to 4°C and 15µl of each reaction was analyzed by agarose gel electrophoresis. 0.8% agarose gels in 1X TBE were prepared and stained with ethidium bromide in order to visualize PCR amplification products by ultraviolet transillumination at 312nm. PCR products were gel purified using a Qiaquick Gel Extraction Kit (Qiagen Corporation, Valencia, CA) following the manufacturer's instructions.

Purified PCR products were ligated into the T/A cloning plasmid, pGEMT-Easy (Promega Corporation, Madison, WI) and transformed into DH5 alpha electrocompetent *E. coli*. Individual clones were screened for the presence of an insert of the expected size by *Eco*RI restriction enzyme digestion. Plasmid DNA from positive clones was purified using the Qiagen Plasmid Spin Miniprep Kit (Qiagen Corporation, Valencia, CA) according to manufacturer's instructions and eluted in nuclease-free water. DNA from eight cloned PCR products was sequenced for each cell line. DNA sequences were aligned and compared to a reference SPARC promoter sequence (GenBank accession number X82259) in order to determine the methylation status of individual cytosine residues. Only DNA sequences demonstrating complete conversion of non-CpG cytosines were used for analysis.

DNA sequencing

DNA sequencing was performed by MWG Biotechnology and the University of Virginia Core DNA Sequencing Facility unless otherwise stated.

CHAPTER III

RESULTS

A. Effects of SPARC on MCF7 Cell Phenotype

The purpose of the experiments outlined in this section was to determine the extent to which SPARC gene expression influences MCF7 cell phenotype. SPARC gene expression has been correlated with a variety of tumor cell phenotypes including increased cell motility and invasion, decreased cell adhesion and inhibition of cell proliferation (101, 104, 105, 107, 123). However, little is known regarding the functional role of SPARC in regulating breast cancer cell phenotype. In order to gain a better understanding of these events, we used a MCF7 model system in which overexpression of the transcription factor c-Jun results in increased SPARC gene expression and phenotypic changes consistent with malignant progression (46, 51). Many of the alterations in cell phenotype induced by c-Jun are consistent with known functions of SPARC, such as increased cell invasiveness. Therefore, we sought to examine the contribution of SPARC using two approaches. The first was to overexpress SPARC in MCF7 cells in the absence of exogenous c-Jun overexpression. This approach would allow us to determine the extent to which SPARC expression is sufficient to induce alterations in cell phenotype. Our second approach was to inhibit SPARC gene expression in MCF7 cells stably expressing c-Jun. This strategy would allow us to determine the contribution of SPARC to c-Jun induced phenotypic changes. Characterization of these processes will provide a better understanding of the molecular mechanisms of breast cancer progression.

Cloning of the human SPARC protein coding region

In order to use a genetic approach to analyze the contribution of SPARC in MCF7 cell phenotype, we first needed to isolate an expressible human SPARC cDNA clone. To accomplish this goal, we conducted RT-PCR to specifically amplify the full-length human SPARC protein coding region. Total RNA from c-Jun/MCF7 cells, in which SPARC is abundantly expressed, was reverse transcribed. The SPARC cDNA was PCR amplified using a gene specific primer pair which flanked the translation start and stop codons. Restriction enzyme digestion sites were included at the 5' ends of each primer to facilitate directional cloning. The SPARC PCR amplification product was gel purified and cloned into the pGEM7-Zf+ plasmid. DNA sequencing confirmed the identity of the cloned PCR product as the full-length SPARC protein coding sequence (Fig. 5).

Expression of the cloned human SPARC gene by *in vitro* transcription/translation

In order to verify expression of the cloned SPARC gene we conducted *in vitro* transcription and translation as shown in Fig. 6. The SPARC/pGEM7-Zf+ plasmid was linearized with a restriction enzyme 3' of the stop codon and used as the template for *in vitro* transcription reaction using recombinant bacteriophage SP6 polymerase. The resulting SPARC RNA was *in vitro* translated using nuclease treated rabbit reticulocyte lysates in the presence of ^{35}S-methionine. A negative control mock translation reaction, in which template was omitted, was also conducted. *In vitro* translation products were resolved by sodium dodecyl sulfate-polyacrylamide gel electrophoresis (SDS-PAGE) followed by autoradiography in order to detect ^{35}S-methionine labeled SPARC protein. As shown in Fig. 6, analysis of *in vitro* translated SPARC reaction products revealed

ATG AGG GCC TGG ATC TTC TTT CTC CTT TGC CTG GCC GGG AGG
M R A W I F F L L C L A G R
GCC TTG GCA GCC CCT CAG CAA GAA GCC CTG CCT GAT GAG ACA
A L A A P Q Q E A L P D E T
GAG GTG GTG GAA GAA ACT GTG GCA GAG GTG ACT GAG GTA TCT
E V V E E T V A E V T E V S
GTG GGA GCT AAT CCT GTC CAG GTG GAA GTA GGA GAA TTT GAT
V G A N P V Q V E V G E F D
GAT GGT GCA GAG GAA ACC GAA GAG GAG GTG GTG GCG GAA AAT
D G A E E T E E E V V A E N
CCC TGC CAG AAC CAC CAC TGC AAA CAC GGC AAG GTG TGC GAG
P C Q N H H C K H G K V C E
CTG GAT GAG AAC AAC ACC CCC ATG TGC GTG TGC CAG GAC CCC
L D E N N T P M C V C Q D P
ACC AGC TGC CCA GCC CCC ATT GGC GAG TTT GAG AAG GTG TGC
T S C P A P I G E F E K V C
AGC AAT GAC AAC AAG ACC TTC GAC TCT TCC TGC CAC TTC TTT
S N D N K T F D S S C H F F
GCC ACA AAG TGC ACC CTG GAG GGC ACC AAG AAG GGC CAC AAG
A T K C T L E G T K K G H K
CTC CAC CTG GAC TAC ATC GGG CCT TGC AAA TAC ATC CCC CCT
L H L D Y I G P C K Y I P P
TGC CTG GAC TCT GAG CTG ACC GAA TTC CCC CTG CGC ATG CGG
C L D S E L T E F P L R M R
GAC TGG CTC AAG AAC GTC CTG GTC ACC CTG TAT GAG AGG GAT
D W L K N V L V T L Y E R D
GAG GAC AAC AAC CTT CTG ACT GAG AAG CAG AAG CTG CGG GTG
E D N N L L T E K Q K L R V
AAG AAG ATC CAT GAG AAT GAG AAG CGC CTG GAG GCA GGA GAC
K K I H E N E K R L E A G D
CAC CCC GTG GAG CTG CTG GCC CGG GAC TTC GAG AAG AAC TAT
H P V E L L A R D F E K N Y
AAC ATG TAC ATC TTC CCT GTA CAC TGG CAG TTC GGC CAG CTG
N M Y I F P V H W Q F G Q L
GAC CAG CAC CCC ATT GAC GGG TAC CTC TCC CAC ACC GAG CTG
D Q H P I D G Y L S H T E L
GCT CCA CTG CGT GCT CCC CTC ATC CCC ATG GAG CAT TGC ACC
A P L R A P L I P M E H C T
ACC CGC TTT TTC GAG ACC TGT GAC CTG GAC AAT GAC AAG TAC
T R F F E T C D L D N D K Y
ATC GCC CTG GAT GAG TGG GCC GGC TGC TTC GGC ATC AAG CAG
I A L D E W A G C F G I K Q
AAG GAT ATC GAC AAG GAT CTT GTG ATC **TAA**
K D I D K D L V I STOP

Fig. 5. Summary of the human SPARC protein coding sequence. 912 base pair nucleic acid sequence of human SPARC protein coding sequence (GenBank accession number NM_003118) and predicted 303 residue amino acid sequence. Single letter amino acid abbreviations correspond to IUPAC designation.

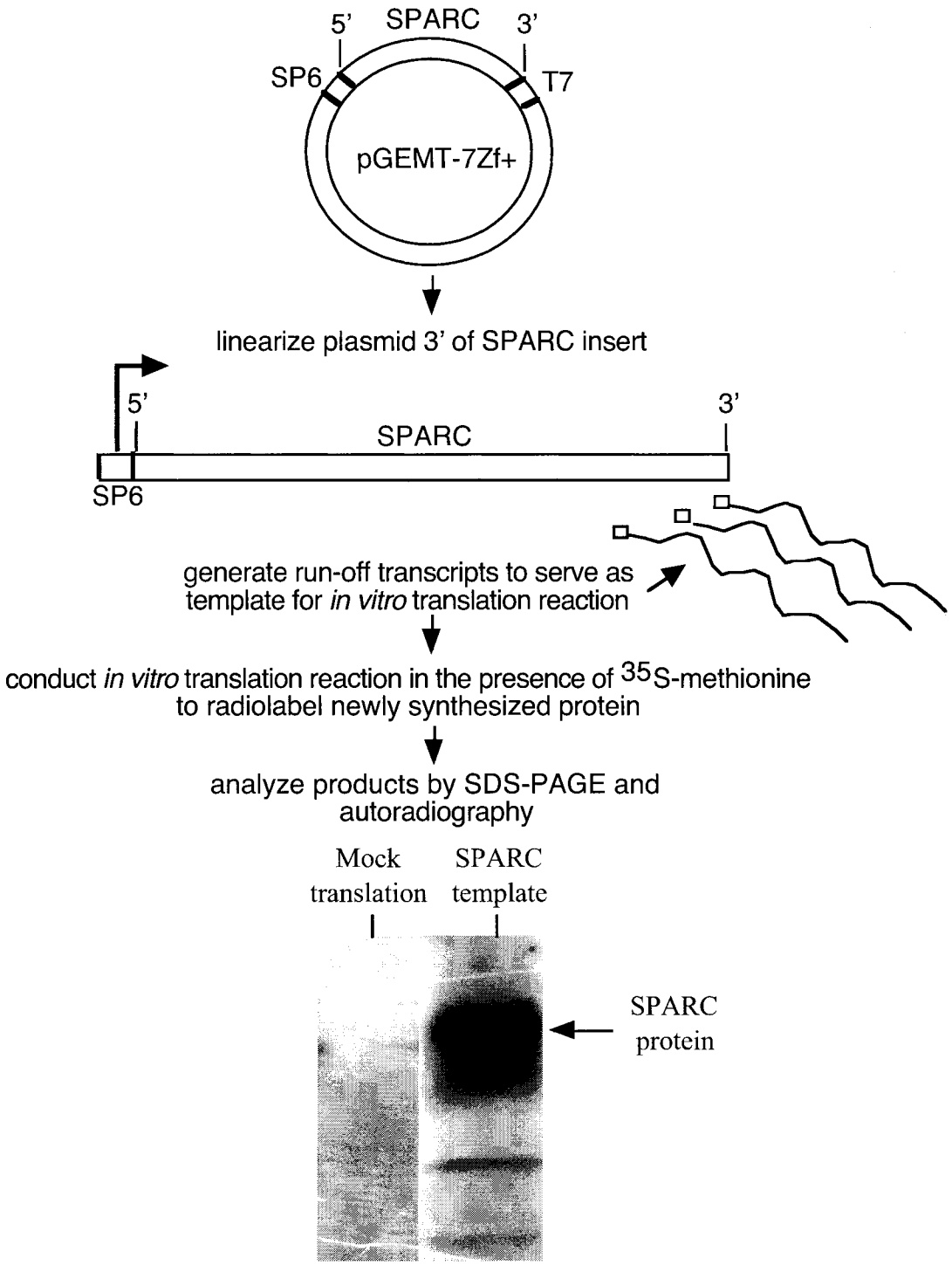

Fig. 6. Expression of cloned human SPARC by *in vitro* transcription/translation. *In vitro* translation rabbit reticulocyte lysate ^{35}S-methionine *in vitro* transcribed RNA no RNA template (mock translation) detected by autoradiography. SPARC protein coding sequence cloned into pGEM7Zf+ plasmid, linearized, *in vitro* transcribed using recombinant bacteriophage SP6 RNA polymerase.

expression of a 34kDa protein. This molecular weight is consistent with SPARC protein that has not been post-translationally modified. *In vivo*, SPARC has been shown to undergo *N*-linked glycosylation at amino acid 99 (Asn) which results in a higher molecular weight protein product (112, 138, 139). However, *in vitro* synthesis of SPARC protein using rabbit reticulocyte lysates is not expected to result in a glycosylated product. A second, lower molecular weight protein present in the SPARC reaction may have been generated from an alternate translation start site, since the band is not present in the mock translation reaction. To our knowledge, there have been no reports of alternate start site usage for SPARC *in vivo*, therefore this lower molecular weight product is most likely an *in vitro* artifact. Based on DNA sequencing (Fig. 5) and *in vitro* transcription/translation analysis (Fig. 6), we conclude that we successfully isolated a full-length, expressible human SPARC cDNA.

Generation of MCF7 stable cell lines constitutively expressing SPARC

Next we sought to generate MCF7 cell lines stably expressing SPARC in order to analyze its role in modulating the MCF7 phenotype. To accomplish this goal, we used retroviral mediated gene transfer to introduce the SPARC gene expression cassette into MCF7 cells. This strategy was chosen over direct transfection of a SPARC mammalian expression plasmid for two main reasons. First, the efficiency of gene transfer using retroviral gene delivery is much higher compared to standard transfection of plasmid DNA. Second, integration of the transgene into the host cell genome is much more efficient due to the presence of viral long terminal repeat (LTR) sequences. A schematic representation of our experimental approach is outlined in Fig. 7. The SPARC protein

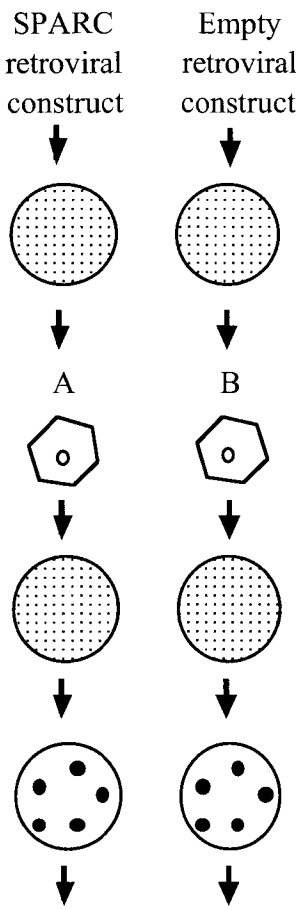

1.) Transfect retroviral constructs into PT67 packaging cell line

2.) Harvest replication deficient retroviruses

A.) SPARC expressing retrovirus

B.) Negative control retrovirus

3.) Infect MCF7 cells

4.) Start antibiotic selection

5.) Ring clone individual antibiotic resistant colonies and assay for SPARC mRNA and protein expression

6.) Assay stable cell clones in phenotype assays (cell proliferation, *in vitro* cell motility and invasion)

Fig. 7. Experimental approach for generating SPARC/MCF7 stable cell lines.

coding region was subcloned into the retroviral expression plasmid, LPCX. This plasmid was transfected into the PT67 packaging cell line to generate infectious, replication deficient retrovirus. In parallel, a negative control retrovirus, without the SPARC gene insert, was also generated. The PT67 packaging cell line stably expresses viral *gag*, *pol* and *env* genes required for virus assembly (140). The LPCX plasmid transfected into these cells provided the viral packaging signal sequence. Virus was harvested from PT67 tissue culture media and then used to infect MCF7 cells. Following infection, MCF7 cells were grown in the presence of the antibiotic puromycin to allow for positive selection of cells containing the stably integrated SPARC or empty vector control gene expression cassettes. Individual antibiotic resistant stable cell colonies were ring cloned and assayed for SPARC expression. Expression of the SPARC transgene is regulated via the cytomegalovirus major immediate early gene promoter. As a result, SPARC is constitutively expressed at high levels in stable cell clones.

Fig. 8 shows semi-quantitative RT-PCR analysis of steady state SPARC mRNA levels in three independently isolated stable SPARC/MCF7 cell clones. These results indicate that SPARC expression in each of the three clones was comparable to the levels observed in c-Jun/MCF7 cells. Next, SPARC protein expression was analyzed by Western blot analysis of whole cell lysates using a SPARC specific antibody (Fig. 8). The molecular weight of SPARC protein was estimated to be 43kDa, consistent with published reports and consistent with SPARC expressed in c-Jun/MCF7 cells (111, 125, 141). A higher molecular weight band was occasionally observed and may represent non-specific background due to insufficient washing during the Western blot procedure. Based on the results presented in Fig. 8, we conclude that three independent

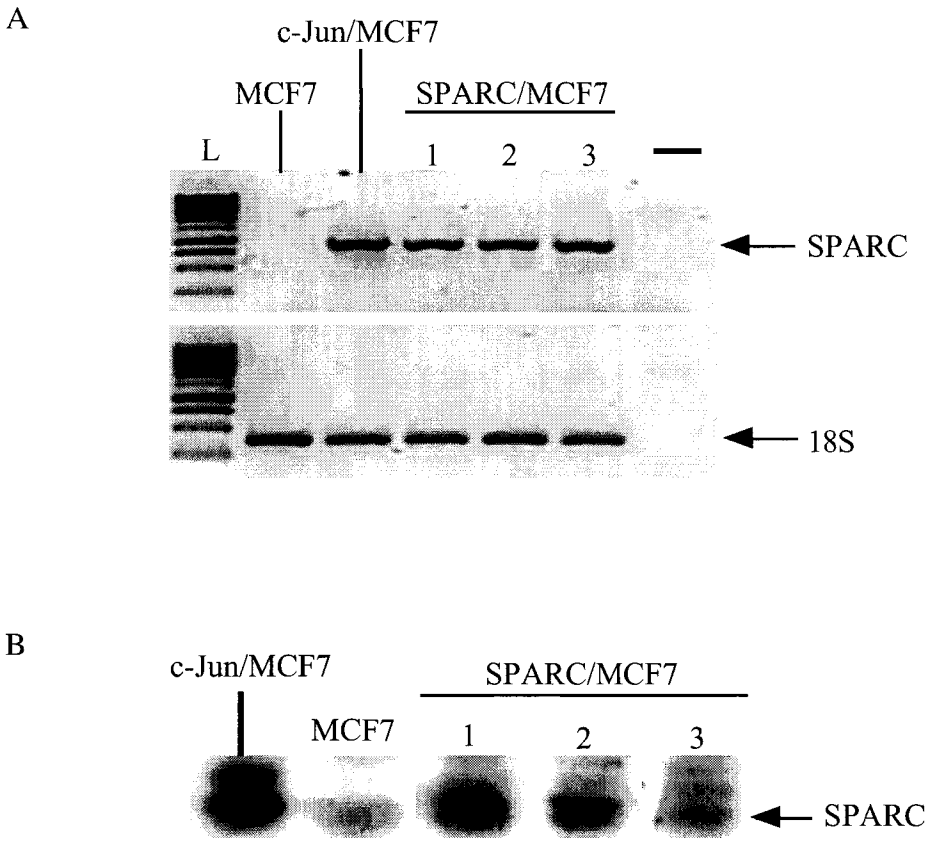

Fig. 8. Analysis of SPARC mRNA and protein expression in SPARC/MCF7 stable cell lines. *A*, Semi-quantitative RT-PCR demonstrating SPARC mRNA levels in three independent SPARC/MCF7 stable clones (1, 2, 3) using the 18S ribosomal subunit as an internal control (L= DNA molecular weight marker). *B*, Western blot analysis of SPARC protein levels in three independent SPARC/MCF7 stable cell clones using a SPARC specific antibody. Equal amounts of protein (50μg) were loaded in each lane.

SPARC/MCF7 stable cell clones were isolated that express levels of SPARC mRNA and protein comparable to c-Jun/MCF7 cells and would, therefore, be good candidates for phenotypic characterization.

Effect of stable overexpression of SPARC on MCF7 cell proliferation

Increased SPARC expression has been shown to influence a variety of cell phenotypes (101-107). For example, increased expression of SPARC is known to inhibit cell cycle progression resulting in a decrease in cell proliferation (141, 142). Interestingly, we observe a similar phenotype in c-Jun/MCF7 cells in which SPARC mRNA and protein levels are dramatically elevated (46, 51). Therefore, we hypothesized that SPARC may contribute to decreased cell proliferation in our MCF7 model system.

In order to determine if SPARC overexpression, alone, was sufficient to alter the rate of MCF7 cell proliferation, we conducted non-radioactive cell proliferation assays (MTT assays). The MTT assay is a colorimetric assay based on cellular conversion of MTT (3-[4,5-dimethylthiazol-2-yl]-2,5-diphenyl) tetrasodium bromide dye to an insoluble, blue formazan reaction product (143). The degree of color change in each sample has been shown to be directly proportional to cell number (143, 144).

Vector control/MCF7, c-Jun/MCF7 and SPARC/MCF7 stable cell lines were initially maintained in serum-free conditions for 24 hours in order to promote quiescence. Cells were then trypsinized, counted and plated at an equivalent density in complete media containing 10% fetal bovine serum. MTT reactions were quantified by measuring the optical density (OD) of each sample at 24 hour intervals for a total of 96 hours. Results were analyzed by linear regression analysis to determine the slope of a best-fit

line between each optical density reading for each cell line. Proliferation rates for c–Jun/MCF7 and SPARC/MCF7 cells were then expressed relative to vector control/MCF7 cells.

As shown in Fig. 9, the three SPARC/MCF7 stable cell lines exhibited a statistically significant decrease in cell proliferation rate compared to vector control MCF7 cells ($P = <.05$). These results are consistent with previous reports which demonstrated that overexpression of SPARC in the breast cancer cell line, MDA–MB–231, resulted in a decrease in the cell proliferation rate (142). However, SPARC/MCF7 cell lines failed to fully recapitulate the cell proliferation defects induced by c-Jun overexpression. One explanation for this difference is that other c-Jun target genes contribute to regulation of cell proliferation. Consistent with this notion, we have previously shown that overexpression of c-Jun results in altered expression of several cell cycle genes including $p16^{INK4a}$ and $p21^{CIP1/Waf1}$ (51).

Analysis of *in vitro* cell motility and invasion in SPARC/MCF7 stable cell lines

As stated previously, increased SPARC expression is associated with increased cell motility and invasion during wound healing, tissue remodeling and tumorigenesis (101-107). Consistent with these observations, we have previously shown that MCF7 cells overexpressing c-Jun exhibit a dramatic increase in *in vitro* cell motility and invasion (46). In order to determine if SPARC overexpression, alone, was sufficient to induce cell motility and invasion we assayed SPARC/MCF7 stable cell lines using a modified Boyden chamber assay. This assay measures the ability of cells to migrate through a porous membrane in response to a chemotactic stimulus (145).

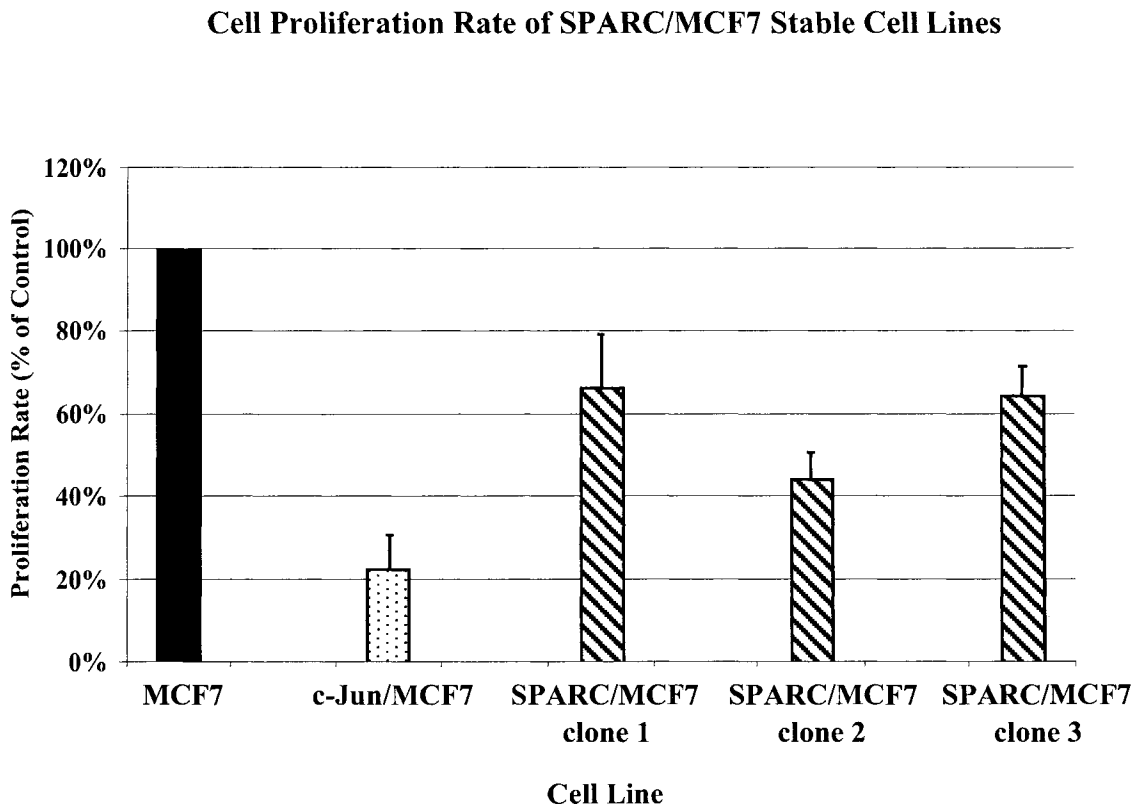

Fig 9. Effect of stable SPARC expression on MCF7 cell proliferation. Cell proliferation rates were determined by MTT assay. The indicated cells lines were plated at the same density in 96-well plates. Samples were assayed at 24, 48, 72 and 96 hours. Optical densities were determine using a microtiter plate reader rate determined slope of the line. Clone 1, 2 and 3 represent three independent SPARC/MCF7 stable cell lines. The cell proliferation rate of vector control/MCF7 cells was set at 100%. The proliferation rate of c-Jun/MCF7 and SPARC/MCF7 cells is expressed as a percentage of MCF7.

An equal number of vector control MCF7, c-Jun/MCF7 and three SPARC/MCF7 stable cell lines were suspended in serum-free growth media and added to the upper portion of a modified Boyden chamber. These cells were separated from the bottom chamber of the apparatus by a gelatin coated porous membrane. The lower chamber contained NIH3T3 conditioned media which served as the chemotactic stimulus. As a result, cells with the capacity to respond positively to the chemoattractant migrated through the pores, ultimately attaching to the underside of the membrane. Following a short (4-5 hour) incubation, the apparatus was disassembled and the cells were stained. Cells remaining on the upper portion of the membrane, which did not migrate through pores, were wiped away and the cells on the bottom were counted using an inverted microscope. Cells in multiple fields of view were counted in order to control for localized variation in cell distribution as well as variations in membrane coating.

In vitro cell invasion assays were conducted in a similar manner to the motility assays. The main difference was that membranes were coated first with collagen IV and then with Matrigel^{TM}. Matrigel^{TM} is a complex mixture of extracellular matrix (ECM) components obtained from Engelbroth-Holm-Swarm (EHS) mouse sarcoma cell cultures (146). This mixture polymerizes on the membrane and forms a barrier that cells must proteolytically degrade in order to migrate through the pore. Therefore, this *in vitro* invasion assay is a measure of a cell's ability to both degrade extracellular matrix components and move in a directional manner. As shown in Fig. 10, SPARC/MCF7 stable cell lines showed no significant difference in motility or invasion when compared to vector control/MCF7 cells. These results suggest that other cellular changes induced by c-Jun are required for acquisition of these phenotypes.

A

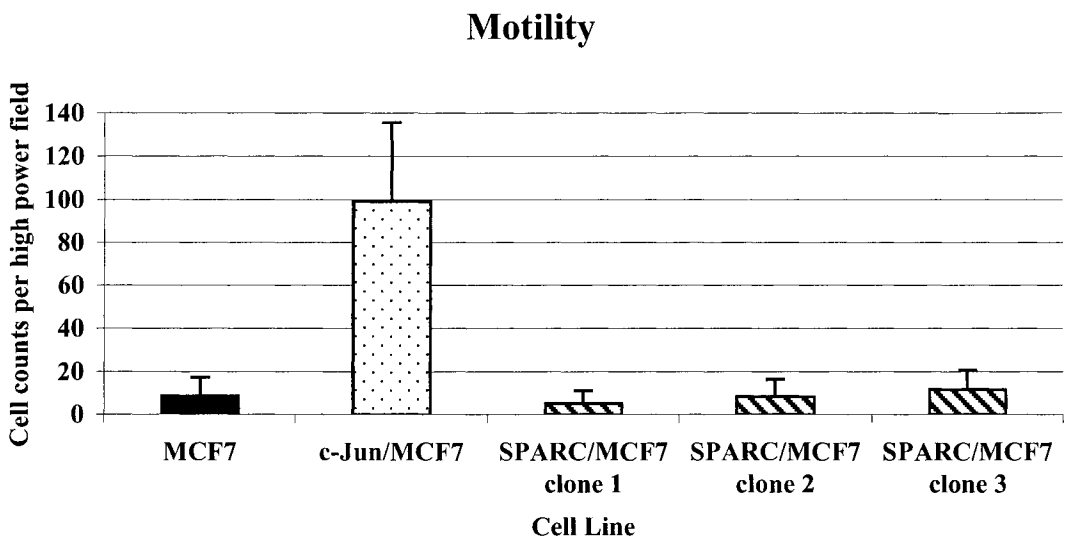

B

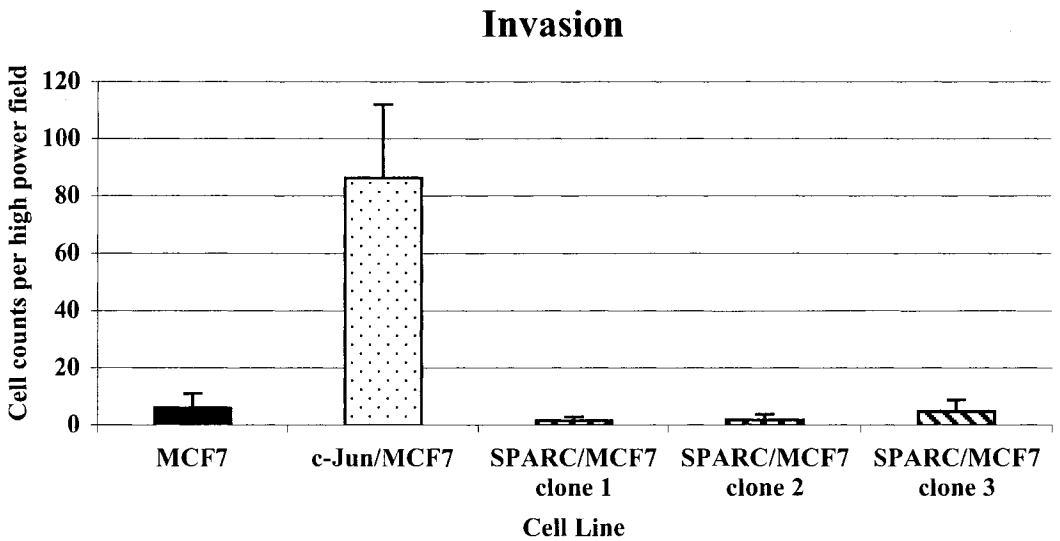

Fig. 10. Analysis of *in vitro* cell motility and invasion demonstrated by SPARC/MCF7 stable cell lines. *A*, Quantitation of cell motility assays done on gelatin coated membranes over a four hour incubation period. *B*, Quantitation of cell invasion assays conducted on Matrigel™ coated membranes over a period of four hours. Each motility and invasion experiment was conducted at least three times. All values are expressed as number of stained cells per high-powered field.

Analysis of the effect of SPARC inhibition on c-Jun induced cell motility and invasion in MCF7 cells

In order to determine if SPARC is involved in migration and invasion exhibited by c-Jun/MCF7 cells we developed a means for its specific suppression. A previous study examining the role of SPARC in human melanoma showed that antisense inhibition of SPARC expression diminished cell adhesion and invasiveness *in vitro* and abrogated tumor formation in mice *in vivo* (126). Therefore, we chose to adopt a similar strategy to determine the contribution of SPARC to c-Jun induced cell motility and invasion in a MCF7 breast cancer model system.

In order to express antisense SPARC in c-Jun/MCF7 cells we constructed replication deficient adenovirus expressing the SPARC cDNA in the antisense orientation. We chose an adenovirus based strategy for gene delivery because this method is more efficient compared to standard transfection procedures. This method results in transient, high levels of expression of the gene of interest. Using this method, we were able to demonstrate 90% of c-Jun/MCF7 cells expressing the control gene beta-galactosidase (Appendix A, Fig. 41). Although this method is limited to transient gene expression, it is still suitable for *in vitro* cell motility and invasion assays because these are short-term assays (4-5 hours). A schematic diagram of our experimental approach is outlined in Fig. 11.

Recombinant, replication deficient adenovirus was produced in the human embryonic kidney cell line, HEK293. These cells stably expresses the adenovirus E1 genes necessary for viral replication (147, 148). Virus was harvested from HEK293 cells and used to infect c-Jun/MCF7 cells. Infection of c-Jun/MCF7cells with an adenovirus

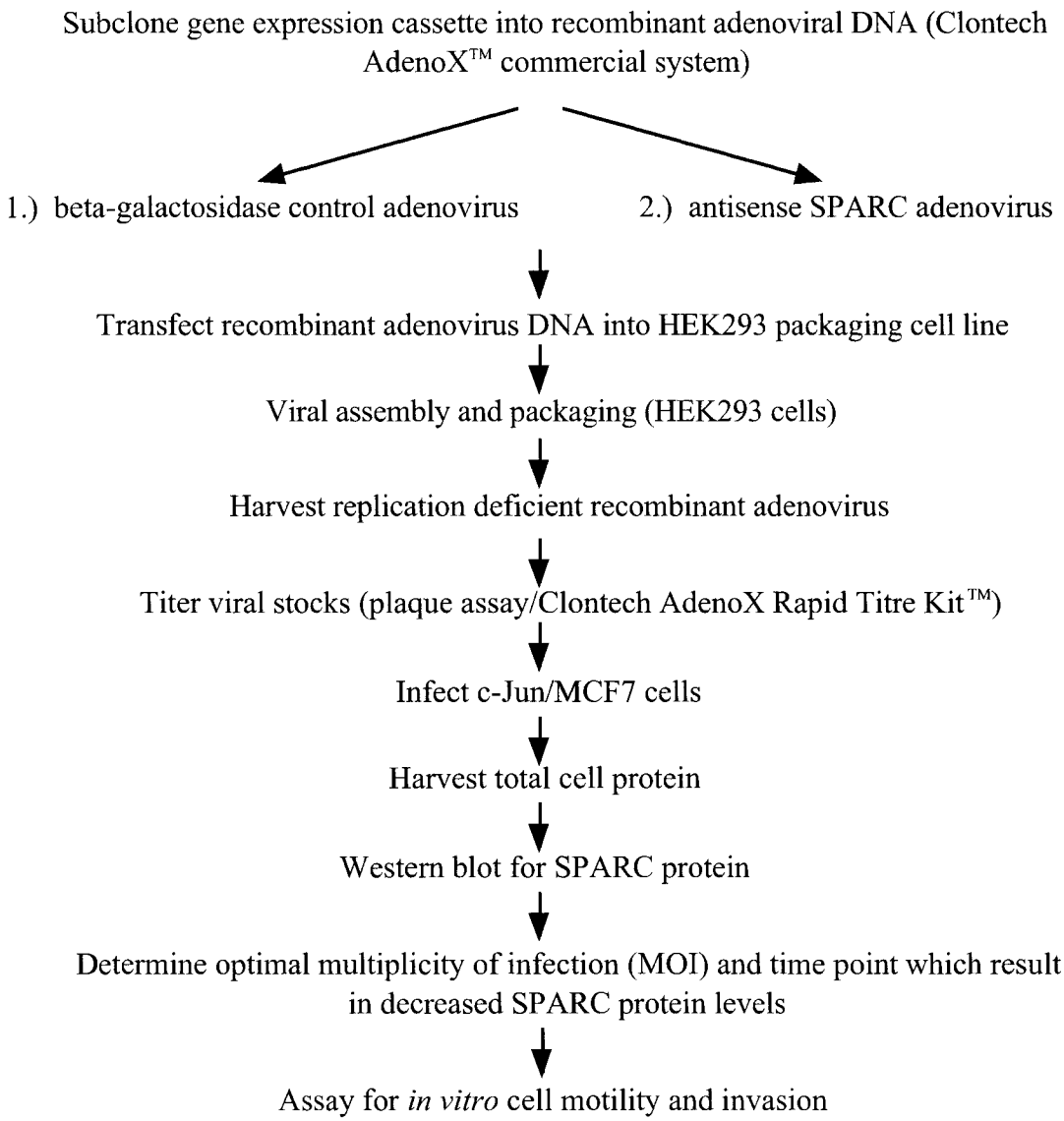

Fig. 11. Experimental approach for suppression of SPARC protein expression using antisense SPARC adenovirus.

expressing the beta-galactosidase gene product was used to determine the optimal multiplicity of infection (MOI) in which most cells became infected without showing cytotoxic effects. This MOI was subsequently used to infect c-Jun/MCF7 cells with the adenovirus expressing SPARC in the antisense orientation. SPARC protein expression was subsequently analyzed by Western blot at 12, 30, 48 and 72 hours post-infection. Fig. 12 demonstrates a marked inhibition in SPARC protein expression 24 hours following infection (MOI=5) with antisense SPARC adenovirus. This time point and MOI was subsequently used to assess motility and invasion of c-Jun/MCF7 cells.

As shown in Fig. 13, c-Jun/MCF7 cells expressing antisense SPARC were significantly less motile than cells infected with the same MOI of control adenovirus. Additionally, c-Jun/MCF7 cells infected with the SPARC antisense virus demonstrated a 70% decrease in invasive capacity when compared to control infected cells. Taken together, these results are consistent with a mechanism by which SPARC upregulation, in response to c-Jun, is a pivotal event leading to the induction of motility and invasion in c–Jun/MCF7cells.

Development of a RNAi mediated approach for stable SPARC inhibition in c–Jun/MCF7 cells

As a follow-up to the transient antisense SPARC studies described above, we sought to develop a system for stable inhibition of SPARC expression in c-Jun/MCF7 cells for future *in vivo* studies. Recent breakthroughs have uncovered a novel approach, termed RNA interference (RNAi), for potent and specific inhibition of gene expression (149-151). Expression of short, 19-23 base pair, small interfering RNAs (siRNAs) has

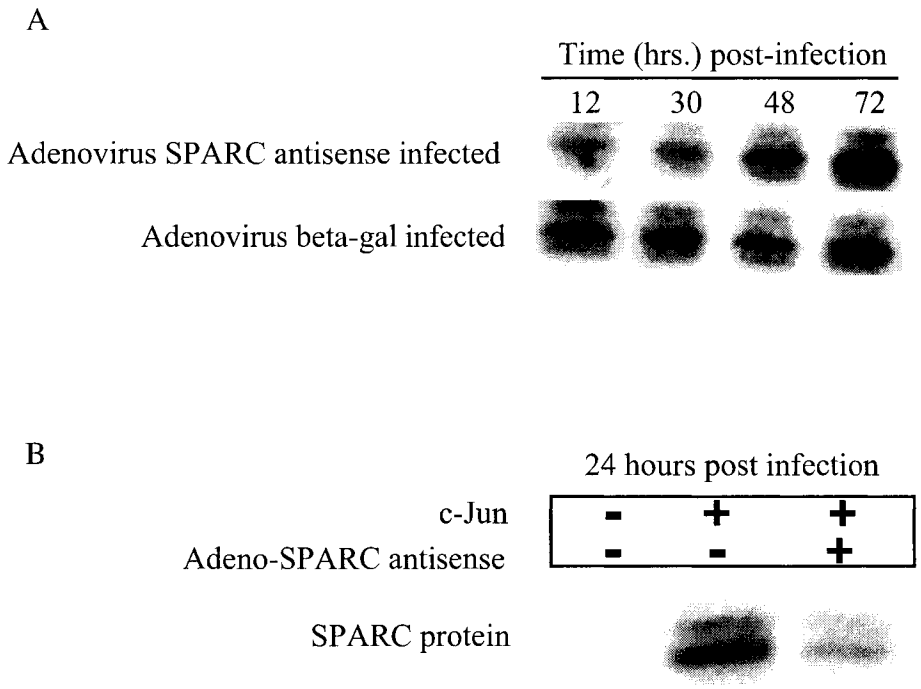

Fig. 12. Analysis of SPARC expression in c-Jun/MCF7 cells infected with antisense SPARC adenovirus. *A*, Western blot analysis of SPARC protein expression at 12, 30, 48 and 72 hours following infection with adenovirus expressing SPARC in the antisense orientation or control adenovirus expressing the beta-galactosidase gene (MOI= 5) in c-Jun/MCF7 cells. *B*, Western blot demonstrating SPARC expression in c-Jun/MCF7 cells 24 hours post-infection with antisense SPARC expressing adenovirus. Equal amounts of total protein (50μg) were loaded in each lane.

A

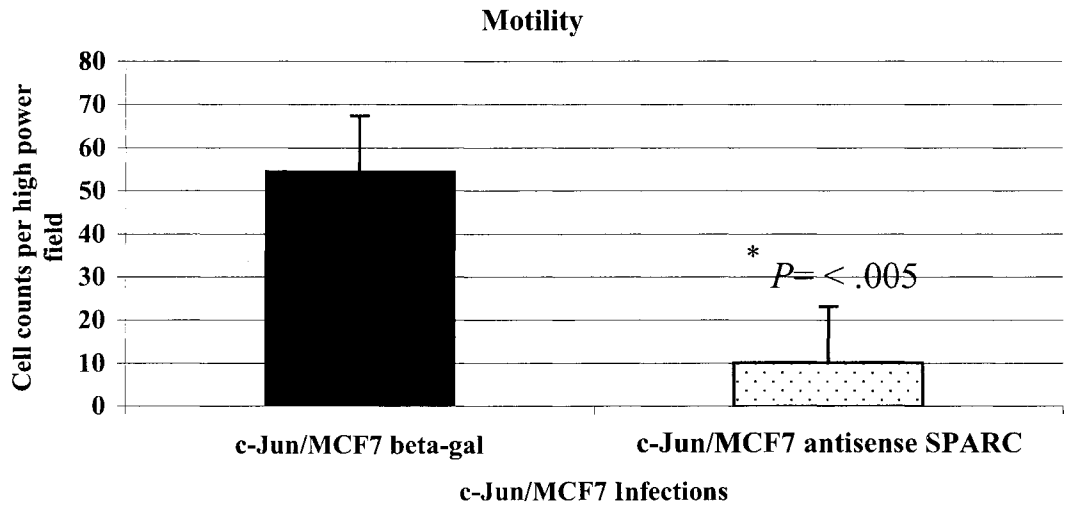

B

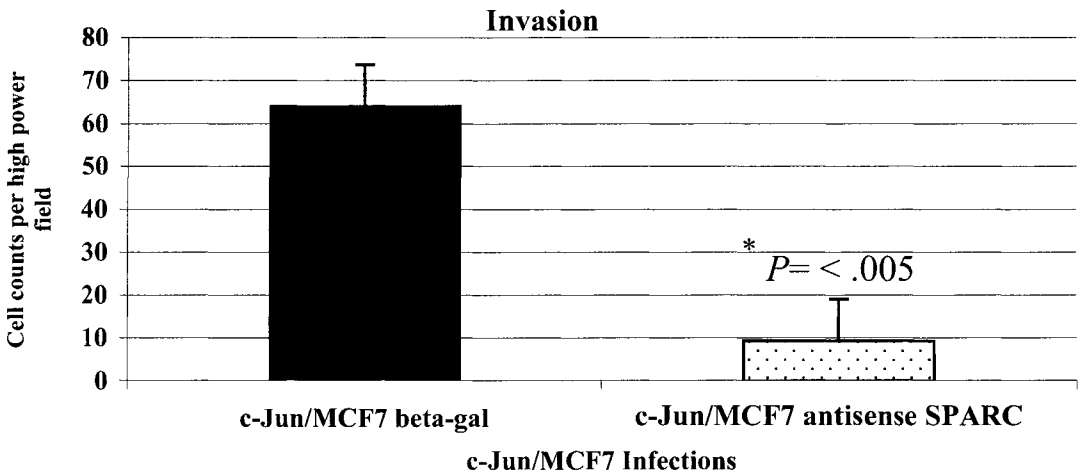

Fig. 13. Analysis of c-Jun/MCF7 *in vitro* cell motility and invasion following antisense inhibition of SPARC expression. *A*, Quantitation of cell motility assays done on gelatin coated membranes over a 4 hour incubation period. *B*, Quantitation of cell invasion assays conducted on Matrigel™ coated membranes over a period of 4 hours. Each infection and motility/invasion assay was repeated at least three times and verified using different viral stocks to control for variability in virus preparations. All values are expressed as number of stained cells counted per high-powered field. Statistics were evaluated using ANOVA (P=<.005).

been shown to promote degradation of complementary cellular mRNAs (149, 150, 152, 153). This process occurs via activation of an RNAi nuclease complex termed the RNA induced silencing complex (RISC). RISC binds to short, double stranded RNA molecules leading to enzymatic degradation of target mRNA thereby decreasing steady state levels (149, 154). A schematic representation of our strategy to inhibit SPARC expression using RNAi is shown in Fig. 14.

One drawback to this method is that it is difficult to predict which sequences will activate the cellular RISC complex. Therefore, we designed four unique siRNA expression cassettes targeted to different regions of the human SPARC mRNA. These expression cassettes were then cloned into the pSilencer-H1-hygro plasmid. This plasmid expresses the siRNA sequences under the control of a RNA polymerase III gene promoter (H1 promoter) which has been shown to promote efficient transcription of short RNA species (34, 155). In addition, the pSilencer-H1-hygro plasmid contains the hygromycin resistance gene allowing for positive selection of stable cell clones. Separate plates of c-Jun/MCF7 cells were transfected with individual SPARC siRNA expression plasmids followed by selection with hygromycin. Hygromycin resistant cells were pooled and maintained as stable cell populations. These cell populations were then analyzed by Western blot to determine SPARC protein levels (Fig. 14). Three of four siRNA sequences designed to inhibit SPARC expression dramatically lowered steady-state levels of SPARC protein. Importantly, levels of c-Jun protein remained unchanged (Fig. 14). Therefore, we conclude from these experiments that we have successfully developed a reagent suitable for inhibiting SPARC protein expression allowing for long-term *in vivo* analysis of these cells. This RNAi approach for SPARC "knock-down" was

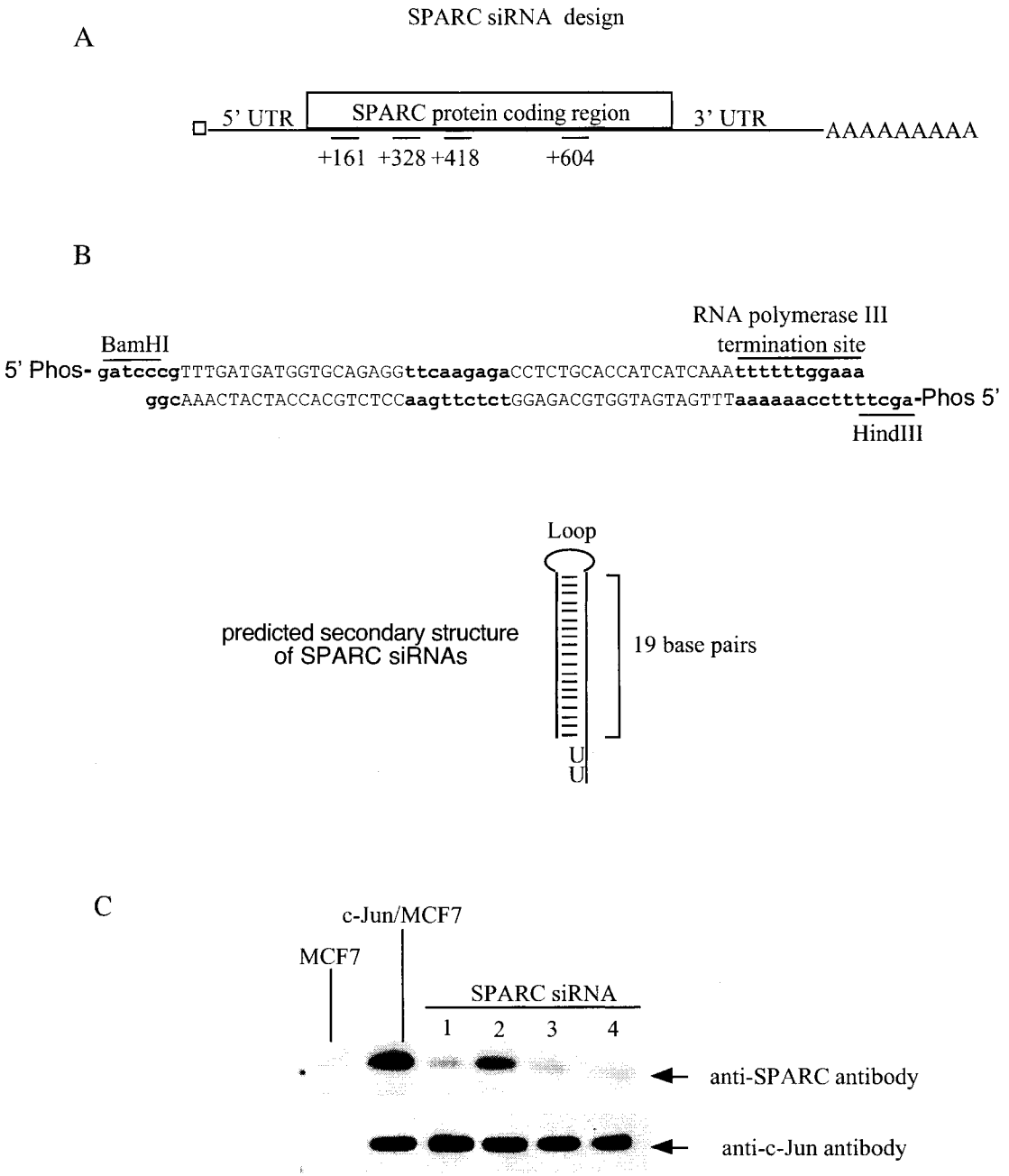

Fig. 14. Experimental approach and characterization of human SPARC specific RNAi. *A*, Schematic representation of the regions of SPARC mRNA targeted by individual siRNA sequences. *B*, Design of siRNA sequences and predicted secondary structure of siRNA transcripts. *C*, Western blot analysis of SPARC protein expression in c-Jun/MCF7 cells stably expressing individual SPARC siRNA sequences (1= +161, 2= +328, 3= +418, 4= +604).

more dramatic than the results we obtained using the antisense SPARC adenovirus. This is likely due to the fact that RNAi promotes active degradation of mRNA in contrast to the antisense SPARC adenovirus.

In summary, the objective of Aim 1 was to determine the role of SPARC gene expression on MCF7 cell phenotype. We addressed this objective by cloning the human SPARC gene and expressing it in MCF7 cells to assess the role of SPARC in the absence of exogenous c-Jun expression. In addition, we expressed SPARC in the antisense orientation in c-Jun/MCF7 cells in order to inhibit SPARC protein expression. This allowed us to examine the contribution to c-Jun induced invasive phenotype. Our conclusions from these experiments were: 1.) SPARC overexpression in MCF7 cells results in a significant decrease in cell proliferation rate 2.) overexpression of SPARC, alone, is not sufficient to promote cell motility and invasion of MCF7 cells and 3.) suppression of SPARC in c-Jun/MCF7 cells significantly inhibits cell motility and invasion. The results presented in this section establish SPARC as a phenotypically relevant c-Jun target gene which contributes to a pro-invasive breast cancer cell phenotype. However the mechanism(s) of SPARC gene regulation by c-Jun had yet to be examined and served as the focus of Aim 2.

B. Mapping the c-Jun Responsive Region of the SPARC Promoter

The experiments described in Aim 1 established that SPARC is a phenotypically relevant c-Jun target gene. Next, we were interested in determining the mechanism(s) by which SPARC gene expression is regulated. In order to address this issue, we examined SPARC promoter activity by transient transfection and promoter/reporter assays. In addition, we characterized protein/DNA interactions involving the SPARC promoter using nuclear extracts from MCF7 and c-Jun/MCF7 cell lines. The studies conducted in Aim 2 sought to identify *cis* regulatory elements of the SPARC promoter which confer c–Jun responsiveness in the context of a MCF7 breast cancer model system.

Analysis of SPARC promoter activity in vector control/MCF7, JunD/MCF7 and c–Jun/MCF7 stable cell lines

The human SPARC promoter was originally described as a 1409 base pair sequence 5' of the major transcriptional start site (129). This sequence was shown to exhibit activity by transient promoter/reporter assays in multiple cell lines including HEK293, HeLa, HepG2, Tera-2 and HT1080 cells (129). Analysis of the human SPARC promoter sequence revealed the presence of three AP-1 like sites which deviate from the consensus context (TGAC/GTCA) by a single nucleotide (Fig. 15). Previous studies conducted by our laboratory have shown that c-Jun/AP-1 is capable of binding to AP-1 like sequences *in vitro* (80). Therefore, we hypothesized that c-Jun may bind to one, or more, of these sites as a means of positively regulating SPARC promoter activity.

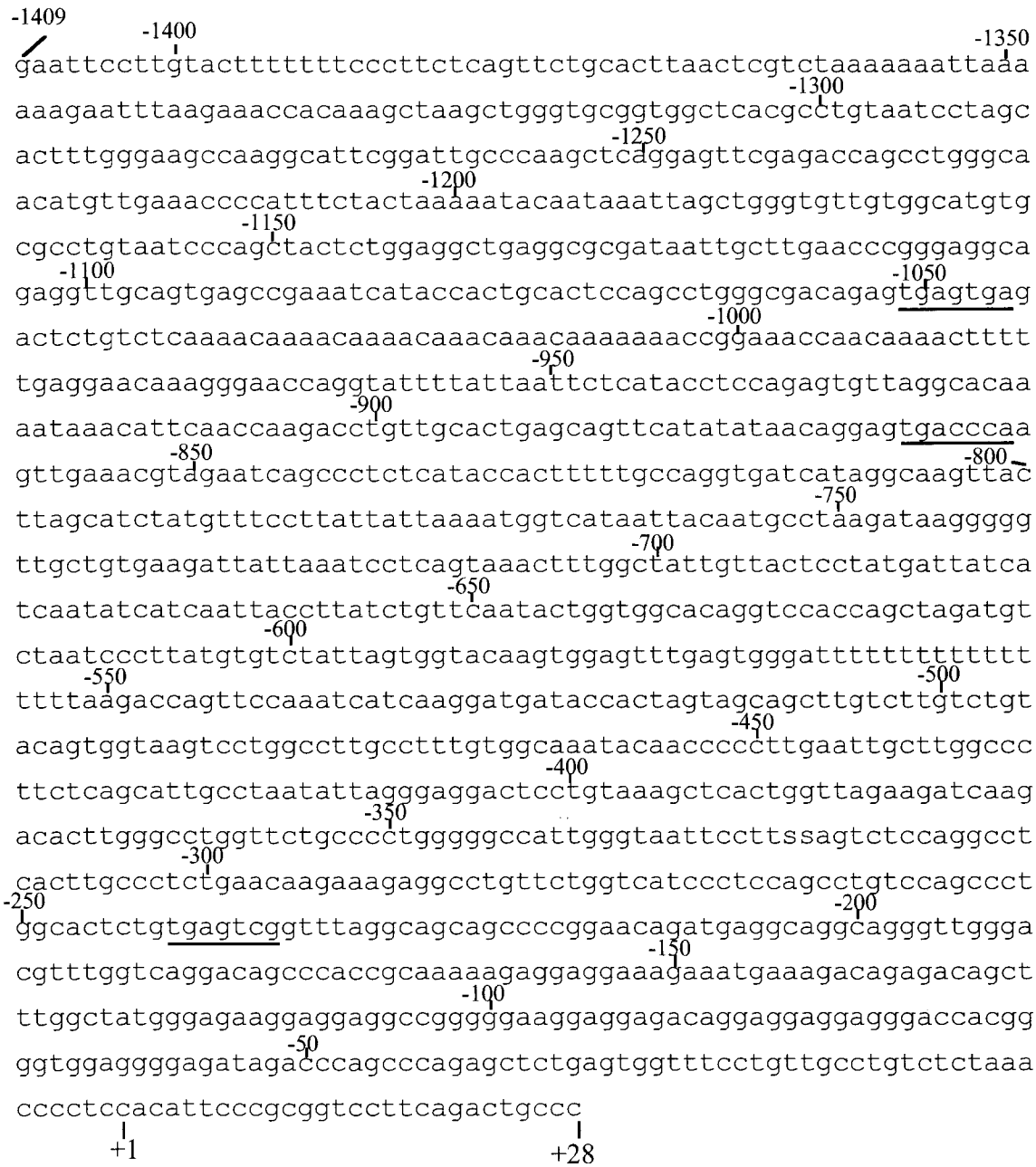

tgagtga= AP-1 "like" site (-1051/-1045)
tgaccca= AP-1 "like" site (-868/-862)
tgagtcg= AP-1 "like" site (-241/-235)

Consensus AP-1 binding site= tgag/ctca

Fig. 15. The DNA sequence of the human SPARC gene promoter. +1 denotes the transcription start site. +2 through +28 denotes additional sequence from the SPARC gene 5' untranslated region and is present in the SPARC promoter/luciferase reporter plasmids used in these studies. AP-1 "like" sites are underlined.

In order to quantify promoter activity, we assayed the human SPARC promoter cloned immediately upstream of the firefly luciferase reporter gene (generous gift from Dr. Marc Castellazzi). This plasmid was transiently transfected into two independent vector control/MCF7, c-Jun/MCF7 and JunD/MCF7 stable cell lines. JunD/MCF7 cells were used in order to determine the extent to which SPARC upregulation was specific to c-Jun. Forty-eight hours after transfection, cellular protein was assayed for luciferase enzyme activity as a measure of SPARC promoter activity. Luciferase values were normalized to protein concentration and represented as fold induction over empty vector control/MCF7 cells.

As shown in Fig. 16, transient transfection of the SPARC promoter/luciferase reporter plasmid (–1409/+28) into c-Jun/MCF7 cells resulted in a 15-30 fold increase in promoter activity when compared to vector control/MCF7 cells. Overexpression of JunD had no significant effect on SPARC promoter activity suggesting that SPARC promoter activation is specific to c-Jun. These results establish that the SPARC promoter is responsive to c-Jun in the context of a transient promoter/reporter assay and would therefore serve as a valuable tool in order to map the c-Jun responsive region(s).

Characterization of protein/DNA interactions at the SPARC promoter AP-1 like sites

Next, we evaluated protein/DNA interactions of three potential AP-1 binding sites at -1051/-1045, -868/-862 and -241/-235 by gel mobility shift analysis. Oligonucleotide primers for each of the non-canonical AP-1 sites were generated and assayed for their ability to bind proteins from nuclear extracts derived from vector control/MCF7,

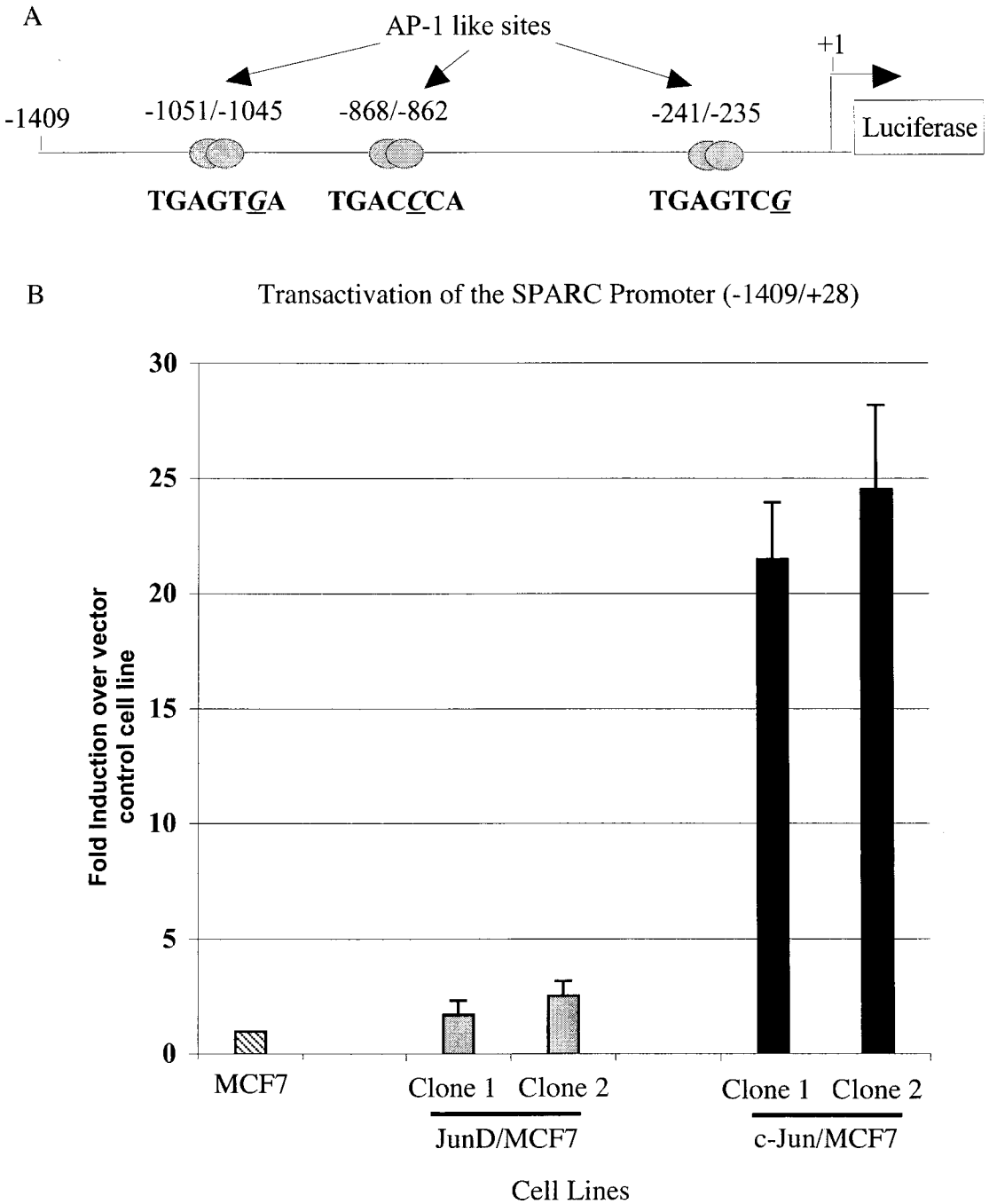

Fig. 16. Analysis of SPARC promoter (-1409/+28) activity in MCF7, JunD/MCF7 and c-Jun/MCF7 stable cell lines. *A*, Schematic diagram indicating the relative location and DNA sequence context of three non-canonical AP-1 sites. Nucleotides underlined and in italics denote sequences which differ from the consensus AP-1 context. *B*, Results of transient transfection analysis of the SPARC promoter (-1409/+28)/luciferase reporter plasmid in the indicated cell lines. Promoter activity is expressed as fold induction over the vector control/MCF7 cells. Relative luciferase values were normalized to protein concentration. Each experiment was done 2-3 times in triplicate.

JunD/MCF7 and c-Jun/MCF7 cells. In addition, a consensus AP-1 probe was analyzed as a positive control for AP-1 binding. Nuclear extracts from each cell line were incubated with ^{32}P radiolabeled DNA probes corresponding to the AP-1 like sequences (Fig. 17). Protein/DNA complexes were resolved on non-denaturing polyacrylamide gels using conditions previously established for AP-1 binding (80). As a negative control, each of the radiolabeled DNA probes were also analyzed in the absence of nuclear extract.

As shown in Fig. 17, only one of the SPARC promoter sites (-1051/-1045) showed appreciable binding of a complex consistent with AP-1 to proteins from c-Jun/MCF7 nuclear extracts. The inability to detect binding to the other two AP-1 like sites at -868/-862 and -241/-235 suggests that these sites are in a poor sequence context for AP-1 complex formation. We detected minimal AP-1 binding activity in vector control/MCF7 nuclear extracts, consistent with previous reports that MCF7 cells possess low endogenous levels of AP-1 activity (95). We also did not detect AP-1 binding in JunD/MCF7 nuclear extracts, consistent with our previous finding that JunD overexpression had no effect on SPARC promoter activity (Fig. 16). Taken together, these results suggest that AP-1 binding activity present in c-Jun/MCF7 nuclear extracts is capable of recognizing the SPARC promoter AP-1 like site at -1051/-1045.

Gel shift competition analysis of the SPARC promoter AP-1 like site at -1051/-1045

Next, we sought to characterize the specificity of protein/DNA interactions on the SPARC promoter -1051/-1045 AP-1 like site by conducting gel shift competition

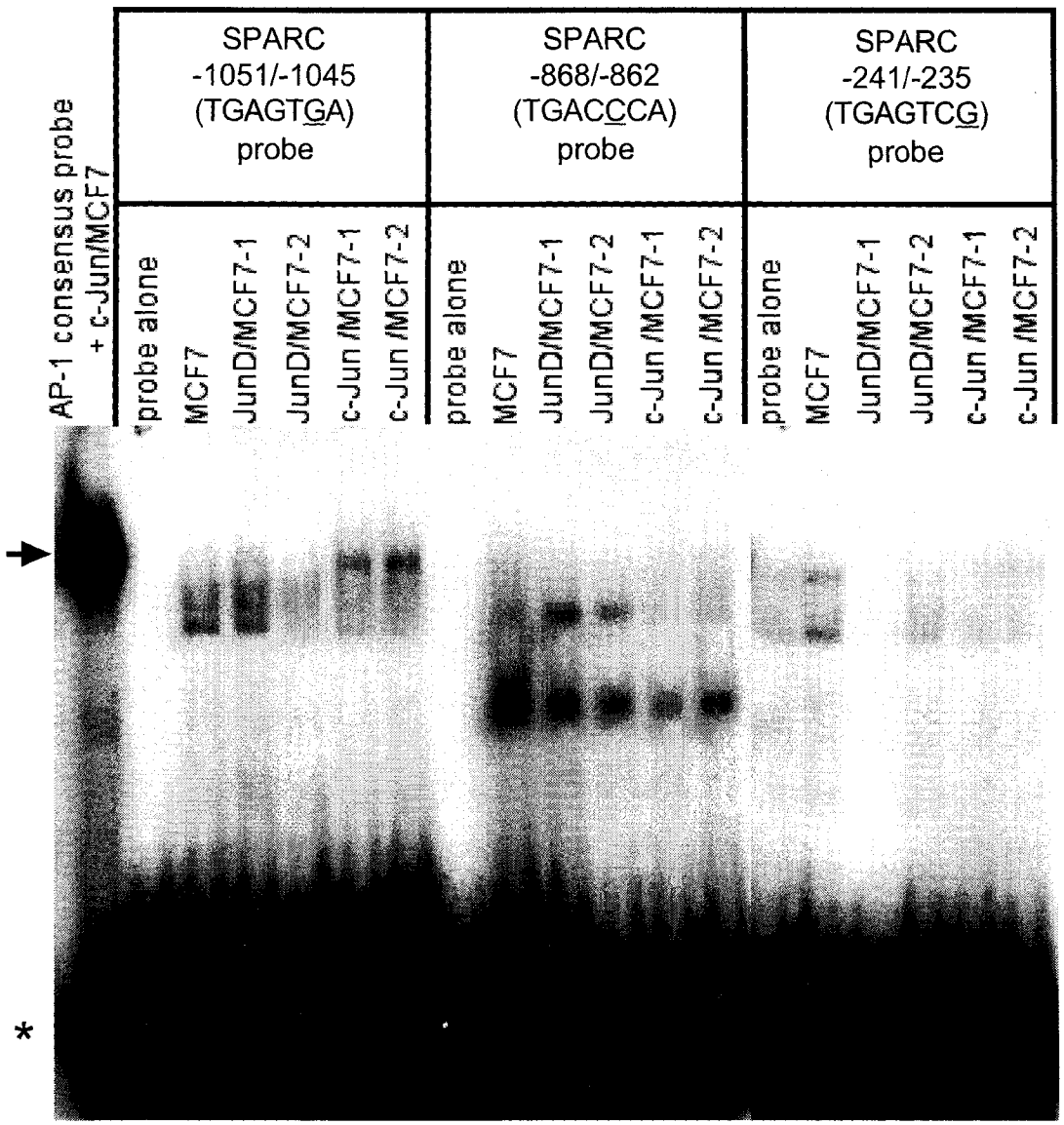

Fig. 17. Gel mobility shift analysis of the SPARC promoter AP-1 like sites at -1051/-1045, -868/-862 and -241/-235. The indicated ^{32}P radiolabeled DNA probes (30,000 cpm) were incubated with either vector control/MCF7, JunD/MCF7 or c-Jun/MCF7 nuclear extracts (8ug). The arrow (→) denotes the position of AP-1 complex formation. The asterisk (*) denotes the location of unbound, radiolabeled probe. MCF7-1 and MCF7-2 designations represent nuclear extracts isolated from individual stable cell line clones.

analysis. Gel shift reactions were conducted in the presence of a non-radiolabeled DNA probe corresponding to an unrelated DNA sequence, without AP-1 binding site, or a consensus AP-1 sequence. We expected that specific AP-1 binding would not be affected by addition of an unrelated DNA probe, whereas addition of a consensus AP-1 probe would inhibit binding in a dose dependent manner.

Nuclear extracts from c-Jun/MCF7 cells were pre-incubated with unlabeled, "cold" AP-1 consensus gel shift probe or an unrelated competitor DNA sequence. Next, the ^{32}P radiolabeled probe containing the SPARC AP-1 like site at -1051/-1045 was added to the reaction. The resulting protein/DNA complexes were resolved on a non-denaturing polyacrylamide gel and visualized by autoradiography. As shown in Fig. 18, the consensus AP-1 competitor completely abolished AP-1 binding to the -1051/-1045 probe at the lowest concentration whereas competition with an unrelated competitor had a modest effect only at higher concentrations. Formation of a lower molecular weight complex decreased with increasing concentrations of either probe suggesting that this represented a non-specific protein/DNA interaction. Taken together, these results demonstrate that the non-canonical AP-1 site at -1051/-1045 is capable of binding proteins with AP-1 binding specificity.

Antibody competition/supershift analysis of the SPARC promoter AP-1 like site at –1051/-1045

In order to identify proteins which specifically recognized the SPARC promoter AP-1 like site at -1051/-1045, we performed antibody competition and supershift analysis (Fig. 19). Addition of antibody to a gel shift reaction can either inhibit specific

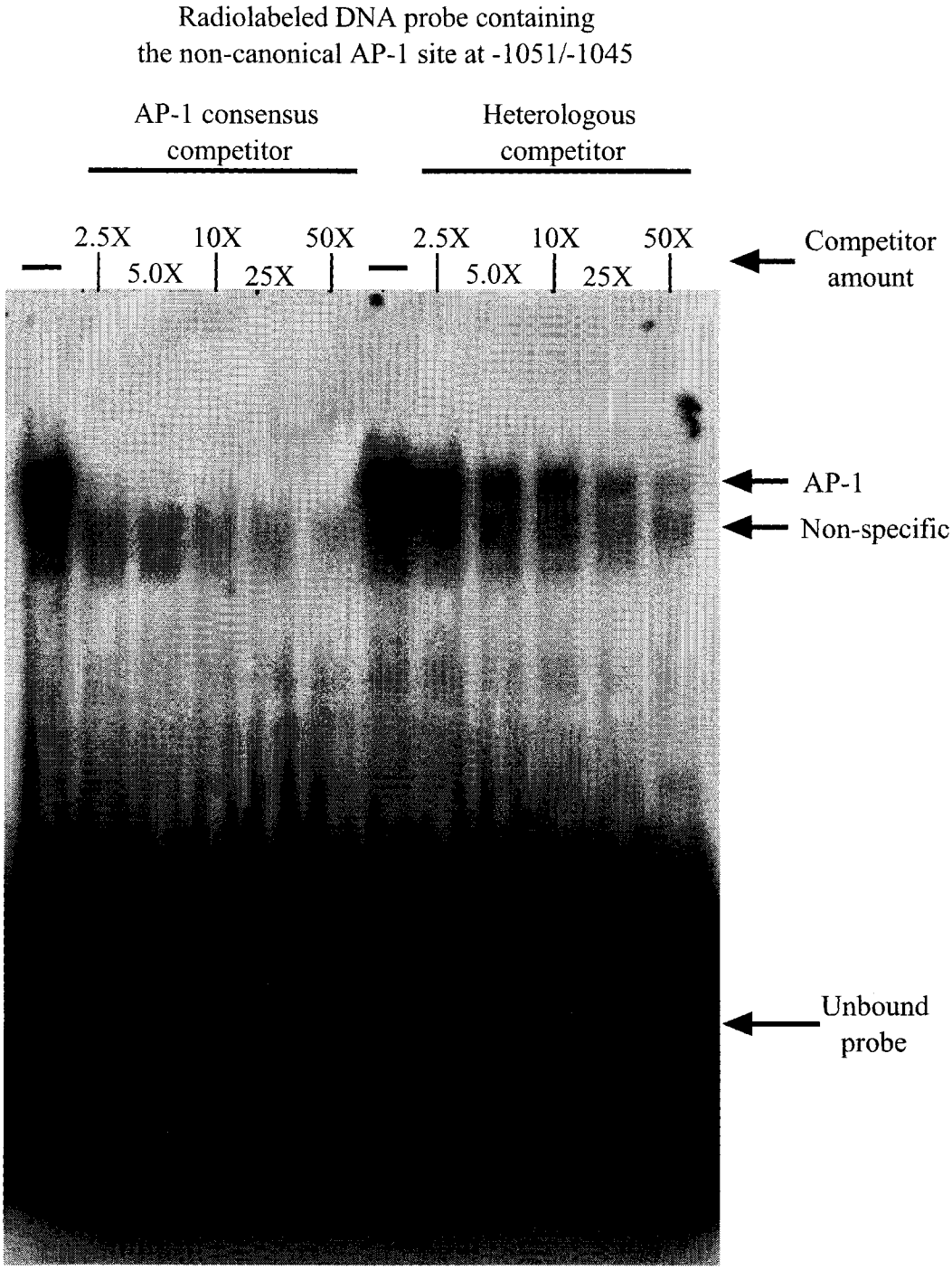

Fig. 18. Gel shift competition analysis of the SPARC promoter -1051/-1045 AP–1 like site. AP-1 binding from c-Jun/MCF7 nuclear extracts to a radiolabeled DNA probe (50,000 cpm) containing the non-canonical AP-1 site at -1051/-1045 where (-) represents no competitor followed by increasing amounts of the indicated AP-1 consensus or unrelated competitors (2.5, 5, 10, 25 and 50X molar excess).

protein/DNA interactions or result in formation of a higher molecular weight complex called a "supershift" depending on the protein domain recognized by the antibody. In either event, this strategy can be used to specifically identify the protein(s) bound to a radiolabeled DNA probe. Our analysis focused on c-Jun and Fra-1 binding because of previous observations suggesting that the AP-1 expression profile in these cells favored this AP-1 dimer combination (Fig. 3) (46).

Nuclear extracts from c-Jun/MCF7 cells were incubated with anti-c-Jun, anti-Fra–1 or a negative control antibody followed by the addition of the ^{32}P radiolabeled gel shift probe (-1051/-1045). As shown in Fig. 19, an antibody directed against the c-Jun DNA binding domain specifically blocked AP-1 binding indicating c-Jun is part of this complex. Because this antibody is directed against the DNA binding domain, the effect seen is a block in binding rather than a supershift (80). Addition of anti-Fra-1 antibody resulted in the formation of a higher molecular weight, supershifted complex indicating that the AP-1 binding activity observed is largely composed of c-Jun/Fra-1 dimers. Incubation with a negative control antibody, against a protein not expected to be present in the complex (p16), did not alter AP-1 binding. Taken together, these results demonstrate that c-Jun/Fra-1 dimers present in c-Jun/MCF7 nuclear extracts are capable of binding to the *SPARC* promoter AP-1 like site at -1051/-1045.

Site directed mutagenesis of the AP-1 like site at -1051/-1045 of the SPARC promoter

In order to determine the functional significance of the AP-1 site located at –1051/-1045, we conducted site-directed mutagenesis and then analyzed the effect on

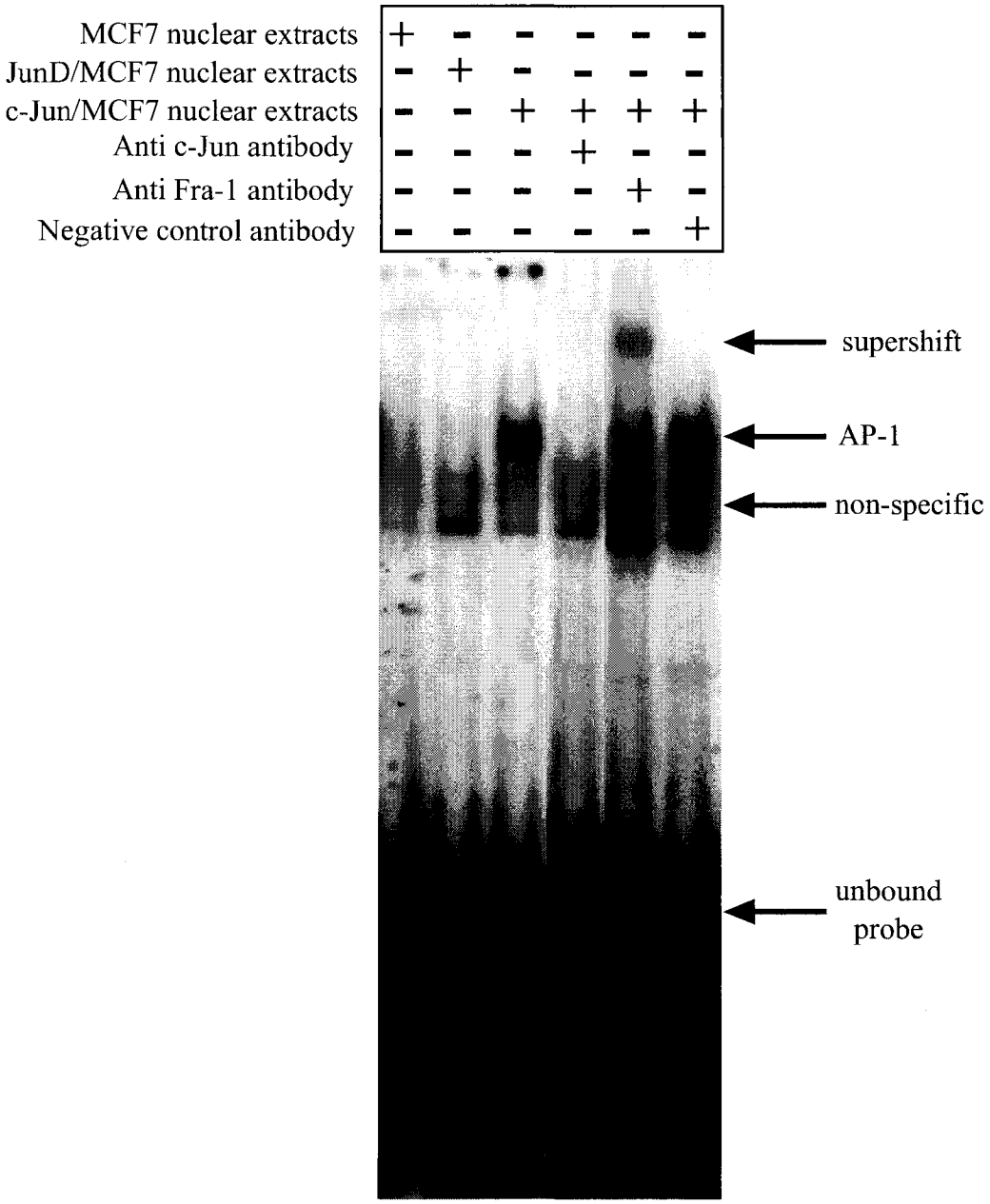

Fig. 19. Antibody competition/supershift analysis of the SPARC promoter -1051/-1045 AP-1 like site. *A*, Promoter schematic indicating the position of several potential AP-1 binding sites in the human SPARC promoter. *B*, Gel shift analysis using the indicated nuclear extracts and antibodies run on a 6% non-denaturing polyacrylamide gel and 50,000 cpm of radiolabeled, double stranded DNA probe (5' gcctgggcgacagagtgagtgagactctgtctcaaaac 3').

AP-1 binding and transactivation. We hypothesized that mutation of this site to a consensus AP-1 context would result in an increase in DNA binding and a concomitant increase in SPARC promoter activity. Conversely, we reasoned that mutation of this site, to a more divergent sequence context, would result in a decrease in AP-1 binding and transactivation potential.

Gel shift probes were constructed in order to change the wild-type -1051/-1045 sequence to a perfect consensus (TGAGTCA) or triple mutant (CGAATGA) sequence context. Gel mobility shift analysis of these mutants using c-Jun/MCF7 nuclear extracts demonstrated that, as expected, mutation to a consensus AP-1 context resulted in much stronger AP-1 binding, whereas the triple mutant abolished binding (Fig. 20*A*).

Next, we examined the effect of these mutations on SPAR*C* promoter activity in vector control/MCF7 and c-Jun/MCF7 cells. The same point mutations used in gel shift analysis were introduced in the context of the full-length promoter using overlapping PCR. Each mutant was subsequently inserted upstream of the firefly luciferase reporter gene. We reasoned that if this site was critical for promoter activation mediated by direct AP-1 binding then mutation to a high or low affinity site would result in a change in transactivation potential relative to the wild-type sequence. On the other hand, if mutation of this site did not affect promoter activation it would suggest that it is either not required or not active when taken out of the full genomic context. Interestingly, transient transfection of the site-directed mutants into c-Jun/MCF7 cells resulted in no significant difference in promoter activity compared to the wild-type sequence context (Fig. 20*B*). These results suggest that the AP-1 binding site at -1051/-1045 does not play a critical role in c-Jun mediated stimulation of SPARC promoter activity.

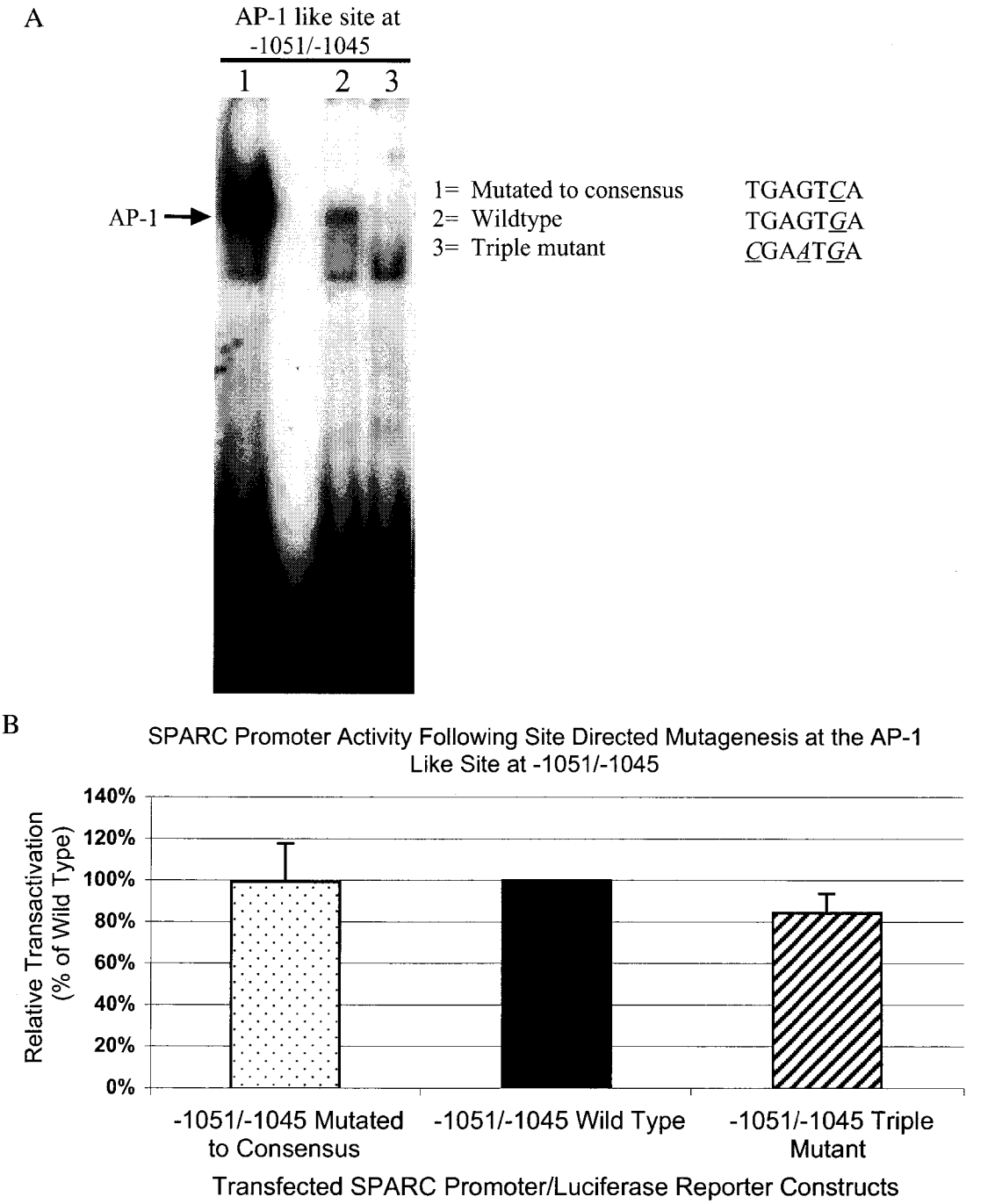

Fig. 20. Analysis of AP-1 binding and promoter activity of -1051/-1045 AP-1 like site mutants. *A*, Gel shift analysis showing AP-1 binding from c-Jun/MCF7 nuclear extracts to the indicated mutated or wild type -1051/-1045 DNA probe (30,000 cpm). *B*, Site-directed mutagenesis was used to introduce point mutations to the non-canonical AP-1 site at –1051/-1045 in the context of the SPARC promoter fragment -1409/+28. Mutant and wild-type promoter/reporter constructs were transiently transfected into c-Jun/MCF7 cells and assayed for activity. Promoter activation is expressed as percent expression relative to the wild-type sequence context. Relative luciferase values were normalized to protein concentration.

Functional analysis of a SPARC promoter deletion mutant spanning the region from -120/+28

Because mutation of the AP-1 site at -1051/-1045, alone, had no effect on c-Jun mediated SPARC promoter activation, we initiated deletion analysis in order to examine the combined effect of removing all three AP-1 like sites. We hypothesized that if AP–1 binding was required then deletion of all potential binding sites would be expected to abrogate c-Jun responsiveness. To accomplish this, we obtained a SPARC promoter fragment containing only nucleotides -120 to +28 relative to the transcriptional start site (generous gift from Dr. Marc Castellazzi). This SPARC promoter construct does not contain any sequence resembling an AP-1 site and was therefore analyzed in vector control/MCF7, JunD/MCF7 and c-Jun/MCF7 cells to determine the effect on promoter activity. Surprisingly, the SPARC promoter fragment spanning from -120 to +28 retained approximately 85% activity relative to the -1409/+28 construct when transfected into c–Jun/MCF7 cells (Fig. 21). These results suggest that the three AP-1 sequences in the SPARC promoter are dispensable and that the major c-Jun responsive region is located within the region spanning -120/+28.

Functional analysis of the SPARC promoter deletion mutant spanning the region from -70/+28

To further resolve the location of the c-Jun responsive element, we constructed an additional 5' promoter deletion mutant which resulted in a promoter fragment spanning from -70/+28 relative to the transcriptional start site. This truncated promoter construct resulted in deletion of a region containing multiple repeats of the sequence, GGA, and a

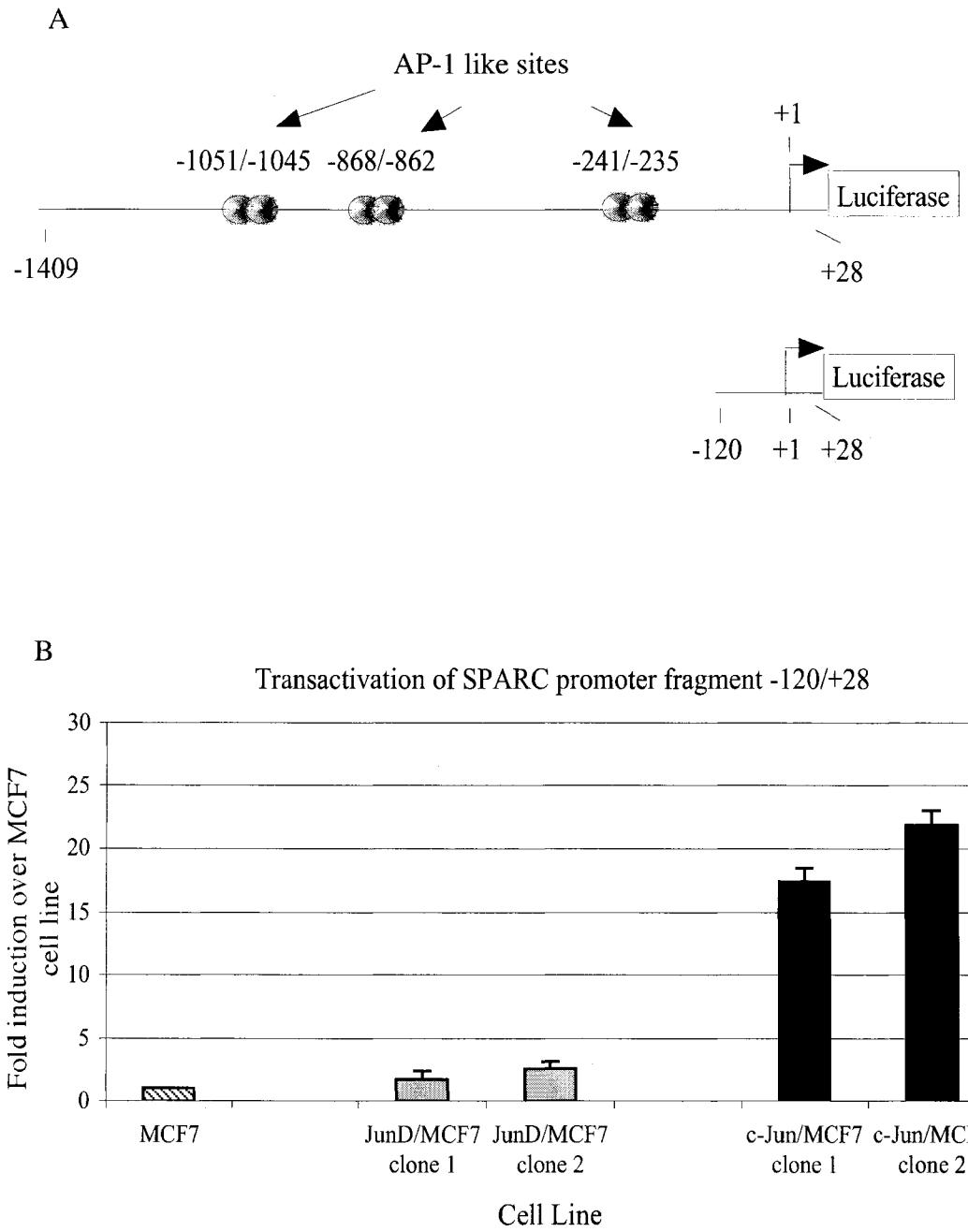

Fig. 21. Analysis of SPARC -120/+28 promoter activity. *A*, Promoter schematic indicating features of the region from -120/+28 of the human SPARC promoter. *B*, Transient transfection of SPARC promoter (-120/+28)/luciferase reporter constructs into MCF7 and c-Jun/MCF7 cells. Promoter activation is expressed as fold induction over the MCF7 cell line. Relative luciferase values were normalized to protein concentration.

GC rich region, both of which have been implicated in regulation of SPARC promoter activity (129, 130, 156, 157). Transient transfection of this construct into c-Jun/MCF7 cells resulted in an 85% reduction in SPARC promoter activity relative to the -120/+28 promoter fragment (Fig. 22). Taken together, these results suggest that the 50 base pair sequence between nucleotides -120 and -70 contains the major c-Jun responsive region.

Gel shift analysis of the c-Jun responsive region spanning nucleotides -120/-83

Next we wanted to characterize protein/DNA interactions involving the c-Jun responsive region of the SPARC promoter. As mentioned previously, this region contains a GC rich element suggesting that transcription factors that recognize this sequence may play a role in SPARC gene regulation. The transcription factor Sp1, and related proteins, have been shown to bind with high affinity to GC rich regions in TATA-less promoters similar to SPARC (140, 158, 159). Therefore, we hypothesized that Sp1 may be involved in SPARC promoter regulation via interaction with the GC rich region located between -120/-83.

We conducted gel mobility shift analysis on vector control/MCF7 and c–Jun/MCF7 nuclear extracts incubated with a ^{32}P radiolabeled DNA probed corresponding to nucleotides -120/-83 of the SPARC promoter. As shown in Fig. 23 analysis of these reactions revealed the presence of similar complexes formed with vector control/MCF7 and c-Jun/MCF7 nuclear extracts suggesting that a common protein, or proteins, may be involved.

In order to determine if any of these complexes contained specific Sp1 binding activity we conducted competition analysis. Addition of a Sp1 consensus probe resulted

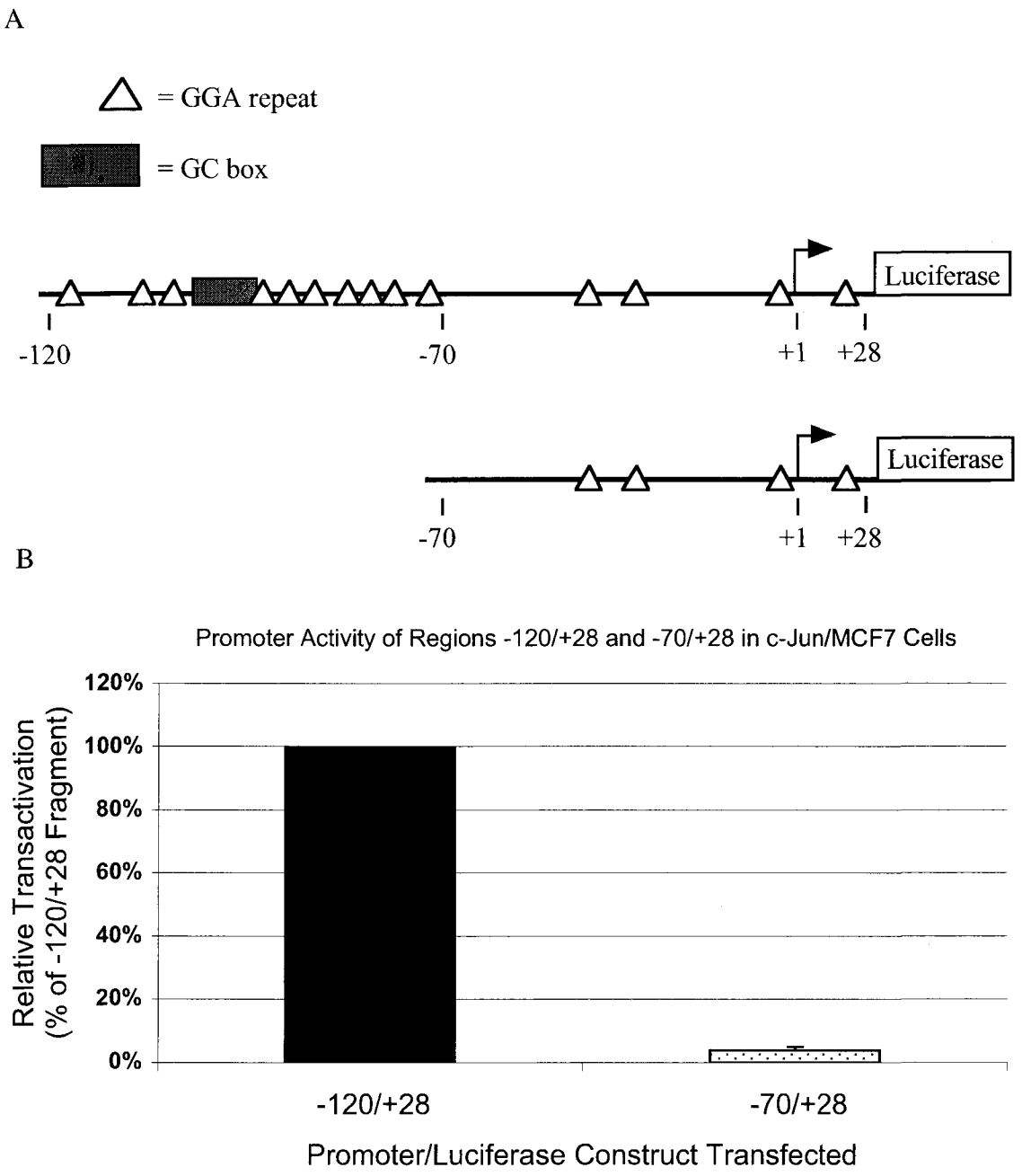

Fig. 22. Analysis of SPARC -70/+28 promoter activity. *A*, Promoter schematic showing the truncated forms of the human SPARC promoter used in these experiments. *B*, Transient transfection of SPARC promoter (-120/+28) and (-70/+28)/luciferase reporter constructs into c-Jun/MCF7 cells. SPARC promoter fragment -70/+28 activity is expressed as percent activation relative to the SPARC promoter -120/+28 luciferase reporter construct. Relative luciferase values were normalized to protein concentration.

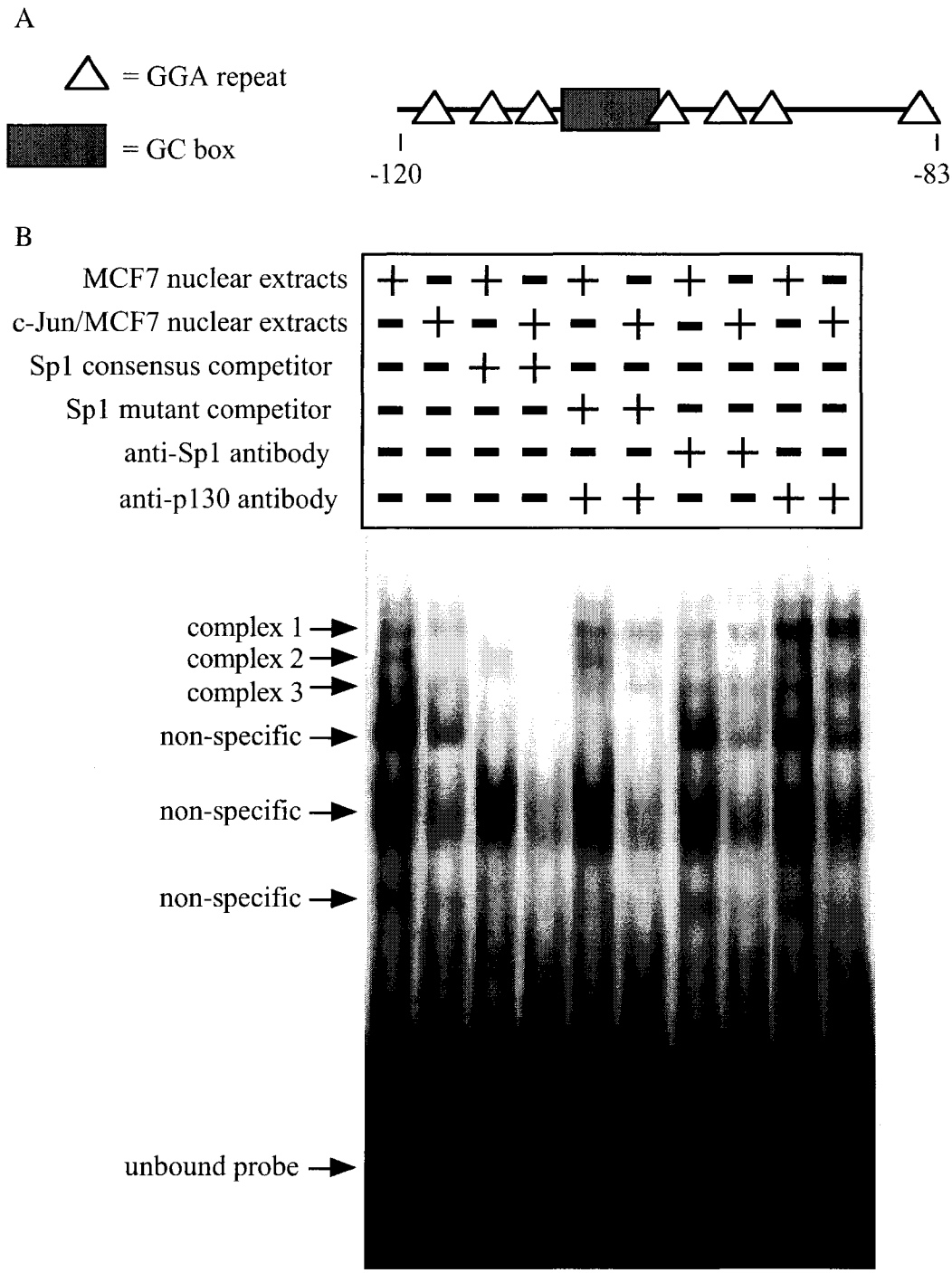

Fig. 23. Analysis of protein/DNA interactions in the region -120/-83 of the SPARC promoter. *A*, Promoter schematic highlighting GC box and GGA repeat motifs. *B*, Gel shift analysis showing various complexes binding to a radiolabeled DNA probe spanning the region of the SPARC promoter from nucleotides -120/-83 using MCF7 and c-Jun/MCF7 nuclear extracts. Sp1 consensus and Sp1 mutant oligonucleotides were used as competitors (100X molar excess) to show the specificity of DNA complex formation.

in specific inhibition of complex 1 and complex 3, whereas incubation with a Sp1 mutant probe had no effect (Fig. 23). These results suggest that protein with Sp1 binding specificity -120/-83 and this activity is present in both extracts.

Next, we attempted to identify Sp1 as part of complex 1 and/or complex 3 by antibody shift analysis. As shown in Fig. 23, addition of Sp1 specific antibody had no effect on the mobility of any of the specific complexes in either vector control/MCF7 or c-Jun/MCF7 nuclear extracts under the conditions tested. One explanation for this result is that another Sp family member, such as Sp2, Sp3 or Sp4, is responsible for the binding we observe. These related zinc finger DNA binding proteins are all capable of binding to GC rich sequences similar to those present in the -120/-83 probe (160, 161). Alternatively, it is possible that Sp1 is actually present in the complexes, but we could not detect it using the reaction conditions tested. One final possibility we considered was that Sp1 antibody was unable to recognize Sp1 protein due to protein/protein interactions which may have masked the epitope(s).

Chromatin immunoprecipitation analysis of c-Jun and Sp-1 binding to the SPARC promoter *in vivo*

Next, we wanted to determine if AP-1 and Sp1 proteins were associated with the SPARC promoter *in vivo*. c-Jun and Sp1 have been shown to interact resulting in synergistic activation of the *p21* and 12(S)-lipoxygenase genes (92, 93). In both cases, c–Jun/Sp1 interaction was shown to occur in the absence of an AP-1 binding site (92, 93). Therefore, we hypothesized that, *in vivo*, c-Jun and Sp1 may co-localize at the SPARC promoter as a means of cooperatively regulating its activity.

Two widely used techniques to study protein/DNA interactions in living cells are *in vivo* DNA footprinting and chromatin immunoprecipitation (ChIP) analysis. *In vivo* DNA footprinting is a sensitive technique that provides a high degree of resolution for analyzing protein/DNA interactions (162). However, this technique provides only indirect evidence regarding the identity of the protein(s) bound to a specific region of genomic DNA. On the other hand, chromatin immunoprecipitation (ChIP) analysis is a technique that provides direct evidence that a protein, alone or in a multi-protein complex, is associated with a specific genomic region *in vivo* (163, 164). Therefore, we chose to use chromatin immunoprecipitation analysis to examine c-Jun, Fra-1 and Sp1 association with the SPARC promoter in vector control/MCF7 and c-Jun/MCF7 cells. Our experimental approach is outlined in Fig. 24.

Protein/DNA interactions were "frozen in time" by reversible chemical crosslinking using formaldehyde. Chromatin was purified and sheared by sonication to generate fragments with an average size of 500-1000 base pairs. Fragments of this size provide a high degree of specificity for the genomic DNA region of interest (163, 164). Following sonication, chromatin was divided into equal amounts to allow for parallel analysis of multiple protein/DNA interactions. This was accomplished by incubating individual chromatin aliquots with antibodies for c-Jun, Fra-1, Sp1 or a negative control antibody. Following immunoprecipitation, protein/DNA complexes were isolated using protein A/agarose beads. Samples were then washed to remove non-specific interactions. Affinity purified chromatin was subsequently eluted from the protein A/agarose beads followed by crosslink reversal. DNA was then isolated from each sample and analyzed

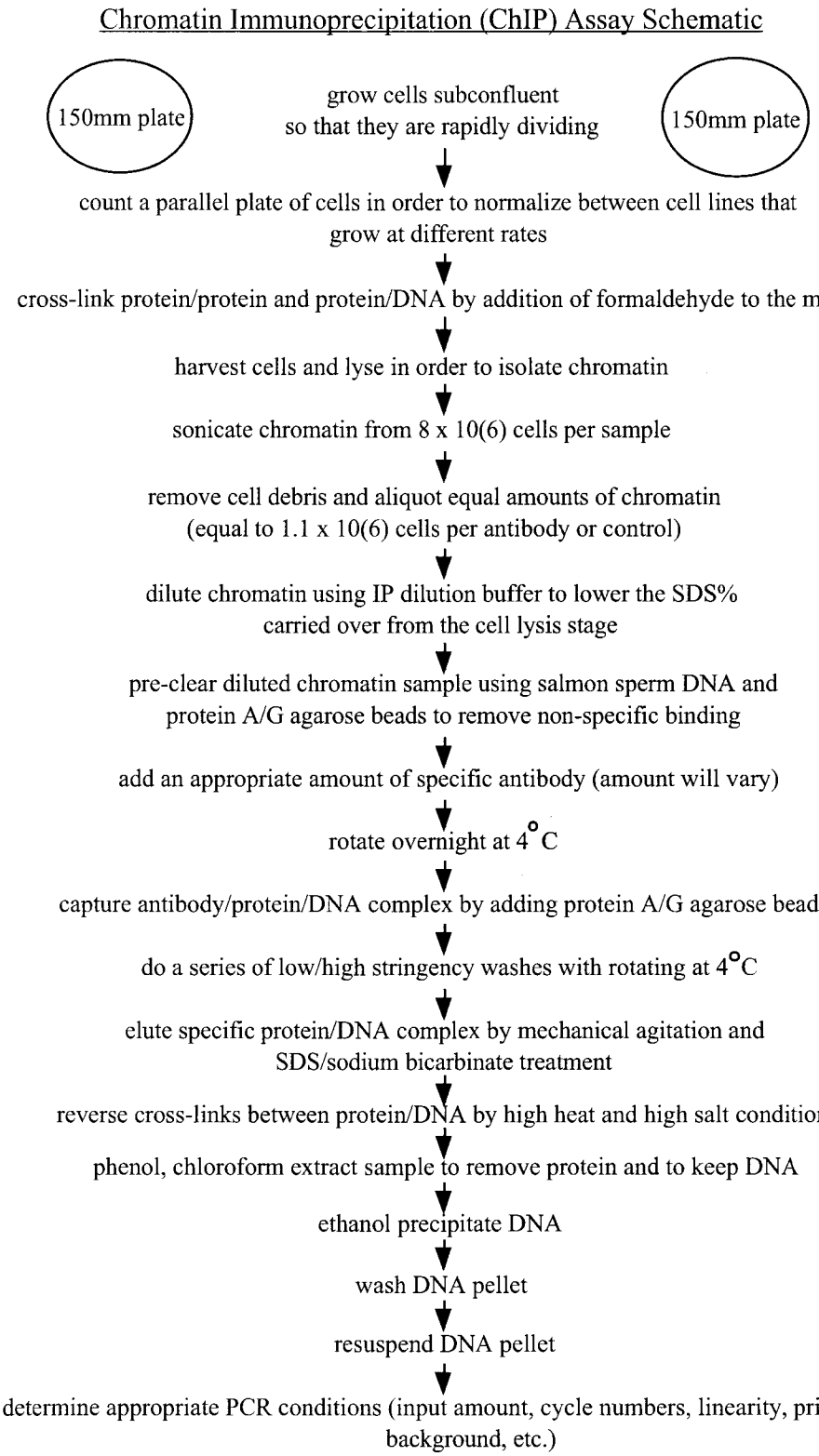

Fig. 24. Experimental approach for determining *in vivo* protein/DNA interactions by chromatin immunoprecipitation analysis.

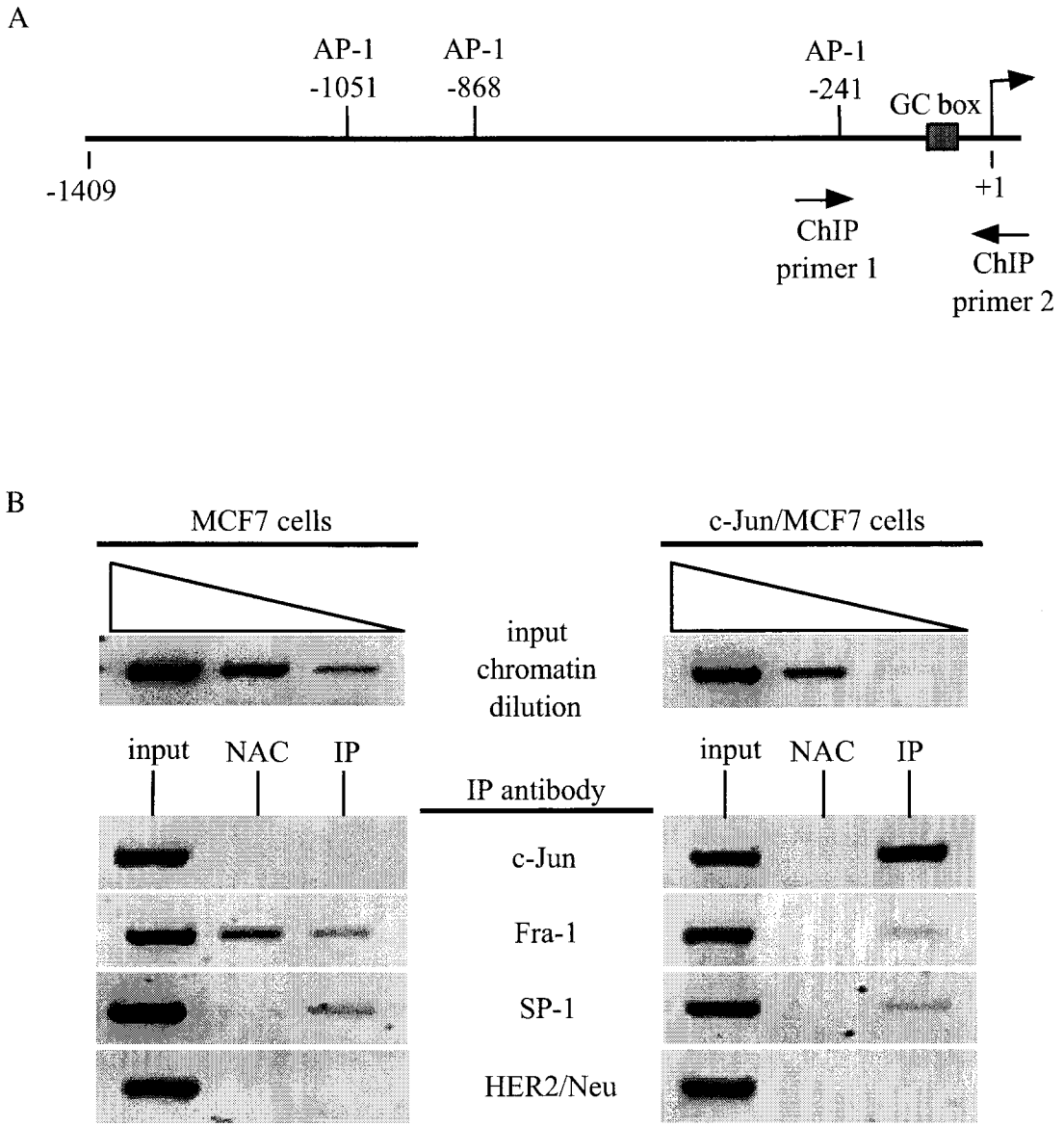

Fig. 25. Chromatin immunoprecipitation analysis of c-Jun, Fra-1 and Sp1 protein binding at the SPARC promoter locus. *A*, Schematic diagram of the human SPARC promoter indicating the location of PCR primers used for ChIP. *B*, PCR analysis of protein associated DNA immunoprecipitated using the indicated antibody. NAC= no antibody control, IP= immunoprecipitation, input= non-immunoprecipitated chromatin template.

by PCR using oligonucleotide primer pairs specific the SPARC proximal promoter region.

Fig. 25 demonstrates the results of chromatin immunoprecipitation analysis of the SPARC proximal promoter region. As expected, c-Jun was present at the SPARC promoter locus only in c-Jun/MCF7 where SPARC gene expression is upregulated. In addition, Fra-1 was present above background only in c-Jun/MCF7 cells. The presence of a PCR amplicon in one of the MCF7 "no antibody control" reactions was most likely due to contamination during PCR since the same sample was tested in other reactions and did not result in this background. Interestingly, Sp1 was present at the SPARC promoter locus in both vector control/MCF7 and c-Jun/MCF7 cell lines consistent with our *in vitro* gel shift analysis suggesting the presence of a common protein with Sp1 binding specificity. It should be noted that, even though the PCR amplicon spans the region from nucleotides -241 to +28, we cannot rule out the possibility that AP-1 sites immediately upstream and/or downstream may contribute to c-Jun and Fra-1 binding observed in the genomic context. This is due to the fact that the average chromatin fragment size is ~750 base pairs. As a result, we may be detecting protein/DNA interactions occurring 250 base pairs upstream or downstream of the region amplified using the primer pair shown in Fig. 25.

Taken together, the results presented in Aim 2 demonstrate that the SPARC promoter region from –120 to -70 contains the major c-Jun responsive element. In addition, we showed that c-Jun, Fra-1 and Sp1 were associated with the SPARC proximal promoter region in c-Jun/MCF7 cells. Interestingly, Sp1 was also bound to this GC rich region in vector control/MCF7 cells where transcription is inactive. These results are

significant because they represent a direct mechanism for c-Jun target gene activation leading to malignant progression.

C. Epigenetic Modifications Associated With SPARC Gene Expression

The results obtained in Aim 2 identified a cytosine and guanine rich region of the SPARC promoter which was critical for c-Jun responsiveness. Further analysis of the SPARC promoter revealed the presence of multiple cytosines in a cytosine-phosphate-guanine (CpG) dinucleotide context. CpG sequences are known to undergo epigenetic modification via DNA methylation (165-167). Importantly, normal genomic DNA methylation patterns have been shown to change during tumorigenesis and oncogenic progression (168-171). Aberrant DNA methylation can lead to gene activation or repression depending on the context. For example, hypermethylation of the tumor suppressor gene *CDKN2A* ($p16^{INK4a}$) results in gene inactivation in many tumors (170, 172, 173). In contrast, hypomethylation of gene regulatory regions correlates with transcriptional activation (174, 175). Interestingly, a recent study demonstrated a correlation between hypermethylation of SPARC exon 1 and decreased SPARC expression in pancreatic cancer cell lines (176). Therefore, we tested the hypothesis that DNA methylation at the SPARC genomic locus may be involved in regulation of SPARC gene expression in a MCF7 breast cancer model system.

Analysis of SPARC gene expression following treatment of MCF7 cells with the DNA methyltransferase inhibitor 5-aza-2'deoxycytidine

CpG methylation is catalyzed by cellular DNA methyltransferase (DNMT) enzymes (170, 177). Previous studies have demonstrated that selective inhibition of DNA methyltransferases is sufficient to reverse genomic DNA methylation patterns leading to reactivation of silenced genes (178-181). Therefore, in order to determine the

effect of DNA methylation on SPARC gene expression in MCF7 cells we used a pharmacological inhibitor of DNA methyltransferase activity, 5-aza-2'deoxycytidine (5–aza-dC). 5-aza-dC is a cytosine nucleotide analog that becomes incorporated into newly synthesized DNA (179-181). When incorporated 5' of a guanine residue, 5–aza–dC irreversibly binds DNA methyltransferase enzymes resulting in demethylation of genomic DNA (182, 183). We reasoned that if the SPARC promoter locus were methylated in MCF7 cells, then inhibition of DNA methyltransferase activity would be expected to result in an increase in SPARC expression.

Vector control/MCF7 and c-Jun/MCF7 cells were grown in the presence or absence of 5-aza-dC for 60 hours. Following treatment, total RNA was isolated and SPARC mRNA levels were determined by semi-quantitative RT-PCR. The invariantly expressed 18S ribosomal subunit served as an internal control to demonstrate that equal amounts of RNA were assayed in each reaction. As shown in Fig. 26, treatment of MCF7 cells with 5-aza-dC resulted in a dose dependent increase in steady-state SPARC message levels. In contrast, 5-aza-dC had no effect on SPARC expression in c–Jun/MCF7 cells where transcription was already active.

Next, we wanted to determine the time course of SPARC gene activation in MCF7 cells following treatment with 5-aza-dC. Cells were grown in the presence of the drug for a total of 72 hours at which point the cells were trypsinized, reseeded and grown in the absence of 5-aza-dC in order to determine the reversibility of SPARC gene activation. Total RNA was harvested at 24 hour intervals following the start of 5-aza-dC treatment and SPARC mRNA levels analyzed by semi-quantitative RT-PCR. As shown in Fig. 26

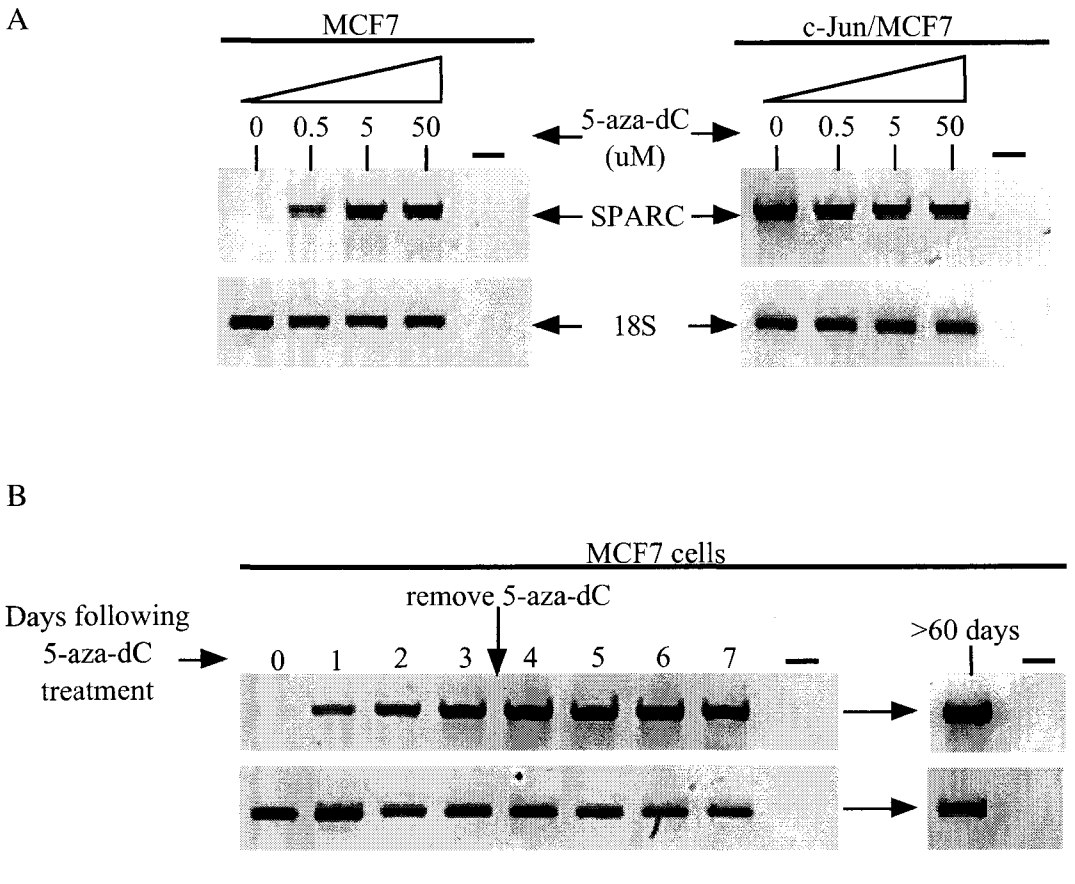

Fig. 26. Analysis of SPARC gene expression following treatment of MCF7 cells with the DNA methyltransferase inhibitor, 5-aza-2'deoxycytidine. *A*, Semi-quantitative RT-PCR analysis of SPARC expression in vector control/MCF7 and c-Jun/MCF7 cells following 5-aza-dC treament at the indicated dose. Cells were treated with increasing doses of 5-aza-dC for 60 hours. Total RNA was then isolated followed by RT-PCR analysis for SPARC expression using 18S as an internal control. *B*, Semi-quantitative RT-PCR analysis of SPARC expression over time following 5-aza-dC treatment (5μM). (-) negative RT-PCR control in which template was omitted from the reaction.

SPARC expression was detected as early as 24 hours after treatment. Surprisingly, SPARC expression persisted in MCF7 cells exposed to 5-aza-dC even after removal of the drug. We reasoned that removal of 5-aza-dC would result in restoration of DNMT activity and, therefore, re-silencing of SPARC expression. One possible explanation for these results is that SPARC mRNA is very stable and therefore, not quickly degraded. As a result, steady state message levels may persist even after repression of SPARC gene transcription. However, this explanation seems unlikely because comparable levels of SPARC transcript were maintained for up to 60 days after 5-aza-dC removal (Fig. 26). An alternative explanation is that DNMT inhibition led to SPARC promoter demethylation that was not re-established following removal of the drug.

Taken together, the results presented in Fig. 26 suggest that, in MCF7 cells, SPARC gene expression is repressed by DNA methylation and activated following DNA demethylation. Therefore, we have identified two events which are capable of activating SPARC gene expression 1.) overexpression of c-Jun and 2.) inhibition of DNA methyltransferase activity.

Low resolution analysis of SPARC promoter DNA methylation in vector control/MCF7 and c-Jun/MCF7 stable cell lines

Since inhibition of DNA methyltransferase activity with 5-aza-dC resulted in an increase in SPARC gene expression, we wanted to determine the extent to which the SPARC promoter region was methylated in MCF7 cells. In addition, we wanted to determine if there was a correlation between SPARC promoter methylation and

transcriptional up-regulation in response to c-Jun. It was our hypothesis that the SPARC promoter was methylated in MCF7 cells, but not in c-Jun/MCF7 cells.

A variety of different methods have been used to determine genomic DNA methylation patterns. These include: cleavage of genomic DNA with methylation sensitive restriction enzymes followed by Southern blot analysis, methylation specific PCR (MSP) and bisulfite DNA sequencing (172, 184, 185). For our initial experiments, we conducted PCR analysis of genomic DNA that had been digested with the methylation sensitive restriction enzyme isoschizomer pair, HpaII and MspI. Both enzymes recognize the sequence 5'-CCGG-3', however, HpaII cannot digest DNA when the internal cytosine is methylated whereas MspI will digest regardless of the methylation status (186). Examination of the SPARC promoter sequence revealed the presence of four HpaII/MspI sites located at both distal and proximal regions. As a result, this approach allowed a rapid determination of DNA methylation at four positions over a 1400 base pair region. Our experimental approach is outlined in Fig. 27.

Genomic DNA was isolated from vector control/MCF7 and c-Jun/MCF7 cells and digested in parallel with HpaII or MspI. Undigested genomic DNA served as a positive control for the PCR reactions while MspI digested samples served as a positive control to demonstrate complete digestion of the genomic DNA. Additionally, we analyzed genomic DNA from three independent clones of each cell line to control for clonal variability.

As shown in Fig. 28, analysis of undigested genomic DNA resulted in successful PCR amplification of the SPARC promoter indicating that reaction conditions were optimal. In addition, analysis of MspI digested samples showed successful digestion of

Experimental approach for low resolution mapping of SPARC promoter methylation

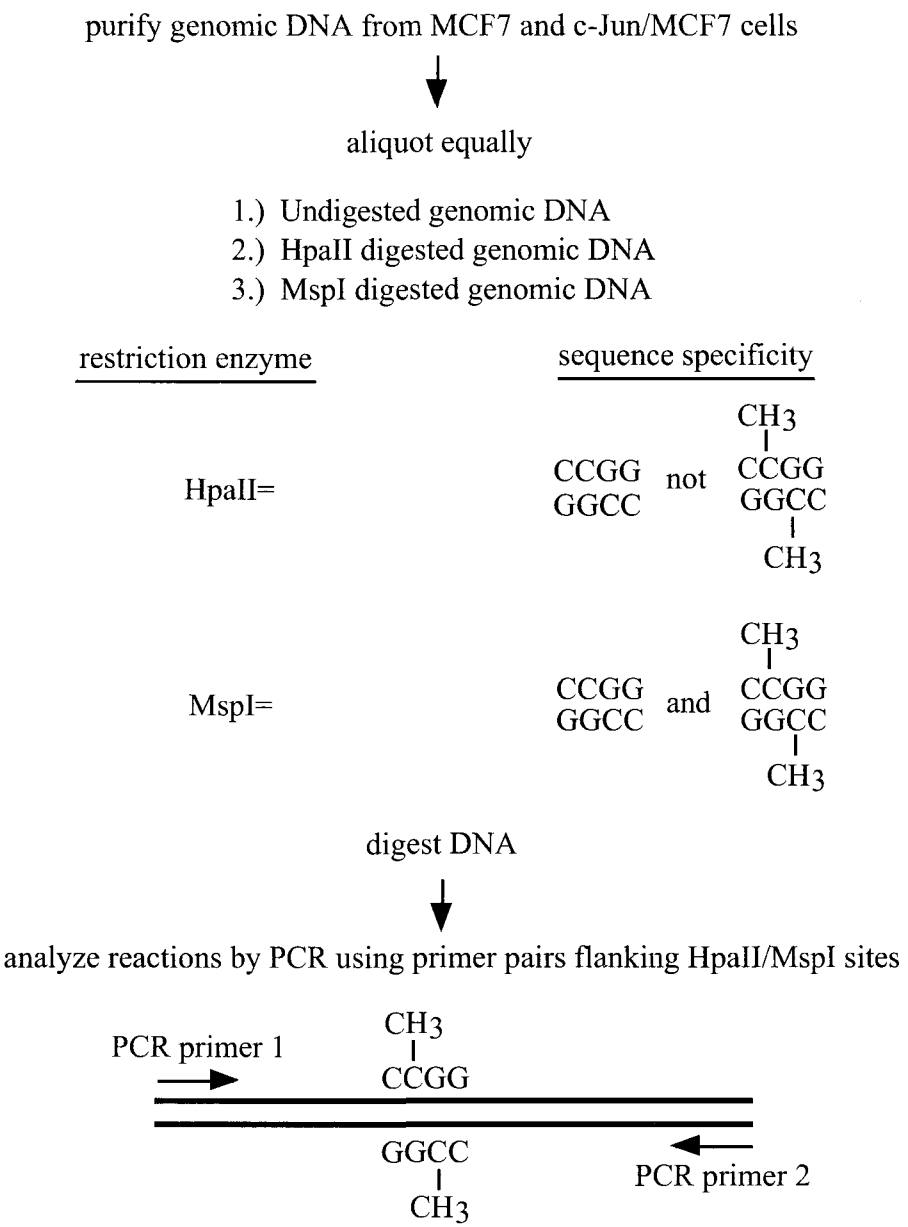

Fig. 27 . Experimental approach for low resolution mapping of DNA methylation at the SPARC promoter locus.

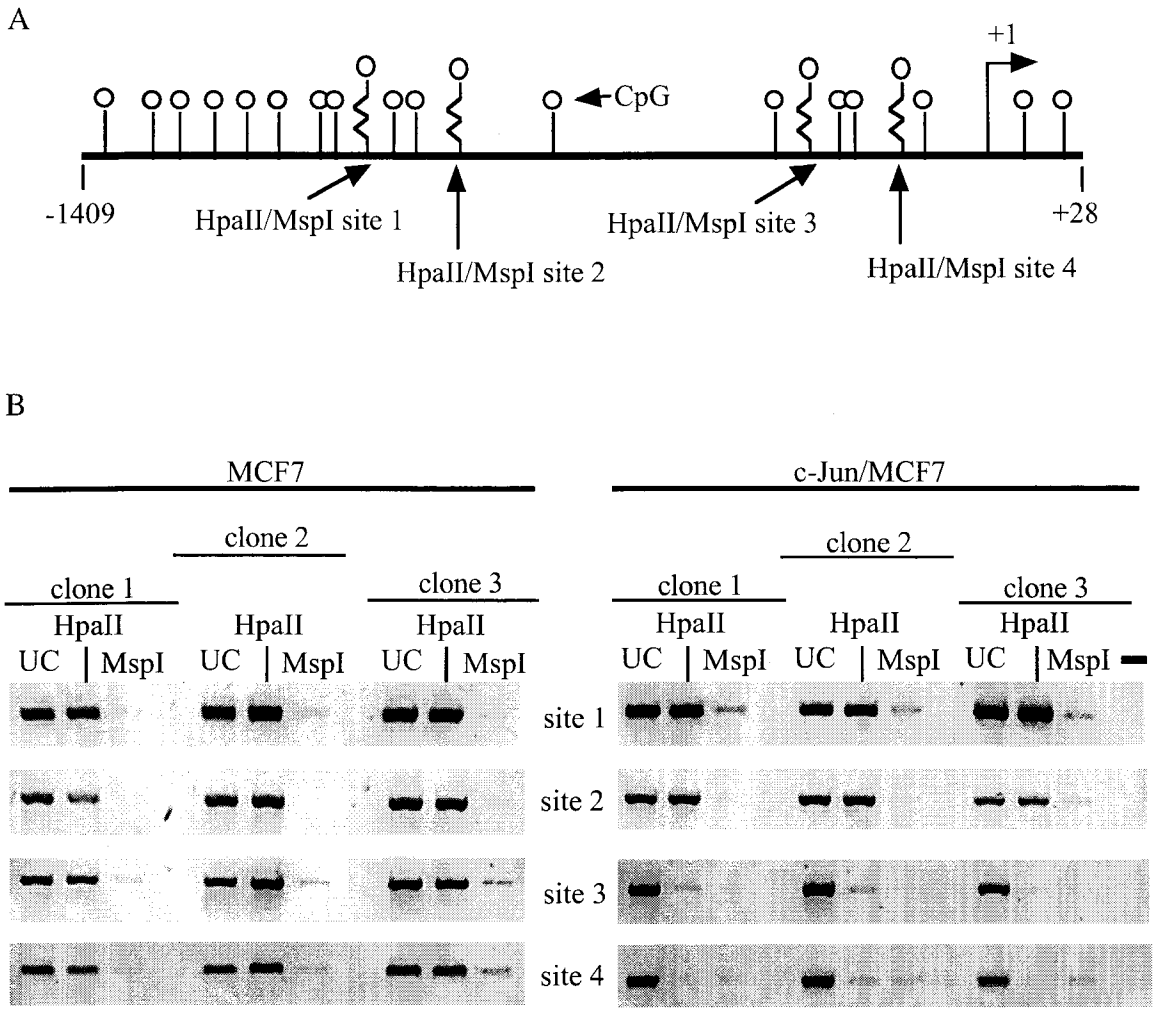

Fig. 28 Analysis of SPARC promoter methylation in MCF7 and c-Jun/MCF7 cells by HpaII/MspI mapping. *A*, Schematic representation of the SPARC promoter indicating HpaII/MspI restriction enzyme recognition sites. *B*, Genomic DNA from three independent MCF7 empty vector control cell lines and c-Jun/MCF7 stable cell lines (clone 1, 2 and 3) was digested with the restriction enzyme isoschizomer pair HpaII/MspI. The restriction enzyme HpaII cannot digest methylated sites (5'–CCGG–3') whereas MspI will digest the same sequence regardless of the methylation status. PCR was conducted on digested DNA using primer pairs flanking individual HpaII/MspI sites. The presence of a band in the HpaII lanes indicates that it is protected from digestion and is therefore methylated. MspI reactions serve as controls to demonstrate complete DNA digestion. UC= uncut, and serves as a positive control for the PCR reaction. The (-) lane serves as a negative PCR control in which template DNA has been left out of the reaction.

all HpaII/MspI sites as indicated by the decrease in PCR amplification product. The presence of low-level background in some MspI digested samples was most likely due to incomplete digestion of genomic DNA. PCR analysis of HpaII reactions in vector control/MCF7 cells resulted in productive amplification suggesting that each of the four HpaII/MspI sites is methylated. In contrast, analysis of HpaII digested DNA from three c-Jun/MCF7 stable cell lines resulted in loss of the PCR amplification product at HpaII/MspI sites #3 and #4. This result indicates that sites #3 and #4 are not methylated *in vivo* in c-Jun/MCF7 cells. Further analysis revealed that the distal HpaII/MspI sites, #1 and #2, remain methylated in all three c-Jun/MCF7 cell lines. Interestingly, the HpaII/MspI site #4 is located within the -120/-70 region that we previously mapped as the major c-Jun responsive region. Taken together, these results demonstrate a localized demethylation of the proximal promoter region in c-Jun/MCF7 cells whereas the distal promoter region is methylated in both vector control/MCF7 and c-Jun/MCF7 cells.

High resolution analysis of SPARC promoter DNA methylation in vector control/MCF7 and c-Jun/MCF7 stable cell lines

The previous HpaII/MspI mapping of SPARC promoter methylation demonstrated that at least two CpG sites become demethylated in response to c-Jun. This demethylation correlates with c-Jun induced transcriptional activation. However, there are other CpG sites, not in a HpaII/MspI context, that may also be differentially methylated. Therefore, we next wanted to determine the methylation status of other CpG sites in order to generate a more detailed map of SPARC promoter methylation.

In order to accomplish this goal, we analyzed methylation using sodium bisulfite modification of genomic DNA followed by DNA sequencing. This method is considered the "gold standard" for methylation mapping because it allows for single nucleotide resolution as well as simultaneous analysis of multiple sites on the same fragment of DNA (185). A schematic diagram of our approach is shown in Fig. 29. Genomic DNA was treated with sodium bisulfite, hydroquinone and sodium hydroxide to chemically convert unmethylated cytosines to uracil (185). Methylated cytosines are resistant to this chemical modification. As a result, it is possible to use DNA sequence analysis to determine the CpG methylation status of the genomic region of interest. Importantly, conversion of all non-CpG cytosines to uracil is used as an internal control to verify that the modification reaction was successful. Following bisulfite modification, genomic DNA served as the template for PCR using primer pairs specific for distal and proximal regions of the SPARC promoter. PCR products derived from modified vector control/MCF7 and c-Jun/MCF7 genomic DNA were then cloned into the T/A cloning plasmid, pGEMT-Easy. Eight cloned PCR products from each cell line were analyzed by DNA sequencing. Each of the cloned inserts represents a single allele amplified from a single cell. As a result, sequencing of multiple clones makes it is possible to determine the percentage of alleles in the cell population which display a given pattern of methylation (185).

The results of bisulfite sequence analysis are graphically represented in Fig. 30. Filled (black) circles indicate methylated CpG residues, whereas empty (white) circles represent unmethylated CpGs. Strikingly, these results demonstrate prominent demethylation of the SPARC promoter in c-Jun/MCF7 cells. This demethylation is

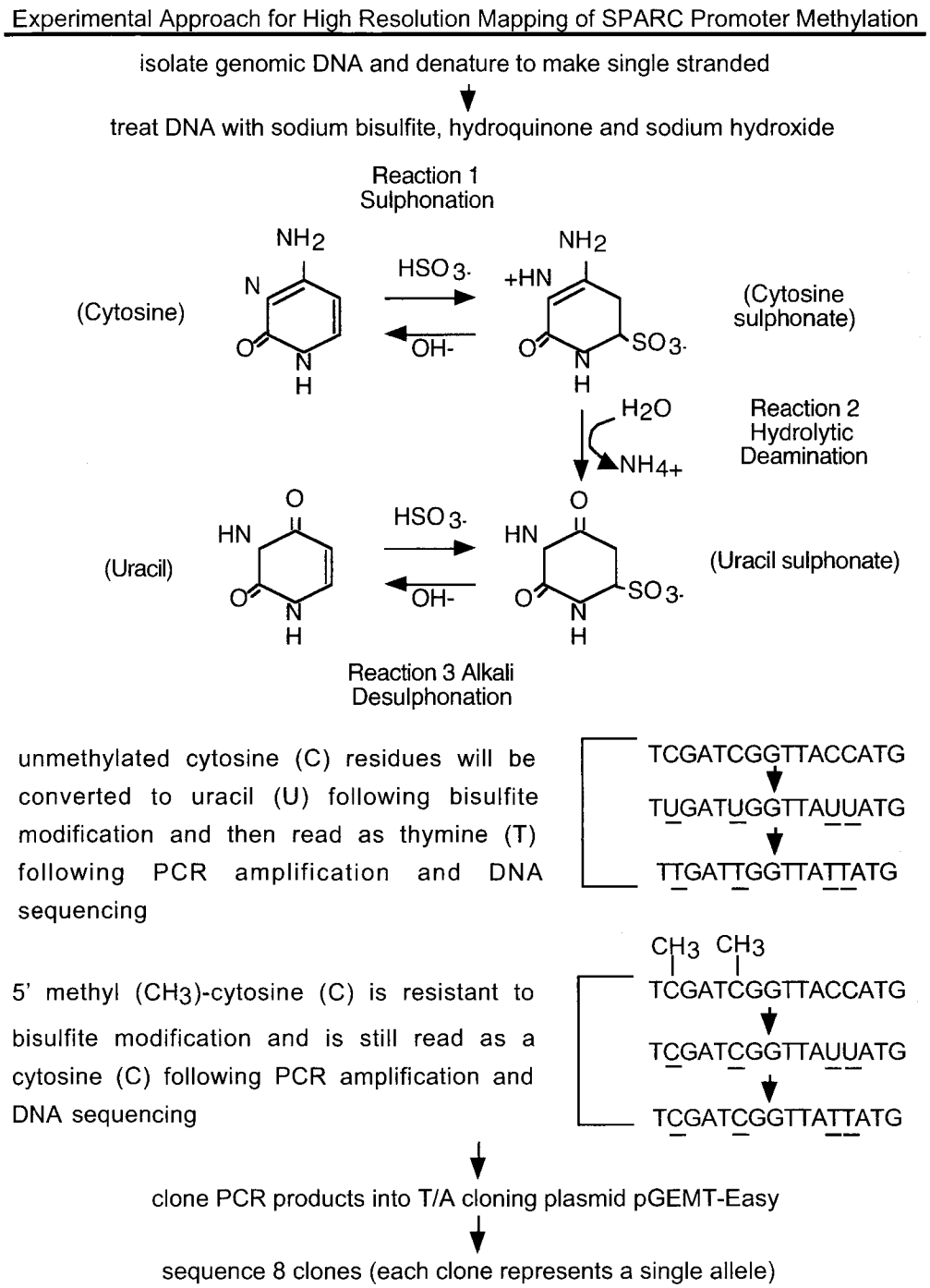

Fig. 29. Experimental approach for high resolution mapping of SPARC promoter methylation by sodium bisulfite genomic DNA modification.

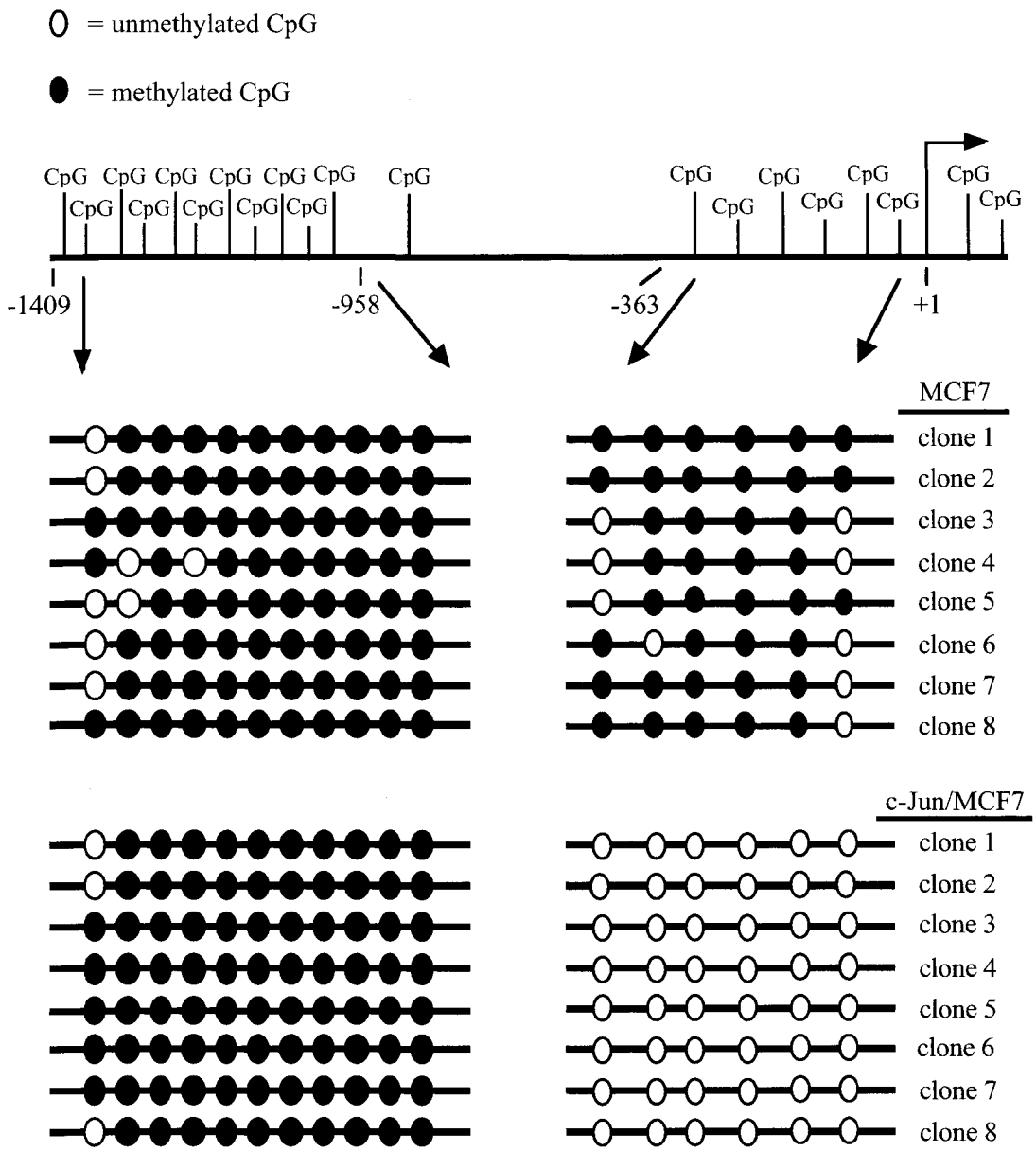

Fig. 30. Results of high resolution, sodium bisulfite mapping of SPARC promoter methylation. Genomic DNA was isolated from MCF7 empty vector control cell line and c-Jun/MCF7 stable cell line. DNA was treated with sodium bisulfite, hydroquinone and sodium hydroxide in order to convert unmethylated cystosine residues to uracil. Methylated cytosines are protected from chemical modification and are not converted to uracil. The proximal and distal regions of the SPARC promoter were then PCR amplified, cloned into plasmid DNA and sequenced. Results are represented graphically where unfilled (white) ovals=unmethylated CpGs and filled (black) ovals=methylated CpGs.

localized to the proximal promoter region and includes the c-Jun responsive region. These results are consistent with our HpaII/MspI methylation mapping experiments (Fig. 28), in which the two HpaII/MspI sites closest to the transcriptional start site were demethylated in c-Jun/MCF7 cells. Taken together, the results of SPARC promoter methylation mapping clearly demonstrate an inverse correlation between SPARC transcript levels and the extent of DNA methylation.

Analysis of the effect of *in vitro* methylation on SPARC promoter activity

Next, we wanted to determine the functional significance of SPARC promoter methylation. It was unclear whether methylation played a functional role in SPARC promoter regulation or whether the change in methylation was a byproduct of transcriptional activation.

In order to address this issue, we conducted *in vitro* methylation of the SPARC promoter -120/+28 luciferase reporter plasmid and assayed for activity by transient transfection. There is a single CpG in the c-Jun responsive region between -120/-70 which corresponds to a HpaII sequence context. Purified plasmid DNA was incubated with recombinant bacterial HpaII methylase in the presence of the methyl donor, *S*–adenosyl methionine (SAM). This resulted in methylation of HpaII/MspI site #4 in the c-Jun responsive region as well as additional sites within the plasmid (Fig. 31). As a control, we prepared a corresponding mock methylated plasmid in which the HpaII methylase was omitted from the reaction. In order to verify the completeness of *in vitro* methylation, an aliquot of HpaII methylated or mock methylated plasmid DNA was analyzed by HpaII and MspI restriction enzyme digestion. Fig. 31, demonstrates that the

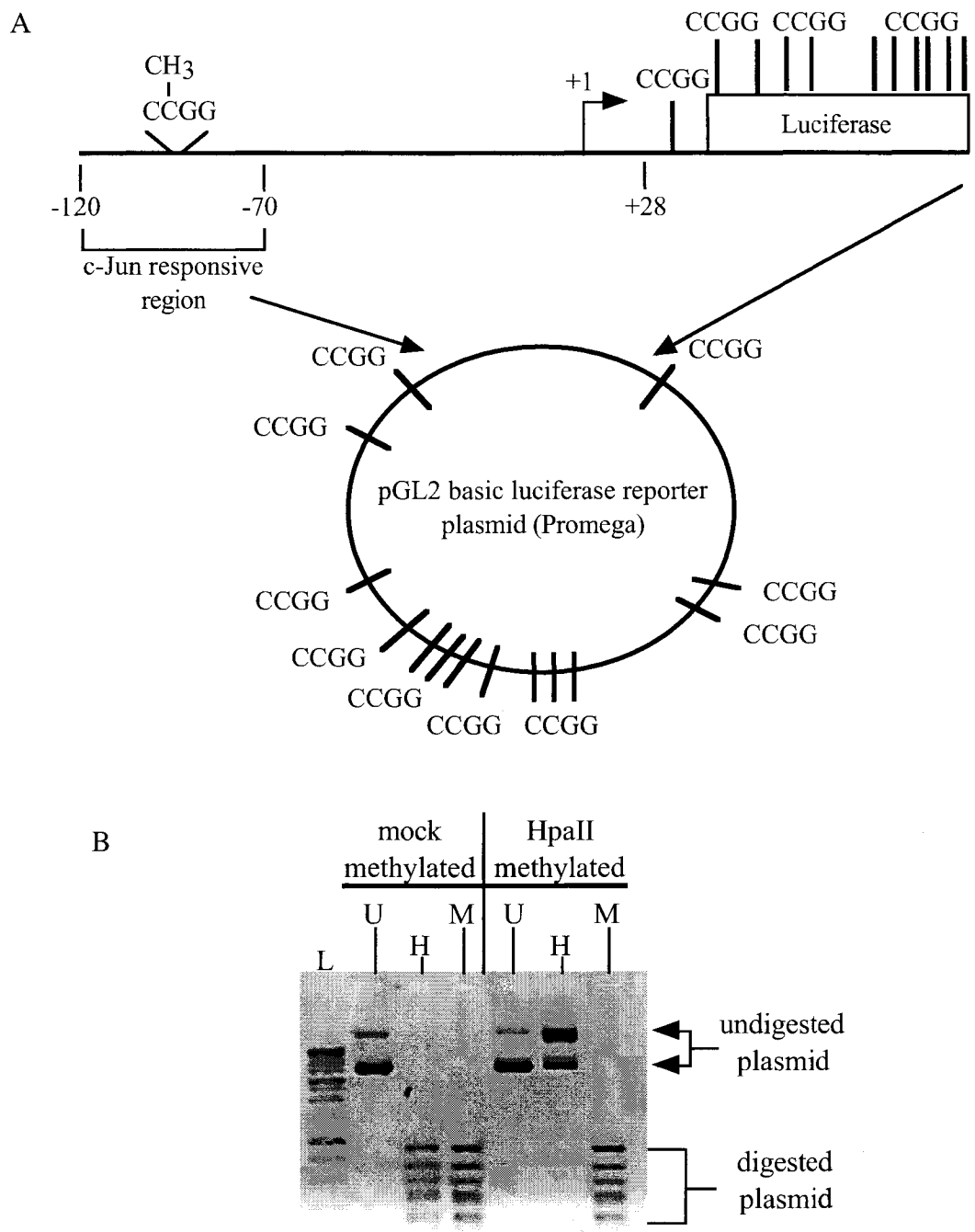

Fig. 31. *In vitro* HpaII methylation of the SPARC promoter (-120/+28) luciferase reporter plasmid. *A*, Schematic representation of all HpaII/MspI sites in the -120/+28 SPARC promoter/luciferase reporter plasmid. CCGG denotes the relative location of HpaII/MspI digestion sites in the pGL2 luciferase reporter plasmid. *B*, Verification of complete HpaII methylation of the SPARC promoter/reporter plasmid. Mock methylated and HpaII methylated plasmids were digested with HpaII or MspI restriction enzyme and analyzed by agarose gel electrophoresis. U= undigested, H= HpaII digested, M= MspI digested.

in vitro methylated plasmid was completely protected from HpaII digestion indicating that it was efficiently methylated.

Next, mock methylated and HpaII methylated SPARC promoter/luciferase reporter plasmids were transiently transfected into vector control/MCF7 and c-Jun/MCF7 cells. Forty-eight hours post-transfection, luciferase values were analyzed as a measure of SPARC promoter activity. As shown in Fig. 32, *in vitro* HpaII methylation of the SPARC promoter (-120/+28)/luciferase reporter plasmid resulted in an 85% decrease in promoter activity in c-Jun/MCF7 cells compared to the mock methylated plasmid. This level of inhibition was similar to the level observed when we deleted the 50 base pair c–Jun responsive region (Fig. 22). As expected, *in vitro* methylation had no effect on SPARC promoter activity in MCF7 cells. Taken together, these results suggest a functional role for SPARC promoter methylation in regulating c-Jun responsiveness.

Analysis of the effect of *in vitro* SPARC promoter methylation on protein/DNA interactions

DNA methylation has been shown to affect transcription by a variety of mechanisms. For example, cytosine methylation can directly inhibit transcription factor binding due to alteration of DNA structure (187, 188). In addition, methylated CpG sequences can serve as recognition sites for methyl binding proteins (189, 190). This can result in competition between sequence specific transcription factors and methyl binding proteins for a common DNA sequence (190). Lastly, methyl binding proteins have been shown to participate in active transcriptional repression via recruitment of histone deacetylase (HDAC) enzymes (190, 191).

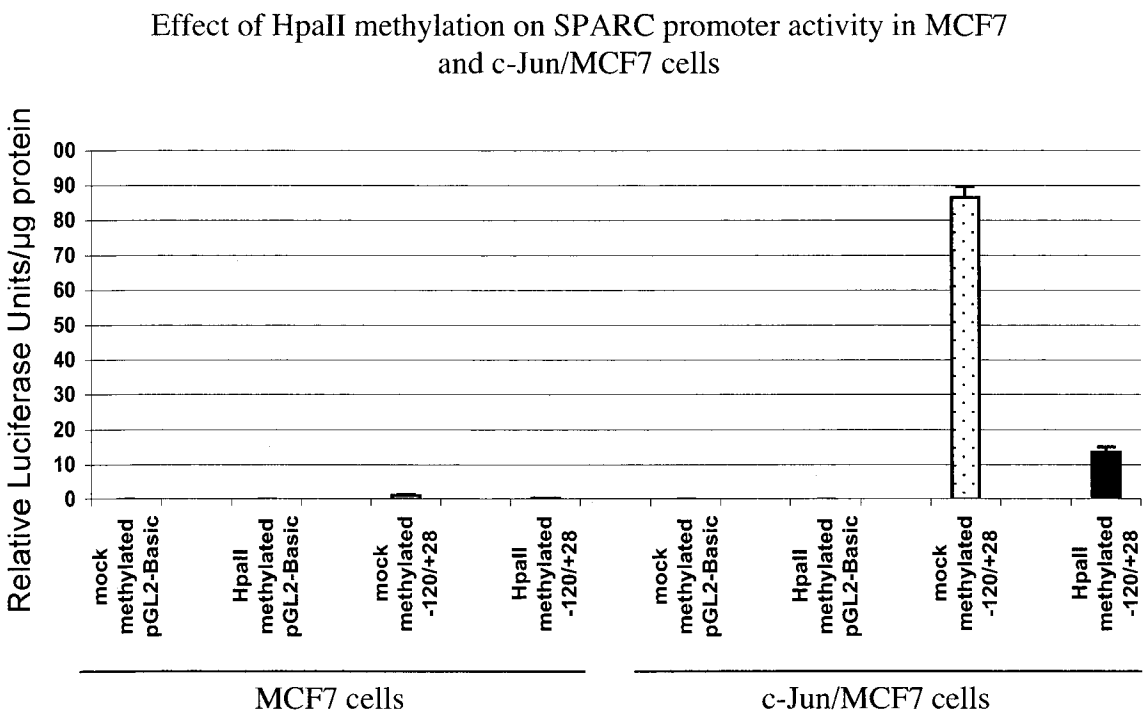

Fig. 32. Effect of *in vitro* SPARC promoter methylation on promoter activity in transient transfection assays. Mock and HpaII methylated plasmids were transfected into vector control/MCF7 and c-Jun/MCF7 cells. Luciferase activity was determined for each sample 48 hours post-transfection. Luciferase values were normalized to protein concentration for each sample and expressed as relative luciferase units/ug of protein. Values represent the average of two independent experiments with each condition tested in duplicate.

In an attempt to characterize the mechanism(s) by which DNA methylation affects SPARC promoter activity, we analyzed the effect of *in vitro* methylation on protein/DNA interactions by gel mobility shift analysis. We hypothesized that DNA methylation may alter protein/DNA interactions at the c-Jun responsive region.

Since our previous gel shift analysis of the -120/-83 region (Fig. 23) did not take into account DNA methylation we re-analyzed this region using mock methylated and HpaII methylated gel shift probes. In order to verify complete methylation of the probe, samples were digested with HpaII and MspI restriction enzymes and analyzed by native polyacrylamide gel electrophoresis. Fig. 33 demonstrates that the *in vitro* methylated probe was completely protected from digestion with HpaII restriction enzyme indicating efficient methylation under these conditions.

Next, *in vitro* methylated and mock methylated probes were analyzed in gel mobility shift assays using nuclear extracts from vector control/MCF7 and c-Jun/MCF7 cells. As shown in Fig. 33, similar band shift patterns were formed with either nuclear extract regardless of the DNA methylation status of the probe. This suggests that *in vitro* protein/DNA interactions at the c-Jun responsive region are unaffected by methylation of HpaII site #4. Based on our previous gel shift competition analysis (Fig. 23) and chromatin immunoprecipitation data (Fig. 25) we believe these complexes to be consistent with Sp family protein/DNA interactions. Interestingly, studies by other laboratories have demonstrated that Sp1 DNA binding is unaffected by cytosine methylation (192). It should be noted that we did not attempt antibody shift analysis for Sp1 in these experiments because we were previously unsuccessful using this approach (Fig. 23). In addition, we did not conduct antibody shift analysis for c-Jun/AP-1 binding

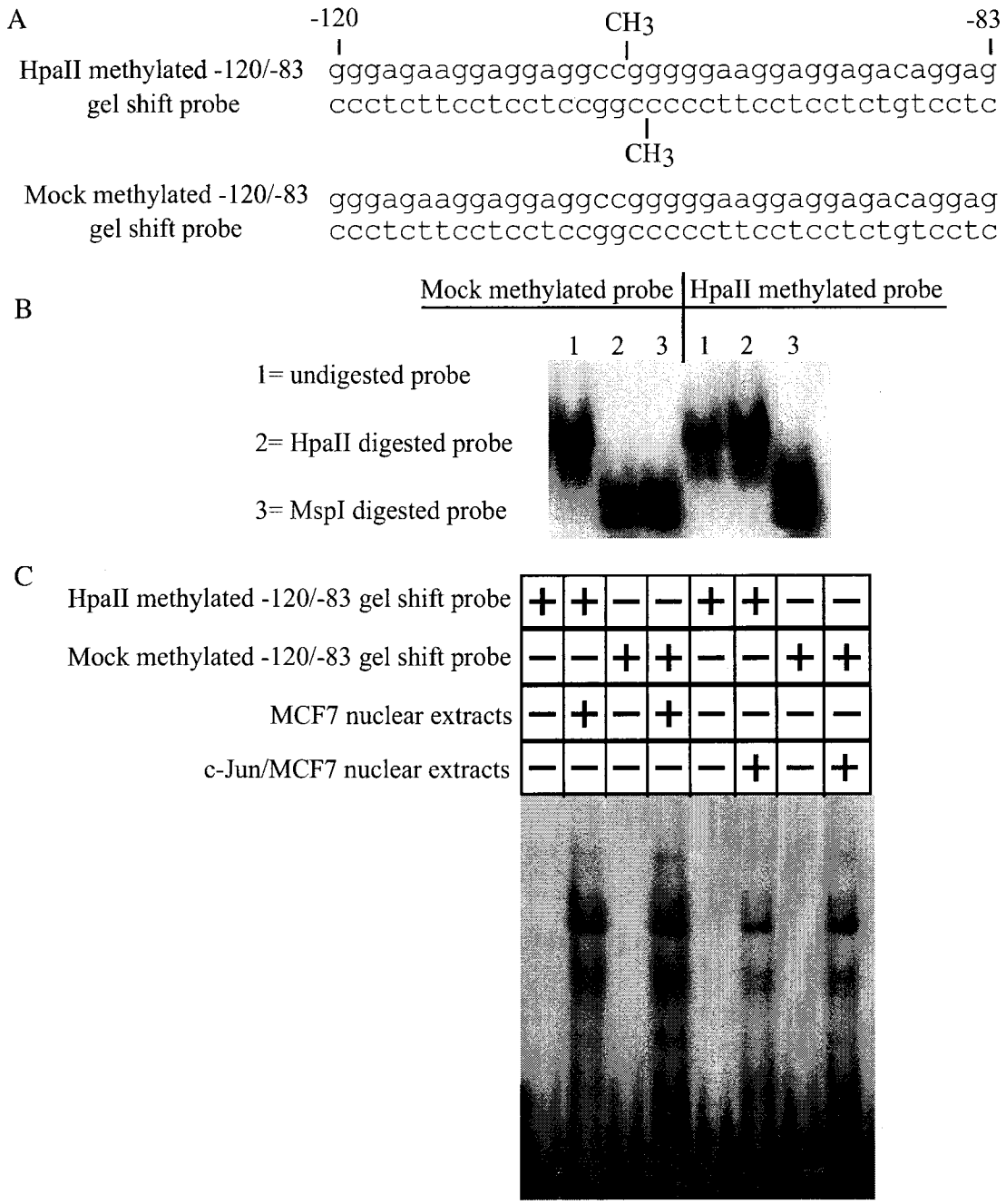

Fig. 33. Effect of *in vitro* methylation of the SPARC promoter –120/-83 region on protein/DNA interactions. *A*, DNA sequence of the gel shift probe used for *in vitro* methylation analysis. The cytosine residue targeted for methylation using recombinant HpaII methylase is indicated by (-CH_3). *B*, HpaII and MspI control digestion reactions demonstrating complete HpaII methylation of the gel shift probe. *C*, Gel shift reactions using mock or HpaII methylated gel shift probes and MCF7 and c-Jun/MCF7 nuclear extracts.

because there was no AP-1 binding site present in the sequence -120/-83. Taken together, our data suggests methylation of the c-Jun responsive region does not inhibit the formation of similar complexes present in both MCF7 and c-Jun/MCF7 nuclear extracts.

Analysis of histone modifications at the SPARC promoter locus

Genomic DNA is arranged in the nucleus as a highly ordered chromatin structure consisting of repeating protein/DNA complexes called the nucleosome (193, 194). A single nucleosome consists of 146 base pairs of DNA coiled around an octameric arrangement of core histone proteins (194-196). This histone core consists of two molecules each of histones H2A, H2B, H3 and H4 (195, 197). Histones H3 and H4 are oriented with the amino terminal protein "tails" radiating outward from the nucleosome core (195). A variety of post-translational modifications are known to occur at these "tail" regions including, acetylation, methylation, phosphorylation, and ubiquitylation (198, 199). Each of these modifications has been associated with either positive or negative regulation of gene expression (200-202). This has led to the "histone code" hypothesis proposed by Allis and Jenuwein which puts forth the idea that the combination of histone tail modifications at a given genomic locus defines the spectrum of transcriptionally active and repressed states (203).

Histone acetylation is a well-characterized modification associated with gene regulation (204, 205). Steady-state histone acetylation patterns are reflective of the balance between histone acetyltransferase (HAT) and histone deacetylase (HDAC) activities. For example, hyperacetylation of histone H3 and H4 has been shown to correlate with increased gene expression, whereas hypoacetylation is associated with

transcriptional repression (199, 201, 206-212). Interestingly, many of the same lysine residues that have been shown to be acetylated can also be methylated (199, 201, 206). A single lysine can be either acetylated or methylated at a given time, but not both. In contrast to acetylation, histone methylation can occur in mono-, di-, or tri-methylated forms (213, 214). Methylation of histone H3 at lysine 4 (K4) is generally associated with gene activation while methylation of histone H3 at lysine 9 (K9) is associated with gene silencing (215-219). Therefore, we expected to see enrichment of methylated histone H3 at lysine 4 in c-Jun/MCF7 cells, whereas in vector control/MCF7 cells we expected to see methylated histone H3 at lysine 9. In addition, we hypothesized that histones associated with the SPARC promoter would be hypoacetylated in MCF7 cells compared to c–Jun/MCF7 cells.

In order to address this hypothesis, we conducted chromatin immunoprecipitation (ChIP) analysis using modification state specific, anti-histone antibodies. A summary of the antibodies used in these studies is shown in Fig. 34. *In vivo* protein/DNA interactions were analyzed following formaldehyde cross-linking of vector control/MCF7 and c–Jun/MCF7 cells. Chromatin from each cell line was isolated and fragmented by sonication. Antibodies were added to diluted chromatin in order to immunoselect protein/DNA complexes specific for individual histone modifications. An antibody specific for HER2/*neu*, a transmembrane receptor protein not expected be at the SPARC promoter, was included as a negative control. In addition, an aliquot of sonicated and crosslinked chromatin was retained and not subjected to immunoprecipitation. This "input" sample was therefore representative of the amount of total chromatin in each immunoprecipitation reaction. Protein/DNA complexes were affinity purified using

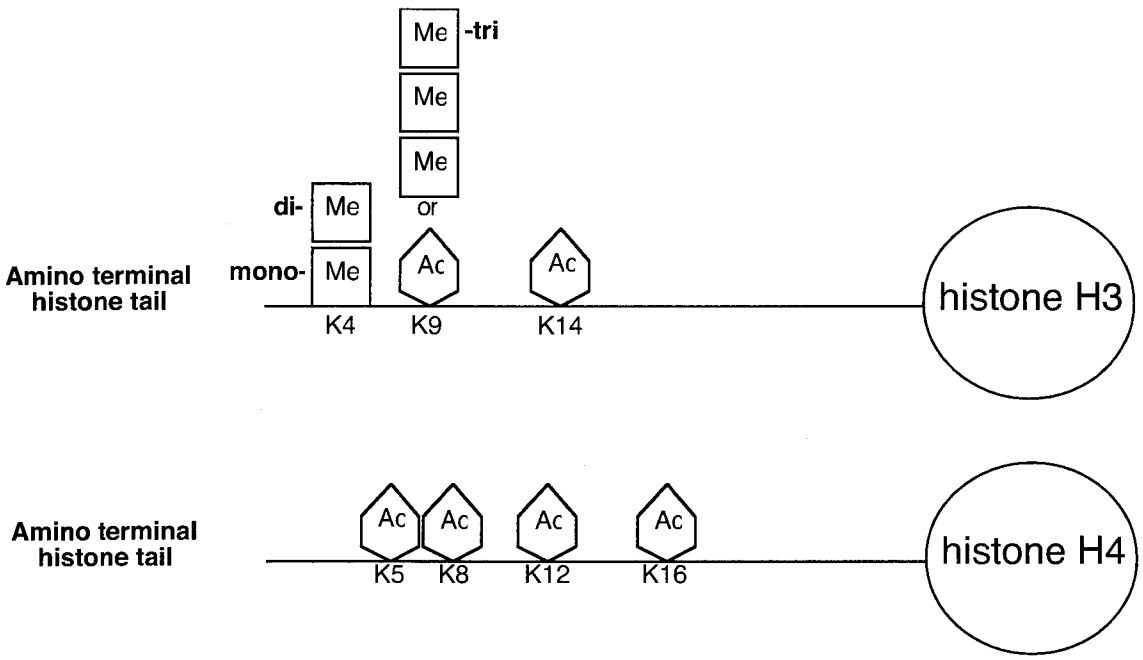

Fig. 34. Schematic representation of histone modifications analyzed by chromatin immunoprecipitation (ChIP) analysis. K= lysine, Ac= acetyl group, Me= methyl group. Numbers following individual lysine residues denote the amino acid position relative to the amino terminus.

protein A/agarose beads. Samples were extensively washed to remove non-specific interactions followed by elution of the immunoselected chromatin. Protein/DNA crosslinks were reversed and the DNA purified. This DNA served as the template for PCR analysis using a primer pair specific for the SPARC proximal promoter region. PCR was conducted using conditions previously shown to be dependent on the amount of input DNA (Fig. 35) and therefore quantitative. PCR amplification products were resolved by agarose gel electrophoresis and quantitated by densitometry. Results were interpreted by comparing the ratio of individual immunoprecipitated DNA signals to the corresponding input DNA signal. The values obtained for each antibody were then compared between cell lines in order to calculate the fold enrichment of each histone modification in c-Jun/MCF7 cells relative to vector control/MCF7 cells.

As shown in Fig. 35, we detected a 2.7 fold enrichment of di-acetylated histone H3 (K9, K14) and a 1.8 fold enrichment of tetra-acetylated histone H4 (K5, K8, K12, K16) at the SPARC promoter region in c-Jun/MCF7 cells relative to vector control/MCF7 cells. Additionally, c-Jun/MCF7 cells demonstrated a 2.8 fold increase in di-methyl histone H3 at lysine 4. Under the conditions tested, we did not observe methylation of histone H3 at lysine 9, a modification strictly associated with constitutive heterochromatin and gene silencing (214, 220, 221). However, we did detect this modification at other genomic loci indicating that the antibody is functional under the conditions tested (Appendix A, Fig. 45).

Taken together, these results demonstrate that the SPARC promoter locus is enriched for histone modifications in c-Jun/MCF7 cells that are consistent with active transcription. However, we were surprised to find these same modifications at the

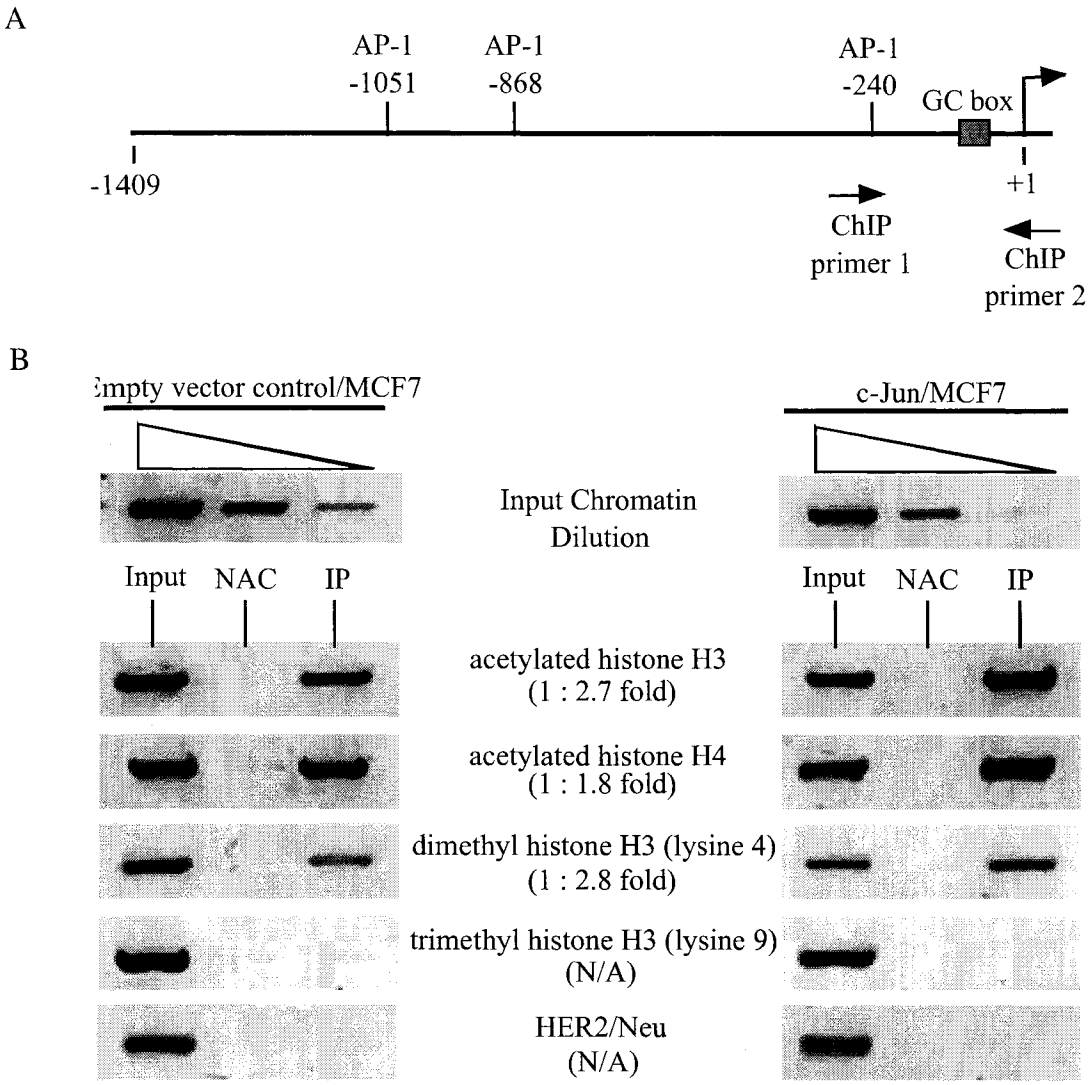

Fig. 35. Chromatin immunoprecipitation analysis of histone modifications at the SPARC promoter locus in MCF7 and c-Jun/MCF7 cells. *A*, Schematic diagram of the SPARC promoter indicating the location of ChIP PCR primers. *B*, Results of PCR analysis of the SPARC promoter region using immunoselected chromatin from vector control/MCF7 and c-Jun/MCF7 cells. Chromatin was immunoprecipitated using the indicated antibodies. PCR amplification products were quantitated by densitometry. The ratio of each immunoprecipitated reaction product, relative to the input chromatin sample, was calculated for each antibody and each cell line. This value was arbitrarily set at one for vector control/MCF7 cells. The corresponding samples from c-Jun/MCF7 cells were then expressed as fold enrichment relative to vector control/MCF7 cells. NAC= no antibody control, IP= immunoprecipitated sample, N/A= quantitation could not be done because the signal for IP reactions was not above background.

transcriptionally inactive SPARC locus in MCF7 cells. We interpret these results to mean that there are subtle differences in histone modifications between vector control/MCF7 and c-Jun/MCF7 cells. This interpretation would be consistent with the localized demethylation of the SPARC promoter observed in c-Jun/MCF7 cells.

Analysis of SPARC expression in MCF7 cells treated with the histone deacetylase inhibitor, trichostatin A

To further characterize the role of histone modification on SPARC gene expression we examined the effect of the histone deacetylase inhibitor, trichostatin A (TSA). TSA has been shown to induce hypoacetylation of histones resulting in an increase in gene expression (222). Furthermore, TSA used in conjunction with the DNA methyltransferase inhibitor, 5-aza-dC, has been shown to result in synergistic activation of transcriptionally silenced genes (223-225).

Vector control/MCF7 were treated with vehicle, 5-aza-dC alone, TSA alone, or a combination of 5-aza-dC and TSA. RNA was then harvested and assayed for SPARC expression by semi-quantitative RT-PCR. As shown in Fig. 36, 5-aza-dC treatment was sufficient to induce SPARC gene expression. This result was consistent with our previous results (Fig. 26) which demonstrated a dose dependent increase in SPARC gene expression following 5-aza-dC treatment. In contrast, treatment of MCF7 cells with TSA alone did not result in an increase in steady-state SPARC mRNA levels. When the DNA methyltransferase inhibitor (5-aza-dC) and histone deacetylase inhibitor (TSA) were used in combination, we saw no additive or synergistic effect on SPARC gene expression.

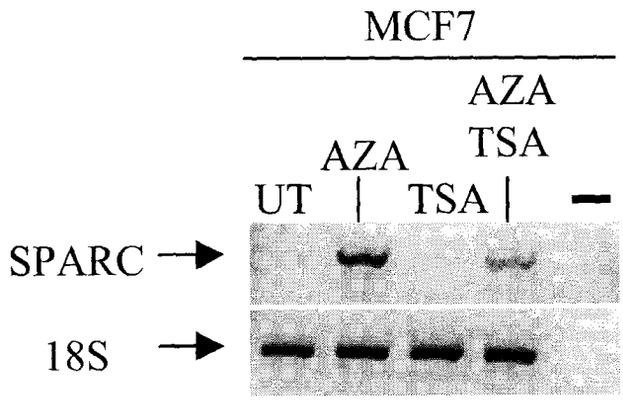

Fig. 36. Analysis of SPARC expression in MCF7 cells following treatment with the histone deacetylase inhibitor, trichostatin A. Cells were treated with vehicle, 5-aza-dC (5μM), trichostatin A (100ng/ml), or a combination of 5–aza-dC (5μM) and trichostatin A (100ng/ml). Total RNA was isolated from each sample and analyzed by for SPARC expression by semi-quantitative RT–PCR. UT= untreated, AZA= 5'aza-2'deoxycytidine, TSA= trichostatin A, (-)= negative RT-PCR control in which template was omitted from the reaction.

Taken together, these results suggest that DNA methylation, not histone acetylation, is the critical epigenetic determinant associated with SPARC gene expression.

CHAPTER IV

DISCUSSION

The gene, SPARC, is highly expressed in many types of cancer, including tumors of the breast. Importantly, SPARC has been shown to directly contribute to tumorigenesis and malignant progression. We have previously shown that constitutive expression of the transcription factor c-Jun results in SPARC gene activation and phenotypic progression in a MCF7 breast cancer model system. The studies described in this dissertation addressed two primary objectives: 1.) to determine the contribution of SPARC to c-Jun induced phenotype in a MCF7 breast cancer model system, and 2.) to determine the mechanisms by which c-Jun regulates SPARC gene expression. In this chapter we will summarize our findings and discuss the results in the context of the literature.

A. The Effects of SPARC on MCF7 Cell Phenotype

Cell Proliferation

The goal of Aim 1 was to determine the effects of SPARC gene expression on MCF7 cell phenotype. Several studies have shown that SPARC is associated with decreased cell proliferation (101, 107, 108). In support of this observation, SPARC expression is inversely correlated with cell proliferation rate in c-Jun/MCF7 cells. However, it was unclear which c-Jun target gene(s) may play a role in regulating this phenotype. In order to address this question, stable cell lines were generated in order to address the extent to which overexpression of SPARC, alone, is sufficient to inhibit MCF7 cell proliferation. The results presented in Fig. 9 demonstrate that constitutive

overexpression of SPARC in MCF7 cells results in an intermediate cell proliferation rate compared to vector control/MCF7 cells and c-Jun/MCF7 cells. Importantly, the results were statistically significant ($P = <.05$) in each of the three SPARC/MCF7 stable cell lines tested.

The exact mechanism by which SPARC alters cell proliferation remains unclear. One possibility is that SPARC attenuates cell signaling required for tumor cell proliferation. In support of this hypothesis, SPARC has been shown to inhibit growth factor receptor signaling via interaction with platelet derived growth factor (PDGF) receptor and vascular endothelial growth factor (VEGF) receptor (102, 104, 117). Another possibility is that altered expression of other c-Jun regulated genes is needed in order to achieve the same level of inhibition seen in c-Jun/MCF7 cells. For example, expression of genes involved in cell cycle regulation, such as $p16^{INK4a}$ and $p21^{CIP1/Waf1}$ may provide an additional effect, in addition to SPARC, resulting in decreased cell proliferation (51).

Cell Motility and Invasion

Next, SPARC/MCF7 stable cell lines were analyzed for their *in vitro* migratory and invasive potential. Previous studies have shown that increased SPARC expression promotes an intermediate attachment state which facilitates cell movement (103, 127). The processes of directional movement and degradation of reconstituted basement membrane are essential steps for tumor invasiveness and malignant progression. These processes are also mechanistically coupled. In order for a cell to exhibit invasiveness it

must be both motile and exhibit increased proteolytic activity in order to break through a reconstituted basement membrane.

In Figure 10, we demonstrate that overexpression of SPARC, in the absence of exogenous c-Jun, is not sufficient to promote MCF7 cell motility and invasion *in vitro* (Fig. 10). This result is in agreement with a previous study which showed that addition of recombinant SPARC to MCF7 cells also failed to promote invasiveness (226).

Next, we addressed the question of whether SPARC expression was required for c-Jun induced cell motility and invasion. To accomplish this goal, an antisense approach was used to inhibit SPARC expression. This approach resulted in a transient decrease in SPARC protein levels (Fig. 12). This decrease in SPARC expression also correlated with a statistically significant decrease in c-Jun induced cell motility and invasion (Fig. 13). These results are consistent with a previous report using a mouse model of malignant melanoma. In this previous study, inhibition of SPARC expression reduced tumor cell invasiveness *in vitro* and abrogated tumor formation in mice *in vivo* (126).

From our studies, it appears that other c-Jun target genes cooperate with SPARC to promote an invasive phenotype. For example, c-Jun/AP-1 has been shown to stimulate expression of the matrix metalloproteases (MMPs). Transient transfection of c-Jun in the invasive breast cancer cell line, MDA-MB-231, stimulates both MMP-2 and MMP-9 expression (227). Furthermore, MMP-9 enzymatic activity was shown to be increased in c-Jun/MCF7 stable cell lines (46). In addition, SPARC enhances MMP-2 proteolytic activity in two invasive breast tumor cell lines (MDA-MD-231 and BT549) as well as the invasive prostate cancer cell lines PC3 and DU145 (226). We hypothesize that SPARC

may be acting in an autocrine and/or paracrine fashion enhancing both MMP expression as well as MMP activation thereby contributing to invasiveness.

However, increased MMP expression may not account for enhanced cell motility. It is possible that expression levels of SPARC modulate cell attachment, thereby, contributing to altered cell motility. SPARC is known to function as an anti-adhesive protein and expression correlates with decreased focal adhesion contacts (102, 104, 119). It is thought that if the cell were too firmly attached to the substratum then cell migration would be inhibited. Conversely, if the cell were too loosely attached, then the cell may undergo apoptosis or anoikis. Since we observe inhibition of both motility *and* invasion, it is unclear whether this is the result of decreased motility alone or also due to decreased proteolytic activity. Future studies using an approach such as gel zymography analysis would be useful in determining the extent to which SPARC regulates MMP enzyme activity. Taken together, the cell proliferation and motility/invasion data are consistent with the hypothesis put forth by Giese and colleagues that tumor cells can "grow" or "go", but cannot do both simultaneously (118, 228).

B. SPARC Promoter Regulation

Mapping the c-Jun Responsive Region

Having established that SPARC is a phenotypically relevant c-Jun target gene, we turned our attention to the regulation of SPARC gene expression. The goals of Aim 2 were to map the c-Jun responsive region(s) of the human SPARC promoter and to identify the *trans* acting factors which contribute to differential SPARC gene activation.

A previous study defined the SPARC promoter as the 1409 base pairs 5' of the transcriptional start site (129). This promoter region was cloned upstream of a luciferase reporter gene and assayed by transient transfection. Figure 16 demonstrates increased SPARC promoter activity in c-Jun overexpressing cell lines, but not empty vector control/MCF7, or JunD/MCF7 cells. These results are consistent with our previous observation that overexpression of JunD did not result in an increase in SPARC gene expression (131). Therefore, we conclude that the related *JUN* family members, c-Jun and JunD, differ in their ability to regulate SPARC promoter activity.

The direct model of c-Jun/AP-1 mediated transcriptional regulation involves dimerization, followed by DNA binding to an AP-1 site and subsequent recruitment of transcriptional coactivators. The culmination of these events is thought to result in stabilization of the transcription pre-initiation complex (53, 61, 70, 96, 99). Sequence analysis of the human SPARC promoter revealed three potential AP-1 binding sites that differed from a consensus context by a single nucleotide. Gel mobility shift analysis was used to examine AP-1 binding activity in empty vector control/MCF7, JunD/MCF7 and c-Jun/MCF7 nuclear extracts. The results demonstrated AP-1 binding only to the –1051/–1045 site and only in c-Jun/MCF7 nuclear extracts (Fig. 17). These results are consistent with our previous promoter/reporter data which showed that c-Jun upregulated the SPARC promoter, but JunD did not. This is also consistent with the relative AP-1 binding activity in c-Jun/MCF7 and JunD/MCF7 nuclear extracts when assayed using a consensus AP-1 element (Appendix A, Fig. 39). The specificity of binding to the –1051/–1045 site was demonstrated by oligonucleotide competition analysis using a consensus AP-1 probe. The results shown in Fig. 18 demonstrated that the major shifted

complex was consistent with AP-1 and this was confirmed using antibodies specific for c-Jun and Fra–1 (Fig. 19). These results suggested a direct role for this site in mediating c-Jun activation of the SPARC promoter. In addition, this result suggests that the other two AP-1 sites (-868/-862 and –241/-235) are not in a favorable sequence context, most likely due to the effects of sequences flanking the core binding site.

c-Jun and Fra-1 are upregulated in invasive breast cancer cell lines and clinical tumor samples (20, 44). Furthermore, c-Jun and Fra-1 appear to be the preferred dimer combination in this MCF7 model system when c-Jun is overexpressed (Fig. 19 and Appendix A, Fig. 39). The functional importance of increased Fra-1 expression was recently shown in a study which demonstrated that overexpression of Fra-1 was sufficient to promote invasiveness *in vitro* (229). Conversely, inhibition of Fra-1 expression by RNAi resulted in decreased invasiveness exhibited by the MDA-MB-231 breast cancer cell line (229). Future studies using a similar RNAi approach in the MCF7 model system would be useful in determining the role of c-Jun/Fra-1 heterodimers in regulating SPARC gene expression and malignant phenotype.

Next, in order to determine the contribution of the –1051/-1045 AP-1 binding site to SPARC promoter regulation, point mutations were made to the core binding sequence. As expected, mutation of this site to a consensus context resulted in increased AP-1 binding in gel mobility shift assays (Fig. 20). Conversely, altering the site so that two additional nucleotides were mutated resulted in a decrease in AP-1 binding (Fig. 20). We reasoned that if the AP-1 site played a role in regulating SPARC promoter activity, then DNA binding would correlate with promoter activity. To test this hypothesis, these mutations were made in the context of the full-length (–1409/+28) SPARC promoter.

Even though we were able to show increased DNA binding *in vitro* by mutating the AP-1 site to a consensus context, this did not result in an increase in SPARC promoter activity in c-Jun/MCF7 cells (Fig. 20). In addition, the mutation which decreased AP-1 binding had no significant effect on SPARC promoter activity. These results suggest that the –1051/-1045 site was not required for c-Jun responsiveness and prompted us to examine the extent to which any of the three AP-1 sites were required.

This question was addressed by analyzing a truncated promoter construct in which ~1300 nucleotides (–1409 to –121) were deleted. This resulted in removal of all obvious AP-1 binding sites. The results presented in Fig. 21 demonstrate that the truncated –120/+28 SPARC promoter retains ~85% of the activity in c-Jun/MCF7 cells when compared to the full-length (-1409/+28) construct. These results suggest two things: 1.) that the major c-Jun responsive region lies within this 148 base pair sequence and 2.) that the AP-1 sites are dispensable for c-Jun responsiveness.

In order to more precisely map the c-Jun responsive region, an additional SPARC promoter deletion mutant was generated. The results presented in Fig. 22 demonstrate that the region between –120 and –70 is required for c-Jun responsiveness. This result is consistent with a previous study which indicated that activation and/or repression is regulated by DNA sequences in the region from –120 to –70 (129). Furthermore, this is the same region previously shown to be required for downregulation of the chicken and human SPARC promoter by v-Jun in primary chicken embryo fibroblasts (130). Since the AP-1 sites were dispensable for c-Jun responsiveness, we hypothesized that another sequence specific transcription factor may confer DNA binding. The presence of a guanine and cytosine (GC) rich sequence between –120 and –70 suggested that Sp family

proteins may bind to this region. Sp1 binds GC rich sequences in TATA-less promoters and can play a dual role as an activator or repressor depending on the context (158, 230, 231). Furthermore, c-Jun and Sp1 cooperate resulting in activation of other genes such as $p21^{WAF1/Cip1}$, keratin 16 and vimentin (93, 232-234).

In order to test this hypothesis, gel mobility shift experiments were conducted. Oligonucleotide competition analysis using a consensus Sp1 probe demonstrated that two complexes (complexes 1 and 3) were specifically inhibited (Fig. 23). These complexes were present in both MCF7 and c-Jun/MCF7 nuclear extracts supporting the idea that Sp1 may play a dual role by binding to this region. Furthermore, chromatin immunoprecipitation (ChIP) analysis demonstrated that Sp1, c-Jun and Fra-1 physically associate with the SPARC promoter locus in intact cells (Fig. 25). Importantly, c-Jun was not bound at an unrelated locus on chromosome 11 (estrogen receptor alpha locus) thereby demonstrating specificity (Appendix A, Fig. 47). Based on the ChIP data, we conclude that SPARC is a *bona fide*, direct AP-1 target gene.

A recent study examined the role of Sp family proteins in regulating the SPARC promoter by utilizing *Drosophila* SL2 cells, which are devoid of endogenous Sp family genes. In this study, increasing amounts of Sp1 or Sp3 expression constructs were co-transfected in SL2 cells, along with either the –120/+28 or –70/+28 SPARC promoter/reporter plasmids (131). The region from –120 to –70 (the previously mapped c-Jun responsive region) was also shown to be required for Sp1 responsiveness in this system (131). These experiments provided the first direct evidence that Sp family proteins are capable of transactivating the SPARC promoter.

Similarly, the chicken promoter is also activated in response to Sp1 in the *Drosophila* SL2 system (156). However, when v-Jun was co-expressed, there was an ~60% decrease in Sp1 dependent transcription (156). This same study showed that v-Jun mediated repression was via a direct mechanism. Chromatin immunoprecipitation demonstrated v-Jun protein physically associated with the plasmid template when transcription was repressed (156). This result is consistent with our current studies where we are able to demonstrate AP-1 and Sp1 binding in a chromatinized context in c–Jun/MCF7 cells (Fig. 25). But, rather than repression, we find that c-Jun activates the human SPARC promoter in these cells. The reason for this dichotomy regarding SPARC gene regulation is not known. It is likely that cell type specific factors play a role in this process since downregulation of SPARC by v-Jun and/or c-Jun is consistent in fibroblasts, whereas upregulation of SPARC occurs in epithelial cells when c-Jun is overexpressed.

We propose that Sp1 serves as a sequence specific DNA binding component at the SPARC locus. c-Jun and Sp1 have been shown to interact so it is tempting to speculate that this may be occurring at the SPARC promoter as a mechanism for transcriptional activation. The interaction between Sp1 and c-Jun is mediated by the glutamine rich region of Sp1 and leucine zipper region of c-Jun (93, 234). This same region of Sp1 interacts with the basal transcription factors including TATA binding protein, TAF4 and TAF7 (235, 236) . In addition, c-Jun interacts with TFIIB, TAF1 and TATA binding protein (96, 97). Therefore, it is possible that AP-1 and Sp1 cooperate to stabilize assembly of the transcription pre-initiation complex.

C. Epigenetic Regulation of SPARC Gene Expression

The results obtained in Aim 2 established that a cytosine and guanine rich region (-120/-70) of the SPARC promoter was required for c-Jun responsiveness. The 5' carbon of cytosine in a cytosine-phosphate-guanine (CpG) context has been shown to undergo methylation (165-167). Importantly, CpG methylation patterns have been shown to change during tumorigenesis (168-171). The degree of DNA methylation in promoters tends to be inversely correlated with gene expression levels. The MCF7 and c-Jun/MCF7 model system used in these studies represents transcriptionally "inactive" (MCF7) and "active" (c-Jun/MCF7) states with respect to SPARC gene expression suggesting active repression or gene "silencing". The goal of Aim 3 was to analyze the epigenetic modifications associated with SPARC gene expression starting with DNA methylation.

The Effect of DNA Methyltransferase Inhibition on SPARC Expression

In order to determine the role of DNA methylation in SPARC gene regulation we used a pharmacological inhibitor of DNA methyltransferase enzymes, 5-aza-2' deoxycytidine (5-aza-dC). This reagent has been used to reactivate genes silenced by DNA methylation (182, 183). The results shown in Fig. 26 demonstrate a dose dependent increase in steady-state levels of SPARC mRNA in MCF7 cells where SPARC was previously undetectable. In contrast, 5-aza-dC had no effect on SPARC levels in c–Jun/MCF7 cells. This suggested that the SPARC promoter is methylated in MCF7 cells, but demethylated in c-Jun/MCF7 cells where SPARC gene expression was already active. These results are consistent with a recent study in which 5-aza-dC treatment of lung cancer cells resulted in increased SPARC gene expression (237).

Next, a time course experiment was conducted in order to determine the kinetics of SPARC gene activation in response to 5-aza-dC. SPARC transcripts were detectable as early as 24 hours following initial treatment with 5-aza-dC (Fig. 26). The maximal effect on SPARC steady state mRNA levels was achieved by 48 hours with no appreciable increase after that. The MCF7 cells used in this study were previously shown to have a doubling time of 37 hours (46). Therefore, it would be expected to take 74 hours for a CpG site to become demethylated on both strands of DNA. Therefore, our results suggest an active, rather than a passive, mechanism of DNA demethylation at the SPARC promoter.

Since, DNA methylation patterns are faithfully conserved during replication, any changes are expected to be maintained in daughter cells. Therefore, we wanted to determine the extent to which demethylation and SPARC gene activation was reversible. 5-aza-dC was removed from the MCF7 growth media and cells were passaged regularly as subconfluent populations for an additional 60 days (Fig. 26). Our results demonstrate that SPARC mRNA levels persist long after 5-aza-dC is removed. This suggests that DNA demethylation may serve as an epigenetic "hit" leading to mitotically heritable gene activation. These observations are important from a clinical standpoint since DNA methyltransferase inhibition is being tested as a therapeutic strategy to reactivate silenced tumor suppressor genes (179). Therefore, it is important to better understand the pleiotropic effects of DNA methyltransferase inhibitors on genes such as SPARC, which are capable of contributing to the malignant phenotype.

Mapping SPARC Promoter DNA Methylation

Our previous experiments using 5-aza-dC suggested that DNA methylation plays a role in regulating SPARC gene expression in MCF7 cells. We hypothesized that this is a mechanism for transcriptional repression in MCF7 cells and that c-Jun relieves this repression. This would provide an explanation for the "off" and "on" type of transcriptional regulation in this model system. In order to determine the extent of SPARC promoter methylation in each cell line, we analyzed the methylation status of CpG sequences using HpaII/MspI mapping. The results confirmed that the SPARC promoter is methylated in MCF7 cells at each of the four HpaII/MspI sites analyzed (Fig. 28). In contrast, the proximal promoter region, including the previously mapped c-Jun responsive element, becomes demethylated in response to c-Jun overexpression. These observations were confirmed and extended by using sodium bisulfite modification of genomic DNA followed by DNA sequencing. Using this approach we were able to determine the methylation status of 17 CpG residues spanning the entire SPARC promoter region. As shown in Fig. 28, the SPARC proximal promoter is demethylated in response to constitutive c-Jun overexpression. Importantly, this demethylation is localized to the 3' region of the promoter including the region previously identified as the c-Jun responsive element.

To our knowledge, this is the first high-resolution map of DNA methylation at the human SPARC gene promoter. It is unclear why there is a discrete boundary between proximal and distal promoter methylation in c-Jun/MCF7 cells. We hypothesize that the physical distance between CpG clusters may buffer, or insulate, the effects occurring in either region making these *cis* elements independent of one another. Another possibility

is that c–Jun/AP-1 specifically targets demethylation to the proximal promoter region. It is unclear from our current studies whether DNA demethylation preceedes, or occurs subsequent to, SPARC gene activation. Future studies using an inducible system to regulate c-Jun expression will be useful in defining the chronology of events leading to SPARC gene activation.

In contrast to what is known about the process of DNA methylation, the process of DNA demethylation is poorly understood. There are several mechanisms by which promoter demethylation and gene reactivation are thought to occur. Evidence suggests that the methyl binding protein, MBD2, exhibits demethylase activity and may be responsible for *de novo* demethylation (238). Alternatively, DNA demethylation can occur via a passive mechanism. This can occur via DNA methyltransferase inhibition resulting in sequential loss of methylation on both strands of DNA following two rounds of replication (239, 240). These mechanisms are not mutually exclusive and future studies will be needed to determine how the SPARC gene locus becomes demethylated in response to c-Jun.

The Effect of Methylation on SPARC Promoter Activity and Protein/DNA Interactions

Next, we sought to determine the extent to which DNA methylation plays a functional role in SPARC promoter regulation. In order to accomplish this, we conducted *in vitro* methylation of the SPARC promoter/luciferase reporter plasmid followed by transient transfection. The SPARC promoter fragment spanning nucleotides –120 to +28 was analyzed, since this region becomes demethylated and contains the

previously mapped c-Jun responsive element. Fortuitously, a single CpG (HpaII site #4) lies within the c-Jun responsive region (Fig. 31). This allowed for specific methylation of this site using recombinant HpaII methylase while leaving other CpGs in the SPARC proximal promoter region unmodified.

As shown in Fig. 31, methylation of HpaII site #4 resulted in a 75% reduction in SPARC promoter activity in response to c-Jun. Since overexpression of c-Jun promotes demethylation at the endogenous SPARC locus, it is tempting to speculate that the residual promoter activity in c-Jun/MCF7 cells is due to progressive demethylation of the *in vitro* methylated plasmid over the 48 hour transfection period. This could be addressed in future studies by analyzing the degree to which methylation is retained on the transfected, *in vitro* methylated plasmid DNA template. By comparing the methylation status over time, it would be possible to determine whether demethylation, in this context, occurs in c-Jun overexpressing cells and the extent to which this might correlate with relative SPARC promoter activity.

Our data supports a model where SPARC promoter methylation is not simply a byproduct of transcriptional repression. Instead, DNA methylation of the c-Jun responsive element is sufficient to repress transactivation. In addition, our studies suggest an explanation for previous observations in which transiently transfected SPARC promoter constructs were active in HeLa and HepG2 cells, but endogenous SPARC gene expression was undetectable (129). We hypothesize that the endogenous genomic locus may be methylated in these cells in contrast to the transfected plasmid DNA.

Next, we examined the effect of *in vitro* methylation on protein/DNA interactions by gel mobility shift analysis. We used the same gel shift probe (-120/-83) which

demonstrated Sp family binding activity in order to determine if specific methylation at HpaII site #4 altered the protein binding pattern (Fig. 33). Previous studies have shown that Sp1/Sp3 DNA binding are not affected by CpG methylation (192). In agreement with these studies, our results demonstrate that similar protein/DNA complexes are observed in the presence, or absence, of HpaII methylation. Based on our previous gel mobility shift data (Fig. 23) and chromatin immunoprecipitation analysis (Fig. 25) we attribute this binding to Sp family proteins. Taken together, our data supports the hypothesis that Sp1 is present at the SPARC locus, regardless of the methylation status. This suggests that Sp1 participates in a repression complex in the absence of c-Jun overexpression and then becomes an activator of SPARC transcription in the presence of c-Jun.

How can Sp1 play dual roles in regulating SPARC gene transcription? One candidate protein which may act as a bifunctional modulator of Sp1 is MCAF (MBD1 chromatin associated factor). MCAF has been shown to function as a both an activator as well as a repressor of gene transcription (241). As the name implies, MCAF can physically associate with the methyl binding protein, MBD1, but has also been shown to bind Sp1 as well (241). Interestingly, the murine homolog of MCAF, mAM, was previously shown to interact with the murine ATFa, a known Jun dimerization partner (242). This interaction between MCAF and ATFa correlates with recruitment of the basal transcription machinery components TFIIE, TFIIH and RNA polymerase II (242). Based on these studies, it is tempting to speculate that MCAF may be a missing link in deciphering the precise mechanism of SPARC gene regulation by Sp1 and AP-1. We envision a scenario where Sp1/MBD1/MCAF exist in a ternary complex at the SPARC

promoter and mediate repression in MCF7 cells. In this case MCAF would confer repressor function to Sp1. Then, following c-Jun overexpression, AP-1 may compete with MBD1 resulting in a Sp1/AP–1/MCAF activation complex. Further biochemical characterization will be required to confirm this hypothesis.

Analysis of DNA Methyltransferase Expression in MCF7 and c-Jun/MCF7 Cells

As a follow up study, we explored the possibility that c-Jun alters the expression of DNMT 1, DNMT3a and/or DNMT3b resulting in aberrant genomic DNA methylation patterns. In support of this hypothesis, previous studies have shown that c-Jun and c-Fos stimulate DNMT1 expression (94, 243). Therefore, we examined the relative expression levels of DNA methyltransferase genes in MCF7 and c-Jun/MCF7 cells.

As shown in Appendix A, Fig. 43, c-Jun overexpression in MCF7 cells induces a modest increase in DNMT1 steady state mRNA levels. However, the most notable difference observed was in the expression pattern of multiple DNMT3b isoforms. By using an oligonucleotide primer pair flanking potential 3' DNMT3b mRNA splice sites, several known splice variants are detectable in MCF7 and c-Jun/MCF7 cells. Interestingly, increased expression of DNMT3b isoforms has been demonstrated in human cancers (244, 245). Specifically, DNMT3b4 expression correlates with DNA hypomethylation at pericentromeric repeats and is associated with chromosome instability in hepatocellular carcinomas (246). In addition, MCF7 cells express primarily DNMT3b2, whereas T24 bladder cancer cells express mainly the DNMT3b3 isoform (247). Several of these alternatively spliced transcripts are expected to yield catalytically inactive isoforms suggesting they may have other, as of yet, undetermined roles in DNA

methylation (178, 248). Taken together, the data suggests that altered expression of DNMT3b isoforms may play a role in regulating SPARC promoter methylation. Exploring this possibility will be the focus of future studies.

Analysis of Histone Modifications at the SPARC Promoter Locus

DNA methylation changes are known to correlate with post-translational modification of histone "tails" (249, 250). Therefore, we used chromatin immunoprecipitation to analyze specific histone modifications at the SPARC promoter locus. Characterization of the proximal promoter region in c-Jun/MCF7 cells revealed changes known to be associated with gene activation (Fig. 35). For example, we observed an increase in acetylated histone H3 and H4 as well as methylation of histone H3, specifically at lysine 4. The fact that there is a basal level of acetylated histones and H3-K4 methylation in empty vector control/MCF7 cells suggests that this is a euchromatic locus, even though gene expression is not active in these cells. In support of this idea, we did not detect tri-methylation of histone H3 at lysine 9, in either cell line, further suggesting that the locus does not reside in a heterochromatic region. To our knowledge, this is the first analysis of histone modifications at the SPARC promoter. These modifications constitute the "histone code" at the locus.

The histone "code", together with DNA methylation patterns, comprise a larger epigenetic "code" recognized by transcriptional regulators. We envision a scenario where chromatin modifying proteins are specifically targeted to the c–Jun responsive region of the SPARC promoter. The net result of such recruitment is transformation of the locus from a repressed state to an activated state. In addition, it is likely that these

c–Jun induced changes antagonize the repression machinery and serve to maintain the activated state of SPARC gene transcription. For example, both AP-1 and Sp1 have been shown to interact with the histone acetyltransferase CBP/p300 (99, 251). Recruitment of CBP/p300 to the SPARC proximal promoter region would be expected to result in an increase in the level of acetylated histones at the locus. This hypothesis could be tested by chromatin immunoprecipitation analysis of the SPARC promoter using a CBP/p300 specific antibody.

A similar mechanism of targeted recruitment may account for elevated levels of H3-K4 dimethylation at the SPARC promoter (Fig. 35). In support of this idea, a recent study demonstrated that the H3-K4 specific methyltransferase, SET7/9, is involved in regulation of the AP–1 target gene, collagenase (252). This study showed that SET7/9 physically associates with the collagenase promoter at low levels prior to collagenase gene induction and then becomes enriched at the locus concomitant with AP–1 binding and transcriptional activation (252). A similar scenario may explain the basal level of H3-K4 methylation observed in MCF7 cells. Therefore, the presence of this modification may render the locus "poised" for activation prior to c-Jun induction.

A final experiment was conducted to demonstrate the extent to which histone acetylation/deacetylation contributes to SPARC gene regulation. MCF7 cells were treated with the histone deacetylase inhibitor trichostatin A (TSA) and SPARC steady state mRNA levels determined by semi-quantitative RT-PCR. TSA is a well characterized, non-competitive inhibitor of histone deacetylase enzymes (222). Previous studies have shown reactivation of silenced genes in response to TSA (223, 224). Depending on the context, treatment with TSA and 5-aza-dC can result in synergistic

activation of gene expression (191, 223, 224). The results presented in Figure 36 show that SPARC expression was increased only by 5-aza-dC and not TSA, alone, or in combination with 5-aza-dC. This result demonstrates that, in MCF7 cells, repression of SPARC gene transcription occurs via a TSA insensitive mechanism. This is consistent with the relative enrichment of acetylated histones at the SPARC locus in MCF7 cells and suggests that maintenance of the repressed state is HDAC independent. This strengthens the argument that, in MCF7 cells, DNA methylation is the dominant epigenetic modification regulating SPARC gene expression.

Analysis of c-Jun Induced Epigenetic Changes at the Human Vimentin and Estrogen Receptor Alpha Gene Loci

In our MCF7 model system, expression of another gene, vimentin, is regulated in an "off" and "on" manner similar to SPARC (51). Vimentin is an intermediate filament protein expressed in cells of mesenchymal origin and has, therefore, been used as a marker for epithelial-to-mesenchymal transition observed in invasive breast cancers (253). An early study demonstrated that AP-1 was responsible for serum and PMA (phorbol 12-myristate 13-acetate) inducibility of vimentin gene expression (254). This study also showed that tandem AP-1 elements located ~700 base pairs upstream of the transcription start site were necessary and sufficient for this effect (254). These sites were subsequently shown to exhibit AP-1 binding *in vitro* and a recent study demonstrated that AP-1 and Sp1 cooperate resulting in synergistic activation of the human vimentin promoter (234, 254). However, there has been no direct evidence that

AP-1 and/or Sp1 physically associate with the vimentin promoter in an endogenous, genomic context.

In contrast to SPARC, the vimentin promoter is a classical CpG island with 56 CpG sequences over a 600 base pair region surrounding the tandem AP-1 sites (Appendix A, Fig. 44). The results presented in Appendix A, Fig. 44 demonstrate that this locus is almost completely methylated in empty vector control/MCF7 cells where transcription is repressed. However, there is a dramatic and widespread loss of DNA methylation in response to c-Jun overexpression. In contrast to the SPARC gene locus, the widespread demethylation of the vimentin promoter CpG island demonstrates that c-Jun is capable of inducing more than just localized changes in DNA methylation during target gene activation. In addition, chromatin immunoprecipitation analysis demonstrated that c-Jun and Fra-1 physically associate with the vimentin promoter in the demethylated state (Appendix A, Fig. 45). These experiments provide the first direct evidence that vimentin is a direct AP-1 target gene. It is likely that in this case, c-Jun and Fra-1 utilize two adjacent AP-1 sites since they are in a consensus context and this region was previously shown to be required for AP-1 responsiveness. Similar to what we observed at the SPARC locus, Sp1 was present at the vimentin promoter under conditions where transcription was repressed or activated. This further suggests a bi-functional role for Sp1 in transcriptional activation.

In contrast to the SPARC locus, chromatin immunoprecipitation analysis of the vimentin promoter in MCF7 cells revealed histone modifications consistent with a heterochromatic, transcriptionally silent locus (Appendix A, Fig. 45). One of the most striking changes induced by c-Jun was loss of histone H3-lysine 9 tri-methylation, a

modification strictly associated with classic epigenetic gene silencing. This result also serves as a positive control, demonstrating that the negative result obtained at the SPARC promoter using the anti-tri-methyl histone H3-K9 antibody (Fig. 35) is a "real" negative result.

Based on characterization of epigenetic changes at the SPARC and vimentin gene loci, we wanted to determine if any c-Jun target genes were regulated in an opposite manner. Therefore, we chose to examine the estrogen receptor alpha (ERa) gene locus. ERa expression is "on" in growth factor dependent MCF7 cells and "off" in estrogen independent and tamoxifen resistant c-Jun/MCF7 cells (46). The ERa locus is known to become hypermethylated in invasive, ERa negative, breast cancer cells and this correlates with loss of ERa expression (183, 255, 256). However, the mechanisms driving this process are unclear. In order to characterize the methylation status of the ERa promoter in our model system, we conducted HpaII/MspI mapping as shown in Appendix A, Fig. 46. The results demonstrate a localized hypermethylation in response to c-Jun overexpression. Specifically, the CpG rich region immediately 3' of the promoter "A" transcription start site becomes completely methylated and this correlates with transcriptional repression. This is in agreement with the current paradigm where the degree of promoter methylation inversely correlates with the level of gene transcription.

Next, we conducted chromatin immunoprecipitation analysis in order to determine the histone modifications and protein/DNA interactions at the estrogen receptor alpha locus. The results presented in Appendix A, Fig. 47 show that Sp1 is present at the locus only in MCF7 cells when transcription is active. Importantly, this demonstrates that Sp1 is not ubiquitously present under all conditions tested in our

studies. Interestingly, c-Jun and Fra-1 are not associated with the ERa locus, at least not in the hypermethylated region analyzed by ChIP. This suggests that ERa may be an indirect AP-1 target gene. In addition, our analysis revealed hypoacetylation of histone H3 in c–Jun/MCF7 cells during the repressed state and enrichment of methylated histone H3 at lysine 4 in MCF7 cells during active transcription. These changes are in agreement with the current paradigm that histone acetylation and H3-K4 methylation directly correlate with the relative level of gene transcription.

Taken together, our analysis of the SPARC, vimentin and estrogen receptor alpha gene loci highlight the diverse mechanisms by which c-Jun regulates target gene expression. Importantly, these studies were conducted in a biologically relevant model system which recapitulates the phenotypic changes associated with malignant breast cancer progression.

CHAPTER V

CONCLUSIONS

Our hypothesis was that c-Jun binds to the SPARC promoter leading to an increase in SPARC mRNA and protein and a concomitant change to a pro-invasive cell phenotype. Our objectives were 1.) to determine the contribution of SPARC to c-Jun induced phenotype in a MCF7 breast cancer model system and 2.) to determine the mechanism(s) by which c-Jun regulates SPARC gene expression. The results described in Chapter III of this dissertation have led us to propose the following conclusions:

1.) Overexpression of SPARC in MCF7 cells leads to a statistically significant (P= <0.05) decrease in cell proliferation rate.

2.) Overexpression of SPARC, in the absence of c-Jun overexpression, was not sufficient to induce MCF7 cell motility and invasion.

3.) Inhibition of SPARC expression in c-Jun/MCF7 cells results in a statistically significant (P= <0.05) decrease in cell motility and invasion.

4.) Three AP-1 like sites (-1051/-1045, -868/-862, -241/-235) in the SPARC promoter are dispensable for c-Jun responsiveness.

5.) The SPARC promoter region spanning nucleotides –120 to -70 contains the c-Jun responsive element (JRE) required for maximal promoter activation in c-Jun/MCF7 cells.

6.) Sp1 and AP-1 (c-Jun and Fra-1) are present at the SPARC proximal promoter region *in vivo* in c-Jun/MCF7 cells where SPARC is expressed. In MCF7 cells, where SPARC expression is undetectable, only Sp1 is present at the SPARC promoter.

7.) Treatment of MCF7 cells with the DNA methyltransferase inhibitor, 5-aza-2'deoxycytidine (5-aza-dC), results in reactivation of SPARC gene expression, whereas in c-Jun/MCF7 cells, there is no effect on SPARC expression.

8.) Overexpression of c-Jun in MCF7 cells results in localized demethylation of the SPARC proximal promoter region.

9.) *In vitro* methylation of a single HpaII site between –120/-70 of the SPARC promoter abrogates c-Jun responsiveness.

10.) Hypermethylation and hyperacetylation of histone H3 lysine 4 correlates with increased SPARC expression in response to c-Jun.

11.) In MCF7 cells, repression of SPARC gene transcription is maintained by a histone deacetylase independent mechanism.

These conclusions have led us to propose the following model of SPARC gene regulation:

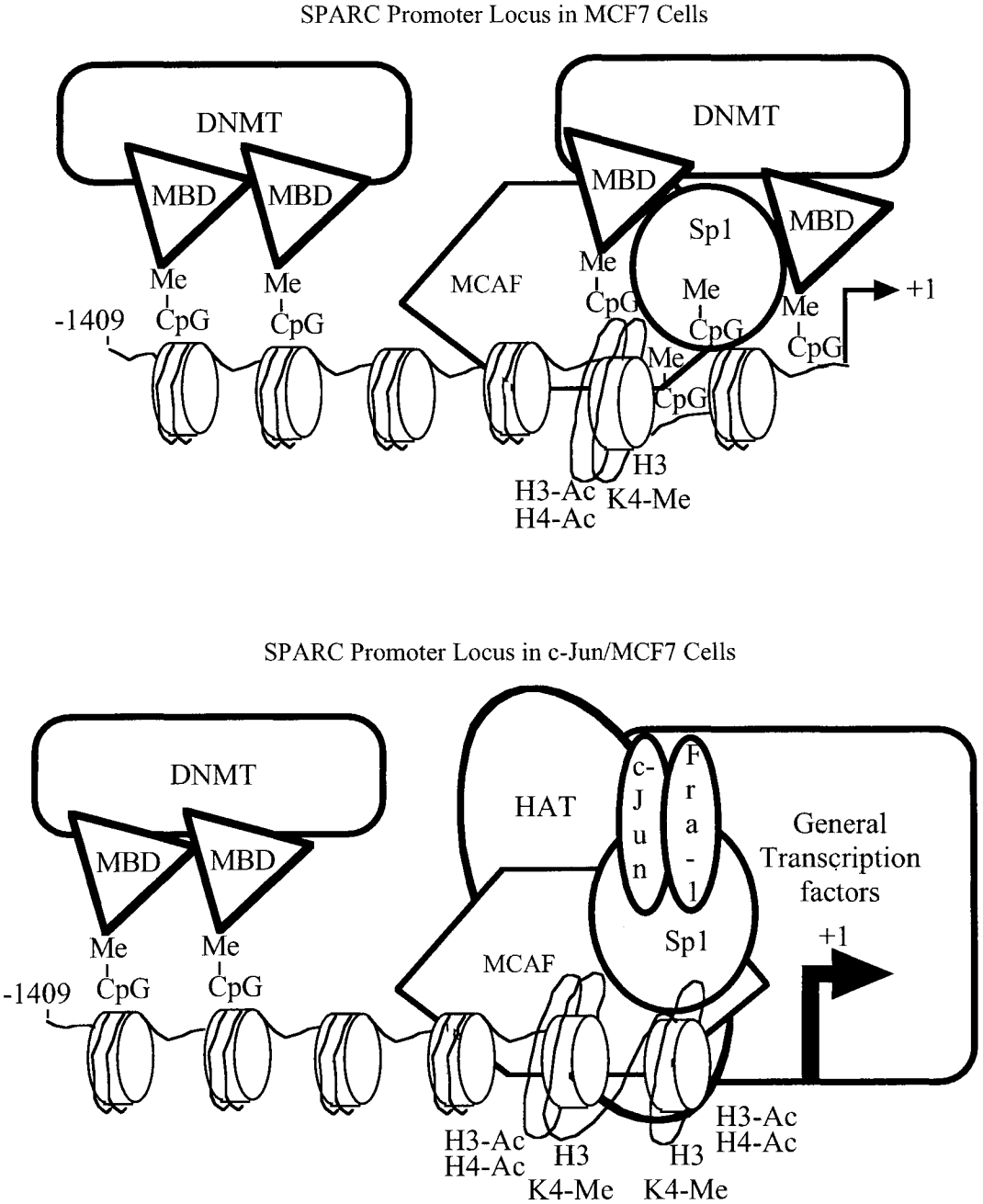

Fig. 37. Proposed model of c-Jun/AP-1 transcriptional regulation of SPARC gene expression. The size of the arrow represents transcription level in each cell line. (HAT) histone acetyltransferase, (MCAF) MBD1 chromatin associated factor, (DNMT1) DNA methyltransferase, (MBD) methyl binding protein, (Ac) acetylation, (Me) methylation.

REFERENCES

1. American Cancer Society. "What are the Key Statistics For Breast Cancer?" 2005, <http://www.cancer.org/docroot/cri/content/cri_2_4_1x_what_are_the_key_statistics_for_breast_cancer_5.asp?sitearea=cri> (17 March 2004).

2. Klein CA. Gene expression sigantures, cancer cell evolution and metastatic progression. Cell Cycle 2004;3(1):29-31.

3. Narod SA, Foulkes WD. BRCA1 and BRCA2: 1994 and beyond. Nat Rev Cancer 2004;4(9):665-76.

4. Simpson PT, Reis-Filho JS, Gale T, Lakhani SR. Molecular evolution of breast cancer. J Pathol 2005;205(2):248-54.

5. Hanahan D, Weinberg RA. The hallmarks of cancer. Cell 2000;100(1):57-70.

6. Birchmeier W, Behrens J, Weidner M, Frixen U, Sachs M, and Vandekerckhove J. Molecular and Cellular Aspects of Tumor Cell Invasion. In: Brugge J, Curran T, Harlow E, and McCormick F, editors. Origens of Human Cancer: A Comprehensive Review. Plainview, New York: Cold Spring Harbor Laboratory Press; 1991. p. 587-99.

7. Tavtigian SV, Simard J, Rommens J, et al. The complete BRCA2 gene and mutations in chromosome 13q-linked kindreds. Nat Genet 1996;12(3):333-7.

8. Anderson DE. Familial versus sporadic breast cancer. Cancer 1992;70(6 Suppl):1740-6.

9. Pavelic K, Gall-Troselj K. Recent advances in molecular genetics of breast cancer. J Mol Med 2001;79(10):566-73.

10. Dickson C, Fantl V, Gillett C, et al. Amplification of chromosome band 11q13 and a role for cyclin D1 in human breast cancer. Cancer Lett 1995;90(1):43-50.

11. Ingvarsson S. Molecular genetics of breast cancer progression. Semin Cancer Biol 1999;9(4):277-88.

12. Tomlinson IP. Mutations in normal breast tissue and breast tumours. Breast Cancer Res 2001;3(5):299-303.

13. Tripathy D, Benz CC. Activated oncogenes and putative tumor suppressor genes involved in human breast cancers. Cancer Treat Res 1992;63:15-60.

14. Pharoah PD, Day NE, Caldas C. Somatic mutations in the p53 gene and prognosis in breast cancer: a meta-analysis. Br J Cancer 1999;80(12):1968-73.

15. Nigro JM, Baker SJ, Preisinger AC, et al. Mutations in the p53 gene occur in diverse human tumour types. Nature 1989;342(6250):705-8.

16. Callahan R, Campbell G. Mutations in human breast cancer: an overview. J Natl Cancer Inst 1989;81(23):1780-6.

17. Garcia I, Dietrich PY, Aapro M, Vauthier G, Vadas L, Engel E. Genetic alterations of c-myc, c-erbB-2, and c-Ha-ras protooncogenes and clinical associations in human breast carcinomas. Cancer Res 1989;49(23):6675-9.

18. Nagai MA, Marques LA, Torloni H, Brentani MM. Genetic alterations in c-erbB-2 protooncogene as prognostic markers in human primary breast tumors. Oncology 1993;50(6):412-7.

19. Slamon DJ, Godolphin W, Jones LA, et al. Studies of the HER-2/neu proto-oncogene in human breast and ovarian cancer. Science 1989;244(4905):707-12.

20. Zajchowski DA, Bartholdi MF, Gong Y, et al. Identification of gene expression profiles that predict the aggressive behavior of breast cancer cells. Cancer Res 2001;61(13):5168-78.

21. Gruvberger S, Ringner M, Chen Y, et al. Estrogen receptor status in breast cancer is associated with remarkably distinct gene expression patterns. Cancer Res 2001;61(16):5979-84.

22. Leygue E, Dotzlaw H, Watson PH, Murphy LC. Altered estrogen receptor alpha and beta messenger RNA expression during human breast tumorigenesis. Cancer Res 1998;58(15):3197-201.

23. Linardopoulos S, Malliri A, Pintzas A, Vassilaros S, Tsikkinis A, Spandidos DA. Elevated expression of AP-1 activity in human breast tumors as compared to normal adjacent tissue. Anticancer Res 1990;10(6):1711-3.

24. Pavelic ZP, Pavelic L, Lower EE, et al. c-myc, c-erbB-2, and Ki-67 expression in normal breast tissue and in invasive and noninvasive breast carcinoma. Cancer Res 1992;52(9):2597-602.

25. Tiniakos DG, Scott LE, Corbett IP, Piggott NH, Horne CH. Studies of c-jun oncogene expression in human breast using a new monoclonal antibody, NCL-DK4. J Pathol 1994;172(1):19-26.

26. Zhang D, Salto-Tellez M, Do E, Putti TC, Koay ES. Evaluation of HER-2/neu oncogene status in breast tumors on tissue microarrays. Hum Pathol 2003;34(4):362-8.

27. Jaiyesimi IA, Buzdar AU, Decker DA, Hortobagyi GN. Use of tamoxifen for breast cancer: twenty-eight years later. J Clin Oncol 1995;13(2):513-29.

28. Nahta R, Esteva FJ. HER-2-targeted therapy: lessons learned and future directions. Clin Cancer Res 2003;9(14):5078-84.

29. Beckmann MW, Niederacher D, Schnurch HG, Gusterson BA, Bender HG. Multistep carcinogenesis of breast cancer and tumour heterogeneity. J Mol Med 1997;75(6):429-39.

30. Duffy MJ, Maguire TM, Hill A, McDermott E, O'Higgins N. Metalloproteinases: role in breast carcinogenesis, invasion and metastasis. Breast Cancer Res 2000;2(4):252-7.

31. Fidler IJ, Hart IR. Biological diversity in metastatic neoplasms: origins and implications. Science 1982;217(4564):998-1003.

32. Liotta LA, Abe S, Robey PG, Martin GR. Preferential digestion of basement membrane collagen by an enzyme derived from a metastatic murine tumor. Proc Natl Acad Sci U S A 1979;76(5):2268-72.

33. Schirrmacher V. Cancer metastasis: experimental approaches, theoretical concepts, and impacts for treatment strategies. Adv Cancer Res 1985;43:1-73.

34. Sui G, Soohoo C, Affar el B, et al. A DNA vector-based RNAi technology to suppress gene expression in mammalian cells. Proc Natl Acad Sci U S A 2002;99(8):5515-20.

35. Gabbert H, Wagner R, Moll R, Gerharz CD. Tumor dedifferentiation: an important step in tumor invasion. Clin Exp Metastasis 1985;3(4):257-79.

36. Sugarbaker E. Patterns of metastasis in human malignancies. In: Cancer Biol Rev; 1981. p. 235-78.

37. Vandel L, Montreau N, Vial E, Pfarr CM, Binetruy B, Castellazzi M. Stepwise transformation of rat embryo fibroblasts: c-Jun, JunB, or JunD can cooperate with Ras for focus formation, but a c-Jun-containing heterodimer is required for immortalization. Mol Cell Biol 1996;16(5):1881-8.

38. Schutte J, Minna JD, Birrer MJ. Deregulated expression of human c-jun transforms primary rat embryo cells in cooperation with an activated c-Ha-ras gene and transforms rat-1a cells as a single gene. Proc Natl Acad Sci U S A 1989;86(7):2257-61.

39. Leaner VD, Kinoshita I, Birrer MJ. AP-1 complexes containing cJun and JunB cause cellular transformation of Rat1a fibroblasts and share transcriptional targets. Oncogene 2003;22(36):5619-29.

40. Kraemer M, Tournaire R, Dejong V, et al. Rat embryo fibroblasts transformed by c-Jun display highly metastatic and angiogenic activities in vivo and deregulate gene expression of both angiogenic and antiangiogenic factors. Cell Growth Differ 1999;10(3):193-200.

41. Johnson R, Spiegelman B, Hanahan D, Wisdom R. Cellular transformation and malignancy induced by ras require c-jun. Mol Cell Biol 1996;16(8):4504-11.

42. Castellazzi M, Dangy JP, Mechta F, et al. Overexpression of avian or mouse c-jun in primary chick embryo fibroblasts confers a partially transformed phenotype. Oncogene 1990;5(10):1541-7.

43. Alani R, Brown P, Binetruy B, et al. The transactivating domain of the c-Jun proto-oncoprotein is required for cotransformation of rat embryo cells. Mol Cell Biol 1991;11(12):6286-95.

44. Bamberger AM, Methner C, Lisboa BW, et al. Expression pattern of the AP-1 family in breast cancer: association of fosB expression with a well-differentiated, receptor-positive tumor phenotype. Int J Cancer 1999;84(5):533-8.

45. Gee JM, Barroso AF, Ellis IO, Robertson JF, Nicholson RI. Biological and clinical associations of c-jun activation in human breast cancer. Int J Cancer 2000;89(2):177-86.

46. Smith LM, Wise SC, Hendricks DT, et al. cJun overexpression in MCF-7 breast cancer cells produces a tumorigenic, invasive and hormone resistant phenotype. Oncogene 1999;18(44):6063-70.

47. Liu P, Kimmoun E, Legrand A, et al. Activation of NF-kappa B, AP-1 and STAT transcription factors is a frequent and early event in human hepatocellular carcinomas. J Hepatol 2002;37(1):63-71.

48. Watts RG, Ben-Ari ET, Bernstein LR, et al. c-jun and multistage carcinogenesis: association of overexpression of introduced c-jun with progression toward a neoplastic endpoint in mouse JB6 cells sensitive to tumor promoter-induced transformation. Mol Carcinog 1995;13(1):27-36.

49. Zoumpourlis V, Papassava P, Linardopoulos S, Gillespie D, Balmain A, Pintzas A. High levels of phosphorylated c-Jun, Fra-1, Fra-2 and ATF-2 proteins correlate with malignant phenotypes in the multistage mouse skin carcinogenesis model. Oncogene 2000;19(35):4011-21.

50. Bergers G, Graninger P, Braselmann S, Wrighton C, Busslinger M. Transcriptional activation of the fra-1 gene by AP-1 is mediated by regulatory sequences in the first intron. Mol Cell Biol 1995;15(7):3748-58.

51. Rinehart-Kim J, Johnston M, Birrer M, Bos T. Alterations in the gene expression profile of MCF-7 breast tumor cells in response to c-Jun. Int J Cancer 2000;88(2):180-90.

52. Maki Y, Bos TJ, Davis C, Starbuck M, Vogt PK. Avian sarcoma virus 17 carries the jun oncogene. Proc Natl Acad Sci U S A 1987;84(9):2848-52.

53. Bohmann D, Bos TJ, Admon A, Nishimura T, Vogt PK, Tjian R. Human proto-oncogene c-jun encodes a DNA binding protein with structural and functional properties of transcription factor AP-1. Science 1987;238(4832):1386-92.

54. Chinenov Y, Kerppola TK. Close encounters of many kinds: Fos-Jun interactions that mediate transcription regulatory specificity. Oncogene 2001;20(19):2438-52.

55. Vogt PK, Bos TJ. jun: oncogene and transcription factor. Adv Cancer Res 1990;55:1-35.

56. Hilberg F, Aguzzi A, Howells N, Wagner EF. c-jun is essential for normal mouse development and hepatogenesis. Nature 1993;365(6442):179-81.

57. Johnson RS, van Lingen B, Papaioannou VE, Spiegelman BM. A null mutation at the c-jun locus causes embryonic lethality and retarded cell growth in culture. Genes Dev 1993;7(7B):1309-17.

58. Bos TJ, Rauscher FJ, III, Curran T, Vogt PK. The carboxy terminus of the viral Jun oncoprotein is required for complex formation with the cellular Fos protein. Oncogene 1989;4(2):123-6.

59. Angel P, Karin M. The role of Jun, Fos and the AP-1 complex in cell-proliferation and transformation. Biochim Biophys Acta 1991;1072(2-3):129-57.

60. Kovary K, Bravo R. Expression of different Jun and Fos proteins during the G0-to-G1 transition in mouse fibroblasts: in vitro and in vivo associations. Mol Cell Biol 1991;11(5):2451-9.

61. Boyle WJ, Smeal T, Defize LH, et al. Activation of protein kinase C decreases phosphorylation of c-Jun at sites that negatively regulate its DNA-binding activity. Cell 1991;64(3):573-84.

62. Lamph WW, Wamsley P, Sassone-Corsi P, Verma IM. Induction of proto-oncogene JUN/AP-1 by serum and TPA. Nature 1988;334(6183):629-31.

63. Peng SS, Chen CY, Shyu AB. Functional characterization of a non-AUUUA AU-rich element from the c-jun proto-oncogene mRNA: evidence for a novel class of AU-rich elements. Mol Cell Biol 1996;16(4):1490-9.

64. Hirai S, Kawasaki H, Yaniv M, Suzuki K. Degradation of transcription factors, c-Jun and c-Fos, by calpain. FEBS Lett 1991;287(1-2):57-61.

65. Treier M, Staszewski LM, Bohmann D. Ubiquitin-dependent c-Jun degradation in vivo is mediated by the delta domain. Cell 1994;78(5):787-98.

66. Horne GM, Anderson JJ, Tiniakos DG, et al. p53 protein as a prognostic indicator in breast carcinoma: a comparison of four antibodies for immunohistochemistry. Br J Cancer 1996;73(1):29-35.

67. Milde-Langosch K, Bamberger AM, Methner C, Rieck G, Loning T. Expression of cell cycle-regulatory proteins rb, p16/MTS1, p27/KIP1, p21/WAF1, cyclin D1 and cyclin E in breast cancer: correlations with expression of activating protein-1 family members. Int J Cancer 2000;87(4):468-72.

68. Cohen DR, Ferreira PC, Gentz R, Franza BR, Jr., Curran T. The product of a fos-related gene, fra-1, binds cooperatively to the AP-1 site with Jun: transcription factor AP-1 is comprised of multiple protein complexes. Genes Dev 1989;3(2):173-84.

69. Gentz R, Rauscher FJ, III, Abate C, Curran T. Parallel association of Fos and Jun leucine zippers juxtaposes DNA binding domains. Science 1989;243(4899):1695-9.

70. Kouzarides T, Ziff E. The role of the leucine zipper in the fos-jun interaction. Nature 1988;336(6200):646-51.

71. Shaulian E, Karin M. AP-1 in cell proliferation and survival. Oncogene 2001;20(19):2390-400.

72. van Dam H, Castellazzi M. Distinct roles of Jun: Fos and Jun: ATF dimers in oncogenesis. Oncogene 2001;20(19):2453-64.

73. Vogt PK. Jun, the oncoprotein. Oncogene 2001;20(19):2365-77.

74. Patel LR, Curran T, Kerppola TK. Energy transfer analysis of Fos-Jun dimerization and DNA binding. Proc Natl Acad Sci U S A 1994;91(15):7360-4.

75. O'Shea EK, Rutkowski R, Stafford WF, III, Kim PS. Preferential heterodimer formation by isolated leucine zippers from fos and jun. Science 1989;245(4918):646-8.

76. Smeal T, Angel P, Meek J, Karin M. Different requirements for formation of Jun: Jun and Jun: Fos complexes. Genes Dev 1989;3(12B):2091-100.

77. Rauscher FJ, III, Sambucetti LC, Curran T, Distel RJ, Spiegelman BM. Common DNA binding site for Fos protein complexes and transcription factor AP-1. Cell 1988;52(3):471-80.

78. Abate C, Curran T. Encounters with Fos and Jun on the road to AP-1. Semin Cancer Biol 1990;1(1):19-26.

79. Benbrook DM, Jones NC. Heterodimer formation between CREB and JUN proteins. Oncogene 1990;5(3):295-302.

80. Hadman M, Loo M, Bos TJ. In vivo viral and cellular Jun complexes exhibit differential interaction with a number of in vitro generated 'AP-1- and CREB-like' target sequences. Oncogene 1993;8(7):1895-903.

81. Ryseck RP, Bravo R. c-JUN, JUN B, and JUN D differ in their binding affinities to AP-1 and CRE consensus sequences: effect of FOS proteins. Oncogene 1991;6(4):533-42.

82. De Cesare D, Vallone D, Caracciolo A, Sassone-Corsi P, Nerlov C, Verde P. Heterodimerization of c-Jun with ATF-2 and c-Fos is required for positive and negative regulation of the human urokinase enhancer. Oncogene 1995;11(2):365-76.

83. Kobierski LA, Chu HM, Tan Y, Comb MJ. cAMP-dependent regulation of proenkephalin by JunD and JunB: positive and negative effects of AP-1 proteins. Proc Natl Acad Sci U S A 1991;88(22):10222-6.

84. Nishitani J, Nishinaka T, Cheng CH, Rong W, Yokoyama KK, Chiu R. Recruitment of the retinoblastoma protein to c-Jun enhances transcription activity mediated through the AP-1 binding site. J Biol Chem 1999;274(9):5454-61.

85. Ubeda M, Vallejo M, Habener JF. CHOP enhancement of gene transcription by interactions with Jun/Fos AP-1 complex proteins. Mol Cell Biol 1999;19(11):7589-99.

86. Stein B, Baldwin AS, Jr., Ballard DW, Greene WC, Angel P, Herrlich P. Cross-coupling of the NF-kappa B p65 and Fos/Jun transcription factors produces potentiated biological function. Embo J 1993;12(10):3879-91.

87. Schule R, Rangarajan P, Kliewer S, et al. Functional antagonism between oncoprotein c-Jun and the glucocorticoid receptor. Cell 1990;62(6):1217-26.

88. Touray M, Ryan F, Jaggi R, Martin F. Characterisation of functional inhibition of the glucocorticoid receptor by Fos/Jun. Oncogene 1991;6(7):1227-34.

89. Yang-Yen HF, Chambard JC, Sun YL, et al. Transcriptional interference between c-Jun and the glucocorticoid receptor: mutual inhibition of DNA binding due to direct protein-protein interaction. Cell 1990;62(6):1205-15.

90. Yang-Yen HF, Zhang XK, Graupner G, et al. Antagonism between retinoic acid receptors and AP-1: implications for tumor promotion and inflammation. New Biol 1991;3(12):1206-19.

91. Bengal E, Ransone L, Scharfmann R, et al. Functional antagonism between c-Jun and MyoD proteins: a direct physical association. Cell 1992;68(3):507-19.

92. Chen BK, Chang WC. Functional interaction between c-Jun and promoter factor Sp1 in epidermal growth factor-induced gene expression of human 12(S)-lipoxygenase. Proc Natl Acad Sci U S A 2000;97(19):10406-11.

93. Kardassis D, Papakosta P, Pardali K, Moustakas A. c-Jun transactivates the promoter of the human p21(WAF1/Cip1) gene by acting as a superactivator of the ubiquitous transcription factor Sp1. J Biol Chem 1999;274(41):29572-81.

94. Slack A, Pinard M, Araujo FD, Szyf M. A novel regulatory element in the dnmt1 gene that responds to co-activation by Rb and c-Jun. Gene 2001;268(1-2):87-96.

95. Daschner PJ, Ciolino HP, Plouzek CA, Yeh GC. Increased AP-1 activity in drug resistant human breast cancer MCF-7 cells. Breast Cancer Res Treat 1999;53(3):229-40.

96. Franklin CC, McCulloch AV, Kraft AS. In vitro association between the Jun protein family and the general transcription factors, TBP and TFIIB. Biochem J 1995;305 (Pt 3):967-74.

97. Lively TN, Ferguson HA, Galasinski SK, Seto AG, Goodrich JA. c-Jun binds the N terminus of human TAF(II)250 to derepress RNA polymerase II transcription in vitro. J Biol Chem 2001;276(27):25582-8.

98. Ransone LJ, Kerr LD, Schmitt MJ, Wamsley P, Verma IM. The bZIP domains of Fos and Jun mediate a physical association with the TATA box-binding protein. Gene Expr 1993;3(1):37-48.

99. Bannister AJ, Oehler T, Wilhelm D, Angel P, Kouzarides T. Stimulation of c-Jun activity by CBP: c-Jun residues Ser63/73 are required for CBP induced stimulation in vivo and CBP binding in vitro. Oncogene 1995;11(12):2509-14.

100. Ogryzko VV, Schiltz RL, Russanova V, Howard BH, Nakatani Y. The transcriptional coactivators p300 and CBP are histone acetyltransferases. Cell 1996;87(5):953-9.

101. Bradshaw AD, Sage EH. SPARC, a matricellular protein that functions in cellular differentiation and tissue response to injury. J Clin Invest 2001;107(9):1049-54.

102. Brekken RA, Sage EH. SPARC, a matricellular protein: at the crossroads of cell-matrix communication. Matrix Biol 2001;19(8):816-27.

103. Greenwood JA, Murphy-Ullrich JE. Signaling of de-adhesion in cellular regulation and motility. Microsc Res Tech 1998;43(5):420-32.

104. Motamed K. SPARC (osteonectin/BM-40). Int J Biochem Cell Biol 1999;31(12):1363-6.

105. Reed MJ, Sage EH. SPARC and the extracellular matrix: implications for cancer and wound repair. Curr Top Microbiol Immunol 1996;213 (Pt 1):81-94.

106. Rosenblatt S, Bassuk JA, Alpers CE, Sage EH, Timpl R, Preissner KT. Differential modulation of cell adhesion by interaction between adhesive and counter-adhesive proteins: characterization of the binding of vitronectin to osteonectin (BM40, SPARC). Biochem J 1997;324 (Pt 1):311-9.

107. Yan Q, Sage EH. SPARC, a matricellular glycoprotein with important biological functions. J Histochem Cytochem 1999;47(12):1495-506.

108. Lane TF, Sage EH. The biology of SPARC, a protein that modulates cell-matrix interactions. Faseb J 1994;8(2):163-73.

109. Schwarzbauer JE, Spencer CS. The Caenorhabditis elegans homologue of the extracellular calcium binding protein SPARC/osteonectin affects nematode body morphology and mobility. Mol Biol Cell 1993;4(9):941-52.

110. Termine JD, Kleinman HK, Whitson SW, Conn KM, McGarvey ML, Martin GR. Osteonectin, a bone-specific protein linking mineral to collagen. Cell 1981;26(1 Pt 1):99-105.

111. Engel J, Taylor W, Paulsson M, Sage H, Hogan B. Calcium binding domains and calcium-induced conformational transition of SPARC/BM-40/osteonectin, an extracellular glycoprotein expressed in mineralized and nonmineralized tissues. Biochemistry 1987;26(22):6958-65.

112. Kaufmann B, Muller S, Hanisch FG, et al. Structural variability of BM-40/SPARC/osteonectin glycosylation: implications for collagen affinity. Glycobiology 2004;14(7):609-19.

113. Lussier C, Sodek J, Beaulieu JF. Expression of SPARC/osteonectin/BM4O in the human gut: predominance in the stroma of the remodeling distal intestine. J Cell Biochem 2001;81(3):463-76.

114. Sakai N, Baba M, Nagasima Y, et al. SPARC expression in primary human renal cell carcinoma: upregulation of SPARC in sarcomatoid renal carcinoma. Hum Pathol 2001;32(10):1064-70.

115. Clezardin P, Malaval L, Ehrensperger AS, Delmas PD, Dechavanne M, McGregor JL. Complex formation of human thrombospondin with osteonectin. Eur J Biochem 1988;175(2):275-84.

116. Mayer U, Aumailley M, Mann K, Timpl R, Engel J. Calcium-dependent binding of basement membrane protein BM-40 (osteonectin, SPARC) to basement membrane collagen type IV. Eur J Biochem 1991;198(1):141-50.

117. Raines EW, Lane TF, Iruela-Arispe ML, Ross R, Sage EH. The extracellular glycoprotein SPARC interacts with platelet-derived growth factor (PDGF)-AB and -BB and inhibits the binding of PDGF to its receptors. Proc Natl Acad Sci U S A 1992;89(4):1281-5.

118. Murphy-Ullrich JE. The de-adhesive activity of matricellular proteins: is intermediate cell adhesion an adaptive state? J Clin Invest 2001;107(7):785-90.

119. Murphy-Ullrich JE, Lane TF, Pallero MA, Sage EH. SPARC mediates focal adhesion disassembly in endothelial cells through a follistatin-like region and the Ca(2+)-binding EF-hand. J Cell Biochem 1995;57(2):341-50.

120. Thomas R, True LD, Bassuk JA, Lange PH, Vessella RL. Differential expression of osteonectin/SPARC during human prostate cancer progression. Clin Cancer Res 2000;6(3):1140-9.

121. Golembieski WA, Rempel SA. cDNA array analysis of SPARC-modulated changes in glioma gene expression. J Neurooncol 2002;60(3):213-26.

122. Le Bail B, Faouzi S, Boussarie L, et al. Osteonectin/SPARC is overexpressed in human hepatocellular carcinoma. J Pathol 1999;189(1):46-52.

123. Yamanaka M, Kanda K, Li NC, et al. Analysis of the gene expression of SPARC and its prognostic value for bladder cancer. J Urol 2001;166(6):2495-9.

124. Massi D, Franchi A, Borgognoni L, Reali UM, Santucci M. Osteonectin expression correlates with clinical outcome in thin cutaneous malignant melanomas. Hum Pathol 1999;30(3):339-44.

125. Ledda F, Bravo AI, Adris S, Bover L, Mordoh J, Podhajcer OL. The expression of the secreted protein acidic and rich in cysteine (SPARC) is associated with the neoplastic progression of human melanoma. J Invest Dermatol 1997;108(2):210-4.

126. Ledda MF, Adris S, Bravo AI, et al. Suppression of SPARC expression by antisense RNA abrogates the tumorigenicity of human melanoma cells. Nat Med 1997;3(2):171-6.

127. Rempel SA, Ge S, Gutierrez JA. SPARC: a potential diagnostic marker of invasive meningiomas. Clin Cancer Res 1999;5(2):237-41.

128. Bellahcene A, Castronovo V. Increased expression of osteonectin and osteopontin, two bone matrix proteins, in human breast cancer. Am J Pathol 1995;146(1):95-100.

129. Hafner M, Zimmermann K, Pottgiesser J, Krieg T, Nischt R. A purine-rich sequence in the human BM-40 gene promoter region is a prerequisite for maximum transcription. Matrix Biol 1995;14(9):733-41.

130. Vial E, Perez S, Castellazzi M. Transcriptional control of SPARC by v-Jun and other members of the AP1 family of transcription factors. Oncogene 2000;19(43):5020-9.

131. Briggs J, Chamboredon S, Castellazzi M, Kerry JA, Bos TJ. Transcriptional upregulation of SPARC, in response to c-Jun overexpression, contributes to increased motility and invasion of MCF7 breast cancer cells. Oncogene 2002;21(46):7077-91.

132. Miller AD. Cell-surface receptors for retroviruses and implications for gene transfer. Proc Natl Acad Sci U S A 1996;93(21):11407-13.

133. Miller DG, Miller AD. A family of retroviruses that utilize related phosphate transporters for cell entry. J Virol 1994;68(12):8270-6.

134. Bradford MM. A rapid and sensitive method for the quantitation of microgram quantities of protein utilizing the principle of protein-dye binding. Anal Biochem 1976;72:248-54.

135. Cory AH, Owen TC, Barltrop JA, Cory JG. Use of an aqueous soluble tetrazolium/formazan assay for cell growth assays in culture. Cancer Commun 1991;3(7):207-12.

136. Dignam JD, Lebovitz RM, Roeder RG. Accurate transcription initiation by RNA polymerase II in a soluble extract from isolated mammalian nuclei. Nucleic Acids Res 1983;11(5):1475-89.

137. Li LC, Dahiya R. MethPrimer: designing primers for methylation PCRs. Bioinformatics 2002;18(11):1427-31.

138. Hughes RC, Taylor A, Sage H, Hogan BL. Distinct patterns of glycosylation of colligin, a collagen-binding glycoprotein, and SPARC (osteonectin), a secreted Ca2+-binding glycoprotein. Evidence for the localisation of colligin in the endoplasmic reticulum. Eur J Biochem 1987;163(1):57-65.

139. Kelm RJ, Jr., Hair GA, Mann KG, Grant BW. Characterization of human osteoblast and megakaryocyte-derived osteonectin (SPARC). Blood 1992;80(12):3112-9.

140. Muller C, Yang R, Beck-von-Peccoz L, Idos G, Verbeek W, Koeffler HP. Cloning of the cyclin A1 genomic structure and characterization of the promoter region. GC boxes are essential for cell cycle-regulated transcription of the cyclin A1 gene. J Biol Chem 1999;274(16):11220-8.

141. Sage H, Vernon RB, Funk SE, Everitt EA, Angello J. SPARC, a secreted protein associated with cellular proliferation, inhibits cell spreading in vitro and exhibits Ca+2-dependent binding to the extracellular matrix. J Cell Biol 1989;109(1):341-56.

142. Dhanesuan N, Sharp JA, Blick T, Price JT, Thompson EW. Doxycycline-inducible expression of SPARC/Osteonectin/BM40 in MDA-MB-231 human breast cancer cells results in growth inhibition. Breast Cancer Res Treat 2002;75(1):73-85.

143. Mosmann T. Rapid colorimetric assay for cellular growth and survival: application to proliferation and cytotoxicity assays. J Immunol Methods 1983;65(1-2):55-63.

144. Tada H, Shiho O, Kuroshima K, Koyama M, Tsukamoto K. An improved colorimetric assay for interleukin 2. J Immunol Methods 1986;93(2):157-65.

145. Boyden S. The chemotactic effect of mixtures of antibody and antigen on polymorphonuclear leucocytes. J Exp Med 1962;115:453-66.

146. Kleinman HK, McGarvey ML, Liotta LA, Robey PG, Tryggvason K, Martin GR. Isolation and characterization of type IV procollagen, laminin, and heparan sulfate proteoglycan from the EHS sarcoma. Biochemistry 1982;21(24):6188-93.

147. Graham FL, Smiley J, Russell WC, Nairn R. Characteristics of a human cell line transformed by DNA from human adenovirus type 5. J Gen Virol 1977;36(1):59-74.

148. Louis N, Evelegh C, Graham FL. Cloning and sequencing of the cellular-viral junctions from the human adenovirus type 5 transformed 293 cell line. Virology 1997;233(2):423-9.

149. Bernstein E, Denli AM, Hannon GJ. The rest is silence. Rna 2001;7(11):1509-21.

150. Elbashir SM, Lendeckel W, Tuschl T. RNA interference is mediated by 21- and 22-nucleotide RNAs. Genes Dev 2001;15(2):188-200.

151. Moss EG. RNA interference: it's a small RNA world. Curr Biol 2001;11(19):R772-5.

152. Elbashir SM, Harborth J, Lendeckel W, Yalcin A, Weber K, Tuschl T. Duplexes of 21-nucleotide RNAs mediate RNA interference in cultured mammalian cells. Nature 2001;411(6836):494-8.

153. Wianny F, Zernicka-Goetz M. Specific interference with gene function by double-stranded RNA in early mouse development. Nat Cell Biol 2000;2(2):70-5.

154. Hammond SM, Caudy AA, Hannon GJ. Post-transcriptional gene silencing by double-stranded RNA. Nat Rev Genet 2001;2(2):110-9.

155. Brummelkamp TR, Bernards R, Agami R. A system for stable expression of short interfering RNAs in mammalian cells. Science 2002;296(5567):550-3.

156. Chamboredon S, Briggs J, Vial E, et al. v-Jun downregulates the SPARC target gene by binding to the proximal promoter indirectly through Sp1/3. Oncogene 2003;22(26):4047-61.

157. Young MF, Findlay DM, Dominguez P, et al. Osteonectin promoter. DNA sequence analysis and S1 endonuclease site potentially associated with transcriptional control in bone cells. J Biol Chem 1989;264(1):450-6.

158. Huber R, Schlessinger D, Pilia G. Multiple Sp1 sites efficiently drive transcription of the TATA-less promoter of the human glypican 3 (GPC3) gene. Gene 1998;214(1-2):35-44.

159. Le Naour F, Prenant M, Francastel C, Rubinstein E, Uzan G, Boucheix C. Transcriptional regulation of the human CD9 gene: characterization of the 5'-flanking region. Oncogene 1996;13(3):481-6.

160. Philipsen S, Suske G. A tale of three fingers: the family of mammalian Sp/XKLF transcription factors. Nucleic Acids Res 1999;27(15):2991-3000.

161. Suske G. The Sp-family of transcription factors. Gene 1999;238(2):291-300.

162. Zaret K. Identifying specific protein-DNA interactions within living cells, or in "in vivo footprinting". Methods 1997;11(2):149-50.

163. Kuo MH, Allis CD. In vivo cross-linking and immunoprecipitation for studying dynamic Protein:DNA associations in a chromatin environment. Methods 1999;19(3):425-33.

164. Orlando V, Strutt H, Paro R. Analysis of chromatin structure by in vivo formaldehyde cross-linking. Methods 1997;11(2):205-14.

165. Cooper DN. Eukaryotic DNA methylation. Hum Genet 1983;64(4):315-33.

166. Razin A, Riggs AD. DNA methylation and gene function. Science 1980;210(4470):604-10.

167. Vanyushin BF, Tkacheva SG, Belozersky AN. Rare bases in animal DNA. Nature 1970;225(5236):948-9.

168. Nephew KP, Huang TH. Epigenetic gene silencing in cancer initiation and progression. Cancer Lett 2003;190(2):125-33.

169. Momparler RL. Cancer epigenetics. Oncogene 2003;22(42):6479-83.

170. Garinis GA, Patrinos GP, Spanakis NE, Menounos PG. DNA hypermethylation: when tumour suppressor genes go silent. Hum Genet 2002;111(2):115-27.

171. Baylin SB, Herman JG, Graff JR, Vertino PM, Issa JP. Alterations in DNA methylation: a fundamental aspect of neoplasia. Adv Cancer Res 1998;72:141-96.

172. Herman JG, Merlo A, Mao L, et al. Inactivation of the CDKN2/p16/MTS1 gene is frequently associated with aberrant DNA methylation in all common human cancers. Cancer Res 1995;55(20):4525-30.

173. Otterson GA, Khleif SN, Chen W, Coxon AB, Kaye FJ. CDKN2 gene silencing in lung cancer by DNA hypermethylation and kinetics of p16INK4 protein induction by 5-aza 2'deoxycytidine. Oncogene 1995;11(6):1211-6.

174. Mesquita P, Peixoto AJ, Seruca R, et al. Role of site-specific promoter hypomethylation in aberrant MUC2 mucin expression in mucinous gastric carcinomas. Cancer Lett 2003;189(2):129-36.

175. Sato N, Fukushima N, Maitra A, et al. Discovery of novel targets for aberrant methylation in pancreatic carcinoma using high-throughput microarrays. Cancer Res 2003;63(13):3735-42.

176. Sato N, Fukushima N, Maehara N, et al. SPARC/osteonectin is a frequent target for aberrant methylation in pancreatic adenocarcinoma and a mediator of tumor-stromal interactions. Oncogene 2003;22(32):5021-30.

177. Holliday R, Pugh JE. DNA modification mechanisms and gene activity during development. Science 1975;187(4173):226-32.

178. Robertson KD. DNA methylation and chromatin - unraveling the tangled web. Oncogene 2002;21(35):5361-79.

179. Christman JK, Mendelsohn N, Herzog D, Schneiderman N. Effect of 5-azacytidine on differentiation and DNA methylation in human promyelocytic leukemia cells (HL-60). Cancer Res 1983;43(2):763-9.

180. Creusot F, Acs G, Christman JK. Inhibition of DNA methyltransferase and induction of Friend erythroleukemia cell differentiation by 5-azacytidine and 5-aza-2'-deoxycytidine. J Biol Chem 1982;257(4):2041-8.

181. Taylor SM, Jones PA. Mechanism of action of eukaryotic DNA methyltransferase. Use of 5-azacytosine-containing DNA. J Mol Biol 1982;162(3):679-92.

182. Bender CM, Zingg JM, Jones PA. DNA methylation as a target for drug design. Pharm Res 1998;15(2):175-87.

183. Ferguson AT, Vertino PM, Spitzner JR, Baylin SB, Muller MT, Davidson NE. Role of estrogen receptor gene demethylation and DNA methyltransferase.DNA adduct formation in 5-aza-2'deoxycytidine-induced cytotoxicity in human breast cancer cells. J Biol Chem 1997;272(51):32260-6.

184. Bird AP, Southern EM. Use of restriction enzymes to study eukaryotic DNA methylation: I. The methylation pattern in ribosomal DNA from Xenopus laevis. J Mol Biol 1978;118(1):27-47.

185. Frommer M, McDonald LE, Millar DS, et al. A genomic sequencing protocol that yields a positive display of 5-methylcytosine residues in individual DNA strands. Proc Natl Acad Sci U S A 1992;89(5):1827-31.

186. Waalwijk C, Flavell RA. MspI, an isoschizomer of hpaII which cleaves both unmethylated and methylated hpaII sites. Nucleic Acids Res 1978;5(9):3231-6.

187. Gaston K, Fried M. CpG methylation has differential effects on the binding of YY1 and ETS proteins to the bi-directional promoter of the Surf-1 and Surf-2 genes. Nucleic Acids Res 1995;23(6):901-9.

188. Umezawa A, Yamamoto H, Rhodes K, Klemsz MJ, Maki RA, Oshima RG. Methylation of an ETS site in the intron enhancer of the keratin 18 gene participates in tissue-specific repression. Mol Cell Biol 1997;17(9):4885-94.

189. Hendrich B, Bird A. Identification and characterization of a family of mammalian methyl-CpG binding proteins. Mol Cell Biol 1998;18(11):6538-47.

190. Ng HH, Bird A. DNA methylation and chromatin modification. Curr Opin Genet Dev 1999;9(2):158-63.

191. Jones PL, Veenstra GJ, Wade PA, et al. Methylated DNA and MeCP2 recruit histone deacetylase to repress transcription. Nat Genet 1998;19(2):187-91.

192. Harrington MA, Jones PA, Imagawa M, Karin M. Cytosine methylation does not affect binding of transcription factor Sp1. Proc Natl Acad Sci U S A 1988;85(7):2066-70.

193. Camerini-Otero RD, Sollner-Webb B, Felsenfeld G. The organization of histones and DNA in chromatin: evidence for an arginine-rich histone kernel. Cell 1976;8(3):333-47.

194. Oudet P, Gross-Bellard M, Chambon P. Electron microscopic and biochemical evidence that chromatin structure is a repeating unit. Cell 1975;4(4):281-300.

195. Luger K, Mader AW, Richmond RK, Sargent DF, Richmond TJ. Crystal structure of the nucleosome core particle at 2.8 A resolution. Nature 1997;389(6648):251-60.

196. Sahasrabuddhe CG, Van Holde KE. The effect of trypsin on nuclease-resistant chromatin fragments. J Biol Chem 1974;249(1):152-6.

197. Hjelm RP, Kneale GG, Sauau P, Baldwin JP, Bradbury EM, Ibel K. Small angle neutron scattering studies of chromatin subunits in solution. Cell 1977;10(1):139-51.

198. Luger K, Richmond TJ. The histone tails of the nucleosome. Curr Opin Genet Dev 1998;8(2):140-6.

199. Peterson CL, Laniel MA. Histones and histone modifications. Curr Biol 2004;14(14):R546-51.

200. Spencer VA, Davie JR. Role of covalent modifications of histones in regulating gene expression. Gene 1999;240(1):1-12.

201. Berger SL. Histone modifications in transcriptional regulation. Curr Opin Genet Dev 2002;12(2):142-8.

202. Jaenisch R, Bird A. Epigenetic regulation of gene expression: how the genome integrates intrinsic and environmental signals. Nat Genet 2003;33 Suppl:245-54.

203. Jenuwein T, Allis CD. Translating the histone code. Science 2001;293(5532):1074-80.

204. Carrozza MJ, Utley RT, Workman JL, Cote J. The diverse functions of histone acetyltransferase complexes. Trends Genet 2003;19(6):321-9.

205. Eberharter A, Becker PB. Histone acetylation: a switch between repressive and permissive chromatin. Second in review series on chromatin dynamics. EMBO Rep 2002;3(3):224-9.

206. Rice JC, Allis CD. Histone methylation versus histone acetylation: new insights into epigenetic regulation. Curr Opin Cell Biol 2001;13(3):263-73.

207. Thiagalingam S, Cheng KH, Lee HJ, Mineva N, Thiagalingam A, Ponte JF. Histone deacetylases: unique players in shaping the epigenetic histone code. Ann N Y Acad Sci 2003;983:84-100.

208. Fischle W, Wang Y, Allis CD. Histone and chromatin cross-talk. Curr Opin Cell Biol 2003;15(2):172-83.

209. Gerber M, Shilatifard A. Transcriptional elongation by RNA polymerase II and histone methylation. J Biol Chem 2003;278(29):26303-6.

210. Jeppesen P, Turner BM. The inactive X chromosome in female mammals is distinguished by a lack of histone H4 acetylation, a cytogenetic marker for gene expression. Cell 1993;74(2):281-9.

211. Kurdistani SK, Grunstein M. Histone acetylation and deacetylation in yeast. Nat Rev Mol Cell Biol 2003;4(4):276-84.

212. Legube G, Trouche D. Regulating histone acetyltransferases and deacetylases. EMBO Rep 2003;4(10):944-7.

213. Dutnall RN. Cracking the histone code: one, two, three methyls, you're out! Mol Cell 2003;12(1):3-4.

214. Lachner M, Jenuwein T. The many faces of histone lysine methylation. Curr Opin Cell Biol 2002;14(3):286-98.

215. Nakayama J, Rice JC, Strahl BD, Allis CD, Grewal SI. Role of histone H3 lysine 9 methylation in epigenetic control of heterochromatin assembly. Science 2001;292(5514):110-3.

216. Nguyen CT, Weisenberger DJ, Velicescu M, et al. Histone H3-lysine 9 methylation is associated with aberrant gene silencing in cancer cells and is rapidly reversed by 5-aza-2'-deoxycytidine. Cancer Res 2002;62(22):6456-61.

217. Jenuwein T. Re-SET-ting heterochromatin by histone methyltransferases. Trends Cell Biol 2001;11(6):266-73.

218. Richards EJ, Elgin SC. Epigenetic codes for heterochromatin formation and silencing: rounding up the usual suspects. Cell 2002;108(4):489-500.

219. Santos-Rosa H, Schneider R, Bannister AJ, et al. Active genes are tri-methylated at K4 of histone H3. Nature 2002;419(6905):407-11.

220. Bannister AJ, Zegerman P, Partridge JF, et al. Selective recognition of methylated lysine 9 on histone H3 by the HP1 chromo domain. Nature 2001;410(6824):120-4.

221. Stewart MD, Li J, Wong J. Relationship between histone H3 lysine 9 methylation, transcription repression, and heterochromatin protein 1 recruitment. Mol Cell Biol 2005;25(7):2525-38.

222. Yoshida M, Kijima M, Akita M, Beppu T. Potent and specific inhibition of mammalian histone deacetylase both in vivo and in vitro by trichostatin A. J Biol Chem 1990;265(28):17174-9.

223. Cameron EE, Bachman KE, Myohanen S, Herman JG, Baylin SB. Synergy of demethylation and histone deacetylase inhibition in the re-expression of genes silenced in cancer. Nat Genet 1999;21(1):103-7.

224. Fahrner JA, Eguchi S, Herman JG, Baylin SB. Dependence of histone modifications and gene expression on DNA hypermethylation in cancer. Cancer Res 2002;62(24):7213-8.

225. Shi H, Wei SH, Leu YW, et al. Triple analysis of the cancer epigenome: an integrated microarray system for assessing gene expression, DNA methylation, and histone acetylation. Cancer Res 2003;63(9):2164-71.

226. Gilles C, Bassuk JA, Pulyaeva H, Sage EH, Foidart JM, Thompson EW. SPARC/osteonectin induces matrix metalloproteinase 2 activation in human breast cancer cell lines. Cancer Res 1998;58(23):5529-36.

227. Bachmeier BE, Albini A, Vene R, et al. Cell density-dependent regulation of matrix metalloproteinase and TIMP expression in differently tumorigenic breast cancer cell lines. Exp Cell Res 2005;305(1):83-98.

228. Giese A, Loo MA, Tran N, Haskett D, Coons SW, Berens ME. Dichotomy of astrocytoma migration and proliferation. Int J Cancer 1996;67(2):275-82.

229. Belguise K, Kersual N, Galtier F, Chalbos D. FRA-1 expression level regulates proliferation and invasiveness of breast cancer cells. Oncogene 2005;24(8):1434-44.

230. Zenzie-Gregory B, Khachi A, Garraway IP, Smale ST. Mechanism of initiator-mediated transcription: evidence for a functional interaction between the TATA-binding protein and DNA in the absence of a specific recognition sequence. Mol Cell Biol 1993;13(7):3841-9.

231. Won J, Yim J, Kim TK. Sp1 and Sp3 recruit histone deacetylase to repress transcription of human telomerase reverse transcriptase (hTERT) promoter in normal human somatic cells. J Biol Chem 2002;277(41):38230-8.

232. Wang CH, Tsao YP, Chen HJ, Chen HL, Wang HW, Chen SL. Transcriptional repression of p21((Waf1/Cip1/Sdi1)) gene by c-jun through Sp1 site. Biochem Biophys Res Commun 2000;270(1):303-10.

233. Wang YN, Chang WC. Induction of disease-associated keratin 16 gene expression by epidermal growth factor is regulated through cooperation of transcription factors Sp1 and c-Jun. J Biol Chem 2003;278(46):45848-57.

234. Wu Y, Zhang X, Zehner ZE. c-Jun and the dominant-negative mutant, TAM67, induce vimentin gene expression by interacting with the activator Sp1. Oncogene 2003;22(55):8891-901.

235. Chiang CM, Roeder RG. Cloning of an intrinsic human TFIID subunit that interacts with multiple transcriptional activators. Science 1995;267(5197):531-6.

236. Saluja D, Vassallo MF, Tanese N. Distinct subdomains of human TAFII130 are required for interactions with glutamine-rich transcriptional activators. Mol Cell Biol 1998;18(10):5734-43.

237. Suzuki M, Hao C, Takahashi T, et al. Aberrant methylation of SPARC in human lung cancers. Br J Cancer 2005;92(5):942-8.

238. Detich N, Theberge J, Szyf M. Promoter-specific activation and demethylation by MBD2/demethylase. J Biol Chem 2002;277(39):35791-4.

239. Juttermann R, Li E, Jaenisch R. Toxicity of 5-aza-2'-deoxycytidine to mammalian cells is mediated primarily by covalent trapping of DNA methyltransferase rather than DNA demethylation. Proc Natl Acad Sci U S A 1994;91(25):11797-801.

240. Yoder JA, Soman NS, Verdine GL, Bestor TH. DNA (cytosine-5)-methyltransferases in mouse cells and tissues. Studies with a mechanism-based probe. J Mol Biol 1997;270(3):385-95.

241. Fujita N, Watanabe S, Ichimura T, et al. MCAF mediates MBD1-dependent transcriptional repression. Mol Cell Biol 2003;23(8):2834-43.

242. De Graeve F, Bahr A, Chatton B, Kedinger C. A murine ATFa-associated factor with transcriptional repressing activity. Oncogene 2000;19(14):1807-19.

243. Bigey P, Ramchandani S, Theberge J, Araujo FD, Szyf M. Transcriptional regulation of the human DNA Methyltransferase (dnmt1) gene. Gene 2000;242(1-2):407-18.

244. Bieche I, Tozlu S, Girault I, Lidereau R. Identification of a three-gene expression signature of poor-prognosis breast carcinoma. Mol Cancer 2004;3(1):37.

245. Girault I, Tozlu S, Lidereau R, Bieche I. Expression analysis of DNA methyltransferases 1, 3A, and 3B in sporadic breast carcinomas. Clin Cancer Res 2003;9(12):4415-22.

246. Saito Y, Kanai Y, Sakamoto M, Saito H, Ishii H, Hirohashi S. Overexpression of a splice variant of DNA methyltransferase 3b, DNMT3b4, associated with DNA hypomethylation on pericentromeric satellite regions during human hepatocarcinogenesis. Proc Natl Acad Sci U S A 2002;99(15):10060-5.

247. Weisenberger DJ, Velicescu M, Cheng JC, Gonzales FA, Liang G, Jones PA. Role of the DNA methyltransferase variant DNMT3b3 in DNA methylation. Mol Cancer Res 2004;2(1):62-72.

248. Robertson KD, Uzvolgyi E, Liang G, et al. The human DNA methyltransferases (DNMTs) 1, 3a and 3b: coordinate mRNA expression in normal tissues and overexpression in tumors. Nucleic Acids Res 1999;27(11):2291-8.

249. Geiman TM, Robertson KD. Chromatin remodeling, histone modifications, and DNA methylation-how does it all fit together? J Cell Biochem 2002;87(2):117-25.

250. Vermaak D, Ahmad K, Henikoff S. Maintenance of chromatin states: an open-and-shut case. Curr Opin Cell Biol 2003;15(3):266-74.

251. Walker GE, Wilson EM, Powell D, Oh Y. Butyrate, a histone deacetylase inhibitor, activates the human IGF binding protein-3 promoter in breast cancer cells: molecular mechanism involves an Sp1/Sp3 multiprotein complex. Endocrinology 2001;142(9):3817-27.

252. Martens JH, Verlaan M, Kalkhoven E, Zantema A. Cascade of distinct histone modifications during collagenase gene activation. Mol Cell Biol 2003;23(5):1808-16.

253. Fuchs IB, Lichtenegger W, Buehler H, et al. The prognostic significance of epithelial-mesenchymal transition in breast cancer. Anticancer Res 2002;22(6A):3415-9.

254. Rittling SR, Coutinho L, Amram T, Kolbe M. AP-1/jun binding sites mediate serum inducibility of the human vimentin promoter. Nucleic Acids Res 1989;17(4):1619-33.

255. Ottaviano YL, Issa JP, Parl FF, Smith HS, Baylin SB, Davidson NE. Methylation of the estrogen receptor gene CpG island marks loss of estrogen receptor expression in human breast cancer cells. Cancer Res 1994;54(10):2552-5.

256. Lapidus RG, Nass SJ, Butash KA, et al. Mapping of ER gene CpG island methylation-specific polymerase chain reaction. Cancer Res 1998;58(12):2515-9.

APPENDIX A

FIGURES

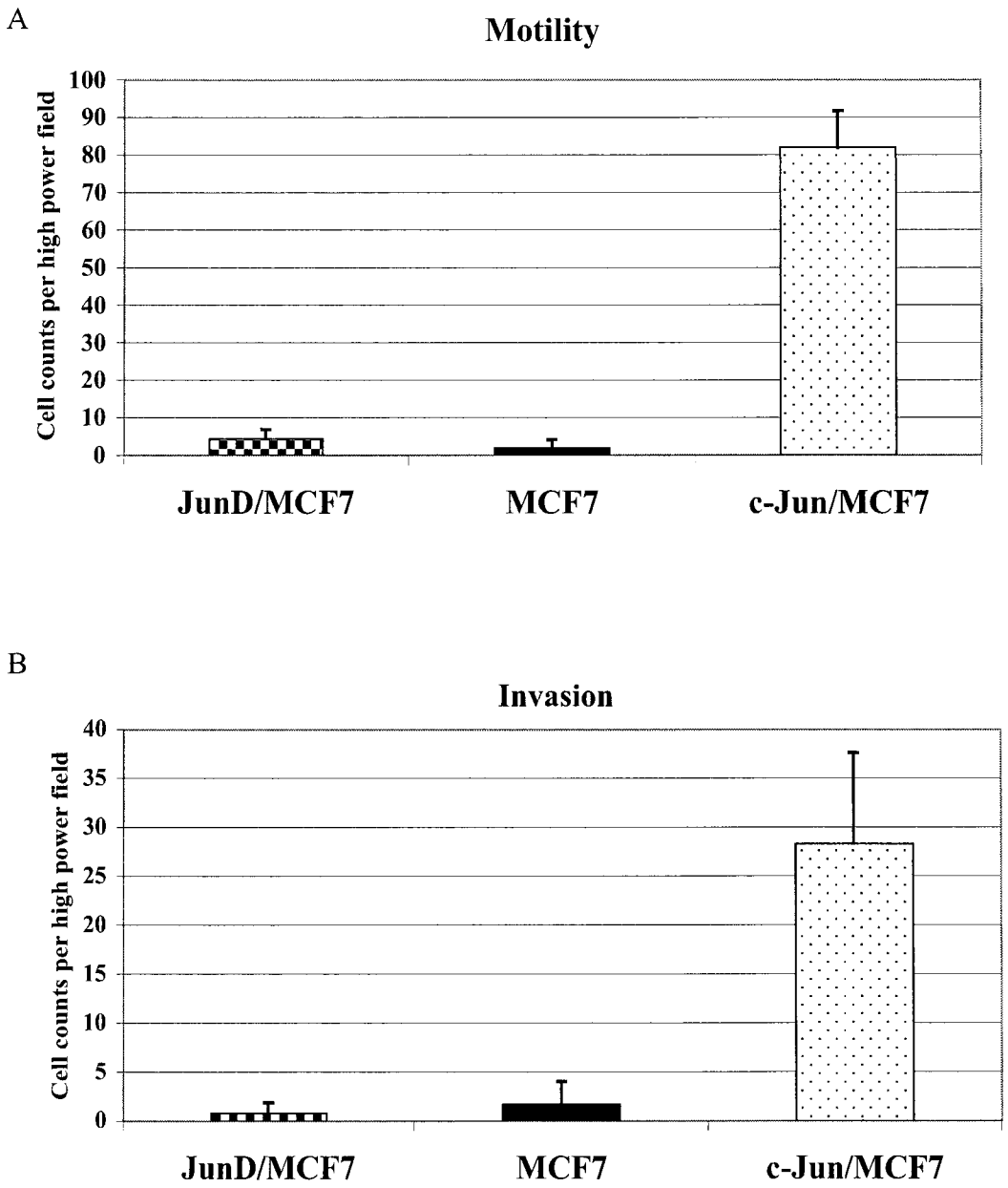

Fig. 38. Analysis of *in vitro* cell motility and invasion demonstrated by JunD/MCF7 stable cell lines. *A*, Quantitation of cell motility assays done on gelatin coated membranes over a 4 hour incubation period. *B*, Quantitation of cell invasion assays conducted on Matrigel™ coated membranes over a period of 4 hours. All values are expressed as the number of stained cells per high power field.

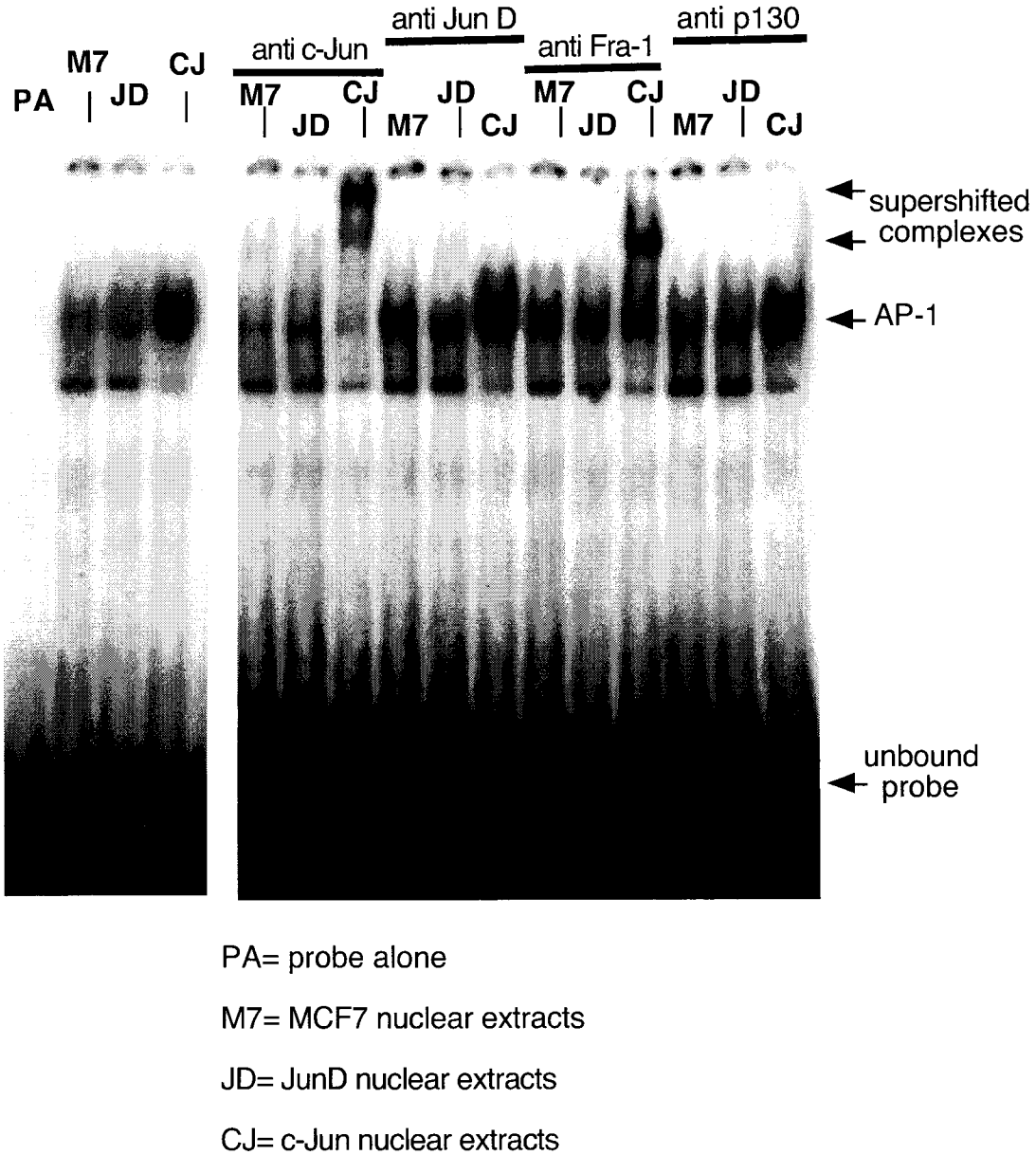

Fig. 39. AP-1 DNA binding activity in nuclear extracts from empty vector control/MCF7, JunD/MCF7 or c-Jun/MCF7 stable cell lines. A radiolabeled oligonucleotide probe corresponding to a consensus AP-1 site from the intron 1 region of the human Fra-1 gene was used in gel shift reactions (25,000cpm). Anti c-Jun, anti JunD, anti Fra-1 or anti p130 (negative control) antibodies were incubated with the radiolabeled probe and nuclear extracts as indicated.

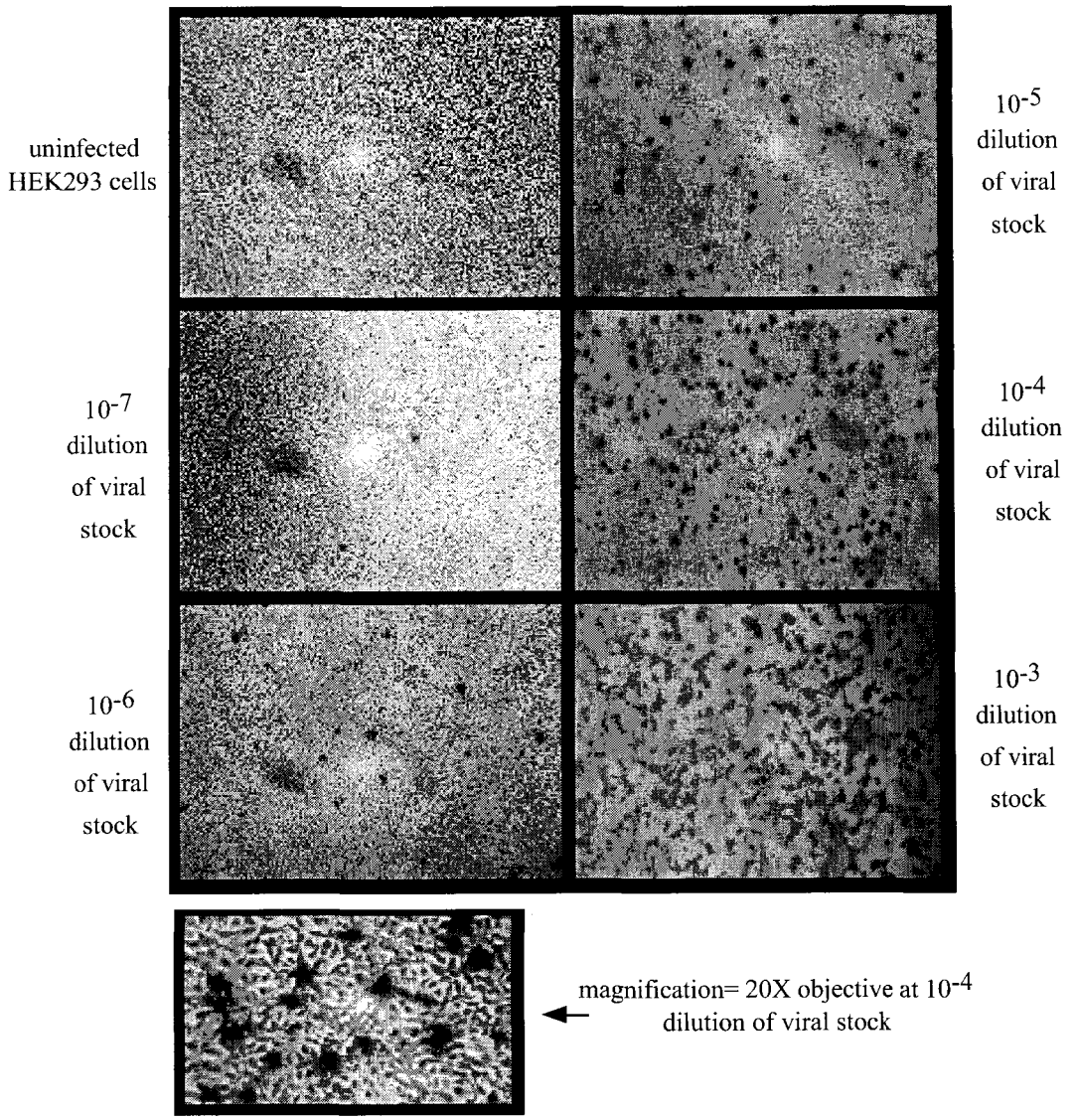

Calculation for determining adenoviral titer

$$\frac{\text{(stained cells/20X field) X (573 fields/well)}}{\text{0.1ml virus X dilution factor}} = \text{pfu/ml}$$

Fig. 40. Determination of recombinant adenoviral titer. Virus was propagated as described in Chapter II. HEK293 cells were infected with the indicated dilutions of virus stock. Cells were assayed 48 hours later for production of adenovirus hexon protein using the Clontech Rapid Titer™ Kit as described in Chapter II.

Mock infected c-Jun/MCF7 cells

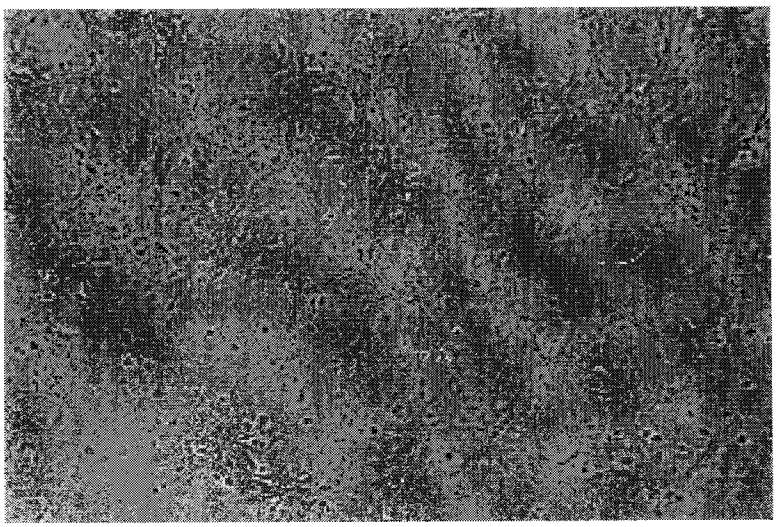

c-Jun/MCF7 cells infected with a beta-galactosidase expressing adenovirus (MOI=5)

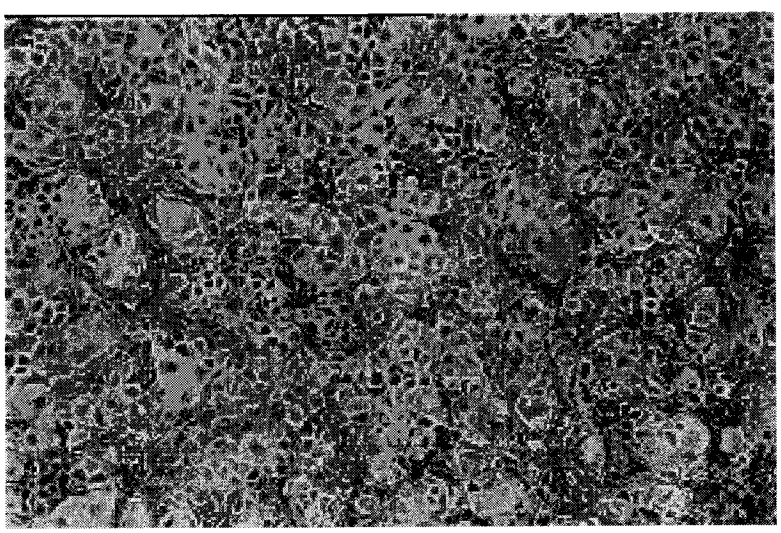

Fig. 41. Infection of c-Jun/MCF7 cells with recombinant adenovirus expressing beta-galactosidase. Magnification= 10X objective.

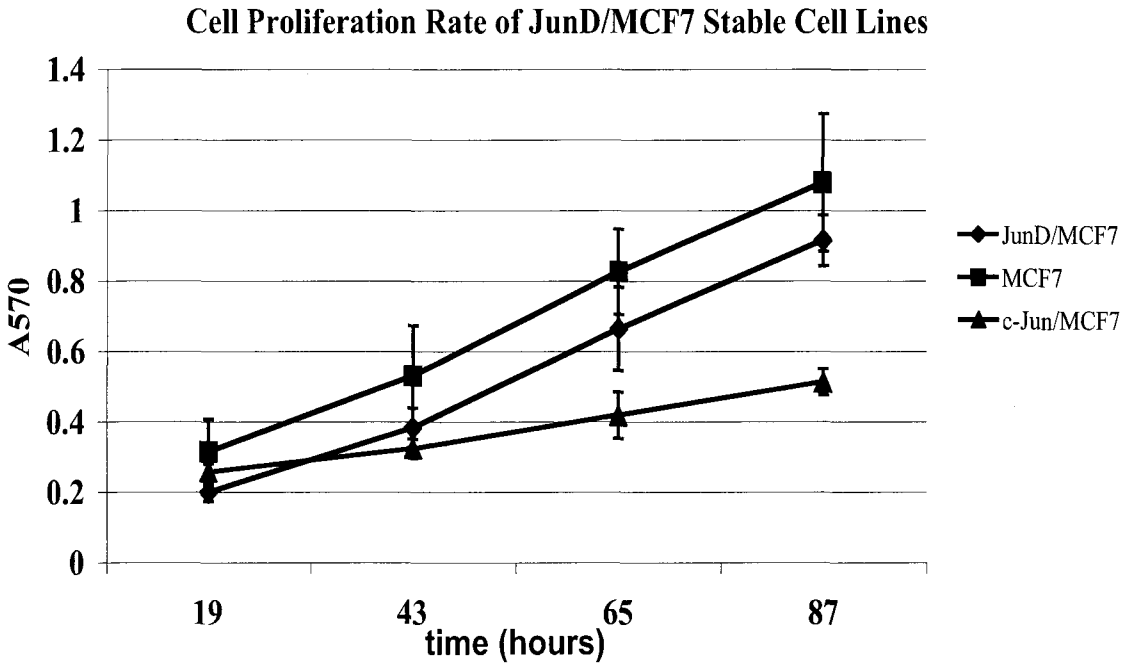

Fig. 42. Effect of stable JunD expression on MCF7 cell proliferation. Cell proliferation rates were determined by MTT assay as described in Chapter II. The indicated cell lines were plated at the same density in 96-well plates. Samples were assayed at 19, 43, 65 and 87 hours. Optical densities were determined using a microtiter plate reader where A= absorbance at 570nm wavelength.

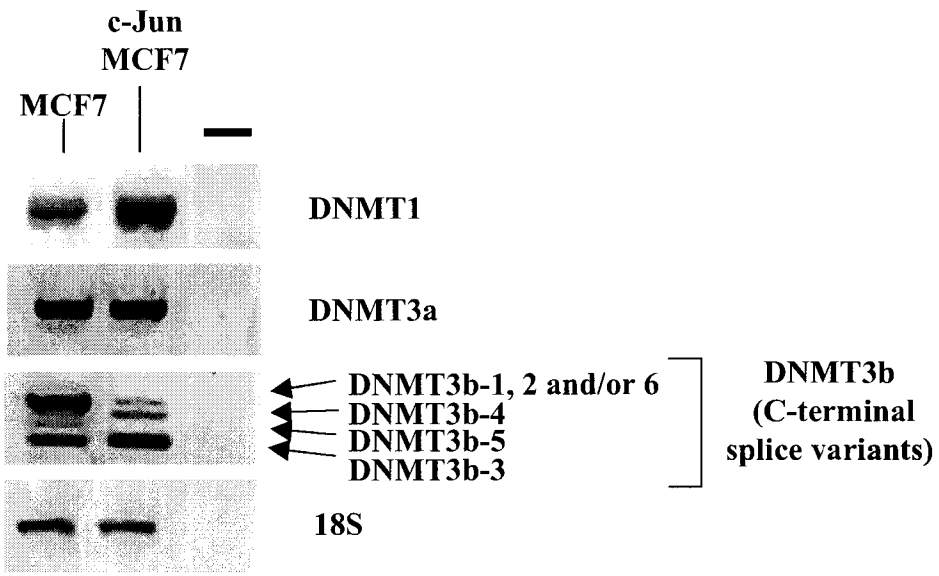

Fig. 43. Semi-quantitative RT-PCR analysis of steady state DNA methyltransferase levels in MCF7 and c-Jun/MCF7 cell lines. DNMT3b RT-PCR primers flank the alternatively spliced 3' coding region. Individual DNMT3b amplicons (upper most and lower most bands) were gel purified and identified by DNA sequencing. DNMT3b-4 and DNMT3b-5 identities are inferred based on amplicon size compared to published reports (242). The 18S ribosomal subunit gene serves as an invariantly expressed, internal control.

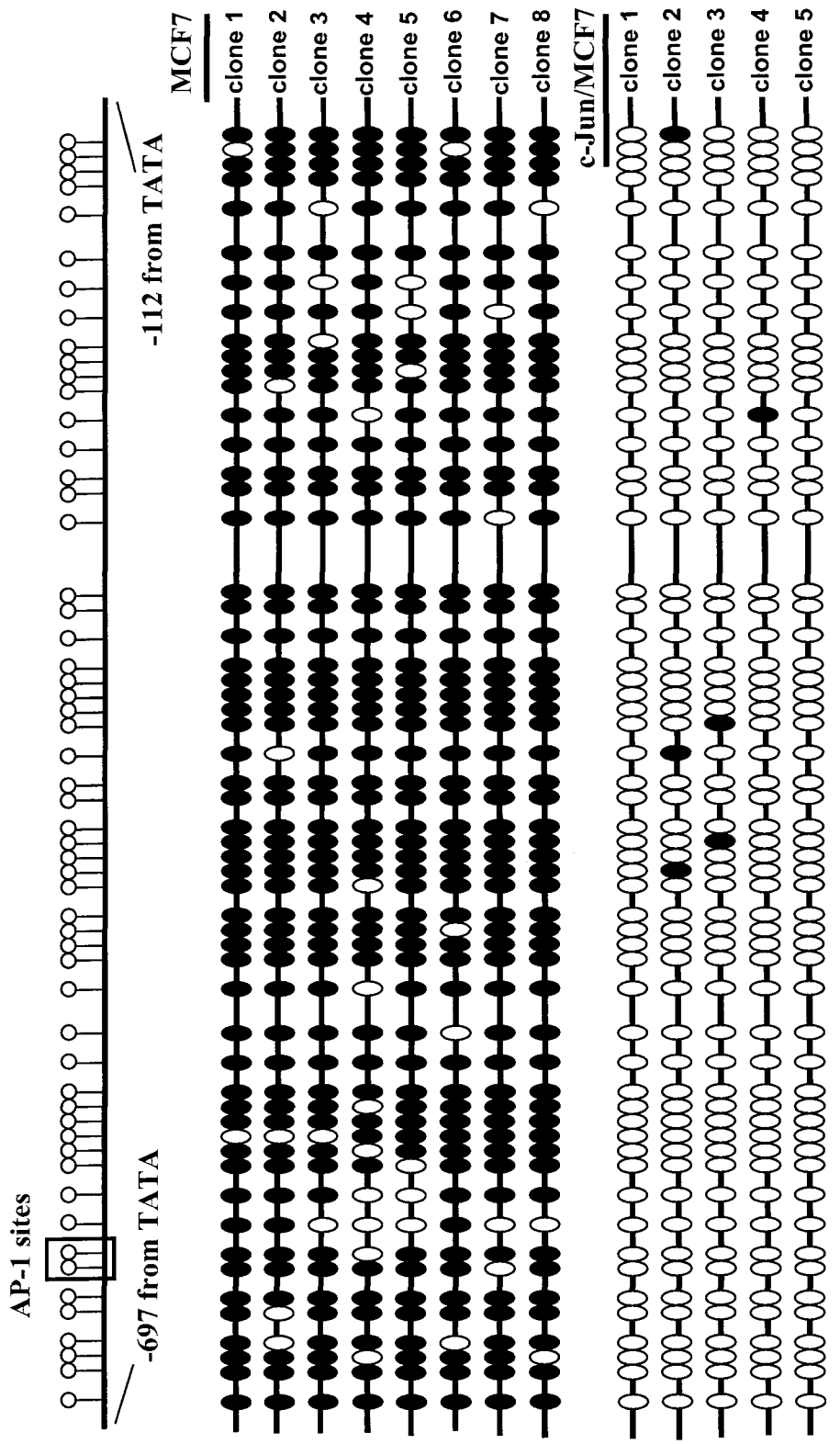

Fig. 44. The vimentin promoter CpG island is highly methylated in MCF7 cells and becomes demethylated in response to c-Jun overexpression. Sequence analysis of sodium bisulfite modified genomic DNA following PCR amplification and isolation of individual clones.

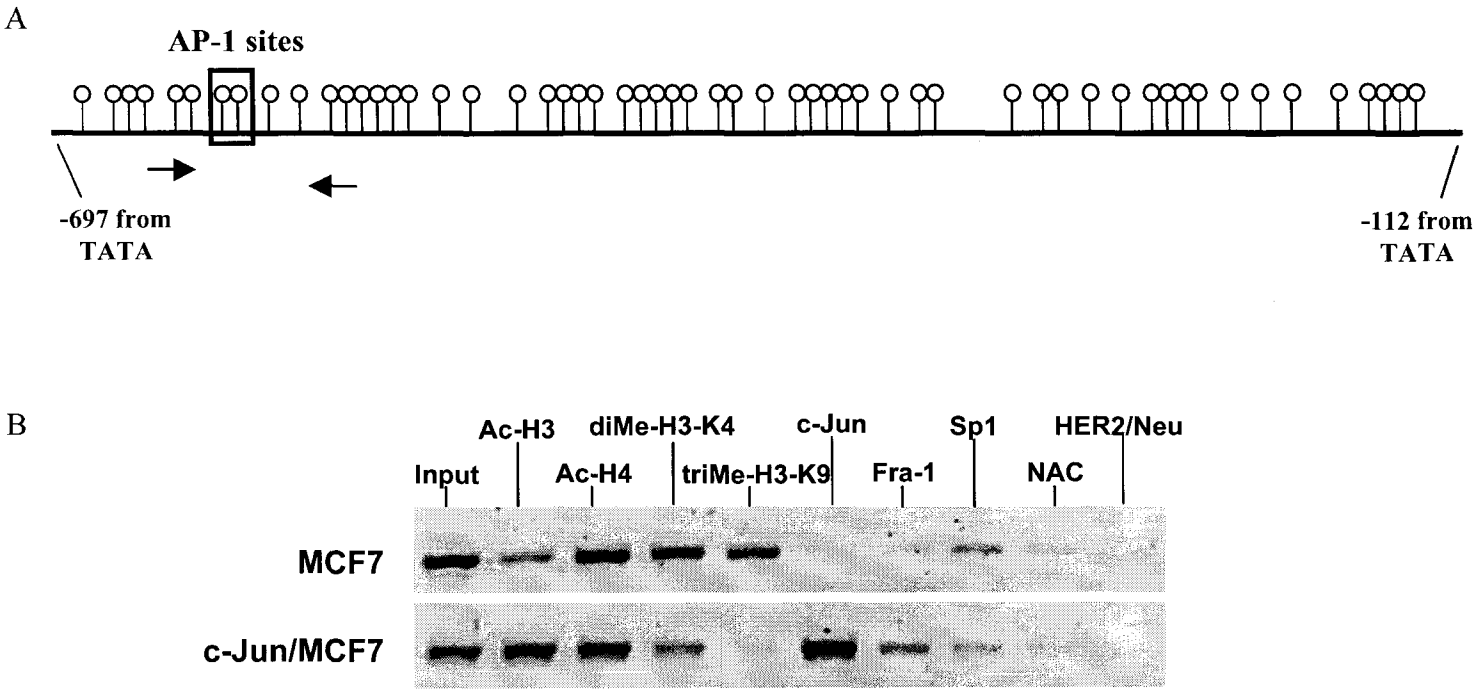

Fig. 45. Chromatin immunoprecipitation analysis of the vimentin gene locus in MCF7 and c–Jun/MCF7 stable cell lines. *A*, Schematic representation of the human vimentin genomic locus. Lollypops denote the location of CpG sequences. Arrows denote the genomic region amplified by PCR during chromatin immunoprecipitation analysis. *B*, Results of chromatin immunoprecipitation analysis using the following antibodies: (Ac-H3) anti diacetylated histone H3, (Ac-H4) anti tetraacetylated histone H4, (diMe-H3-K4) anti dimethyl histone H3 at lysine 4, (triMe-H3-K9) trimethyl histone H3 at lysine 9, anti c-Jun, anti Fra-1, anti Sp1, (NAC) no antibody control. (—)= no template added negative control for PCR reactions.

A

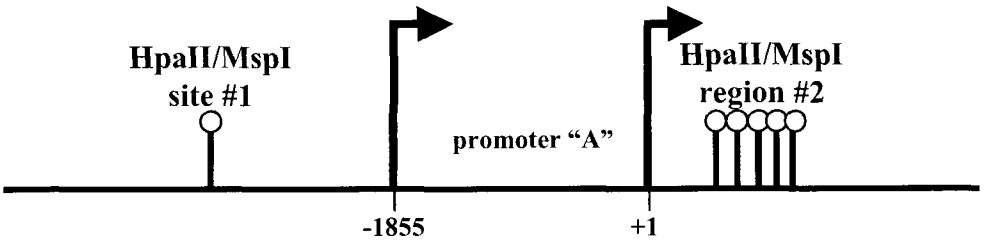

B

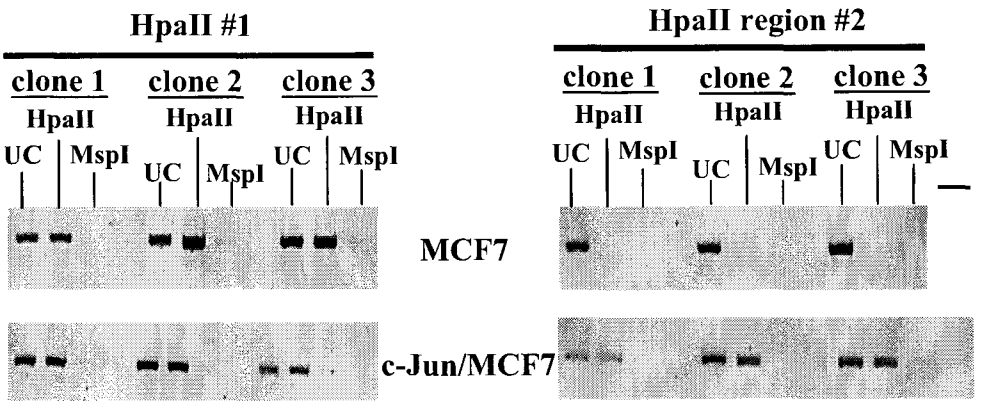

Fig. 46. The estrogen receptor alpha gene locus is hypermethylated in c-Jun/MCF7 cells. *A*, Schematic representation of the a region of the human estrogen receptor alpha gene locus. Arrows indicate transcription start sites. *B*, HpaII/MspI mapping of DNA methylation. Genomic DNA isolated from either MCF7 or c-Jun/MCF7 cells was digested with HpaII, MspI or left undigested (UC). Following digestion, PCR was performed using oligonucleotide primer pairs flanking the HpaII/MspI sites. (—) denotes the negative control PCR reaction in which DNA template was omitted.

A

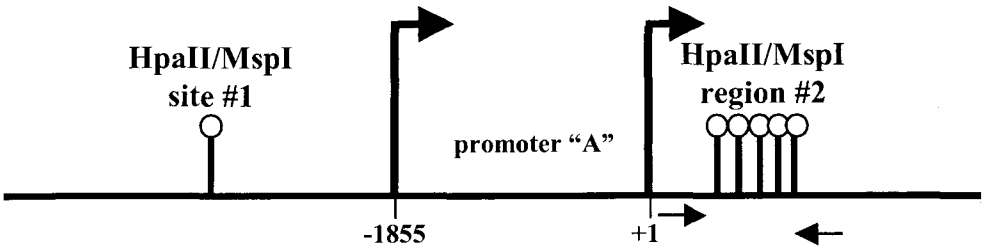

B

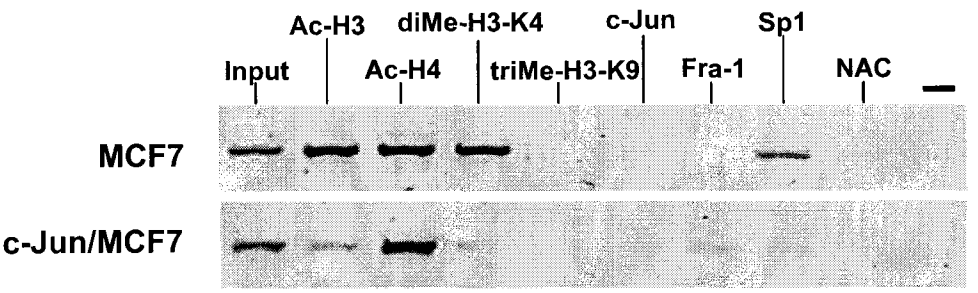

Fig. 47. Chromatin immunoprecipitation analysis of the estrogen receptor alpha gene locus in MCF7 and c-Jun/MCF7 stable cell lines. *A*, Schematic representation of the estrogen receptor alpha genomic locus. The large arrows denote potential transcription start sites. The smaller arrows denote the genomic region amplified by PCR during chromatin immunoprecipitation analysis. Lollypops denote the location of HpaII/MspI sites. (+1) denotes the major transcription start site. *B*, Results of chromatin immunoprecipitation analysis using the following antibodies: (Ac-H3) anti diacetylated histone H3, (Ac-H4) anti tetraacetylated histone H4, (diMe-H3-K4) anti dimethyl histone H3 at lysine 4, (triMe-H3-K9) trimethyl histone H3 at lysine 9, anti c-Jun, anti Fra-1, anti Sp1, (NAC) no antibody control. (—)= no template added negative control for PCR reactions.

APPENDIX B

PERMISSION TO REPRODUCE PUBLISHED MATERIAL

FROM: "Hooker, Sophie (AJ's)" <S.Hooker@nature.com> | Save Address

DATE: Tue, 9 Mar 2004 11:40:05 -0000

TO: "'jbriggs@mail.wistar.upenn.edu'" <jbriggs@mail.wistar.upenn.edu>

Dear Joseph

Thank you for the request to use your article from Oncogene in 2002. Print permission is granted for one-time publication for your dissertation, with the following specifications:

1. Reproduction is intended in a primary journal, secondary journal, CD-ROM, dissertation or book.

2. Nature's copyright permission must be indicated in the reproduction.

3. You must yourself obtain the consent of the author or, where such information is printed in a Nature Publishing Group journal, the photographer/illustrator.

We are certain that all parties will benefit from this agreement and wish you the best in the use of this material. Thank you.

Kind Regards,
Belinda Burgess, on behalf of Sophie Hooker

Sophie Hooker, Permissions Coordinator
Nature Publishing Group
The Macmillan Building
4 Crinan Street
London N1 9XW
UK
tel: +44 0207 843 4893
fax: +44 0207 843 4839

VITA

JOSEPH WILLIAM BRIGGS

Education

1998-2005 Ph.D., Biomedical Sciences
Eastern Virginia Medical School and Old Dominion University
(Department of Microbiology and Molecular Cell Biology, 700 West Olney Road, Eastern Virginia Medical School, Norfolk, VA 23507)

2004-2005 Visiting Scientist
Laboratory of Frank J. Rauscher, III. The Wistar Institute, Philadelphia, PA

1991-1996 B.S., Biology
Old Dominion University, Norfolk, Virginia

Publications

1. Chamboredon S, Briggs J, Vial E, Hurault J, Galvagni F, Oliviero S, Bos TJ, Castellazzi M. v-Jun downregulates the SPARC target gene by binding to the proximal promoter indirectly through Sp1/3. Oncogene. 2003 Jun 26; 22 (26): 4047-61.
2. Briggs J, Chamboredon S, Castellazzi M, Kerry JA, Bos TJ. Transcriptional upregulation of SPARC, in response to c-Jun overexpression, contributes to increased motility and invasion of MCF7 breast cancer cells. Oncogene. 2002 Oct 10; 21 (46): 7077-91.
3. Walter JE, Briggs J, Guerrero ML, Matson DO, Pickering LK, Ruiz-Palacios G, Berke T, Mitchell DK. Molecular characterization of a novel recombinant strain of human astrovirus associated with gastroenteritis in children. Arch. Virol. 2001 Dec; 146 (12): 2357-2367.
4. Basso J, Briggs J, Findlay C, Bos TJ. Directed mutation of the basic domain of v-Jun alters DNA binding specificity and abolishes its oncogenic activity in chicken embryo fibroblasts. Oncogene. 2000 Oct 5; 19 (42): 4876-85.
5. Sehgal A, Briggs J, Rinehart-Kim J, Basso J, Bos TJ. The chicken c-Jun 5' untranslated region directs translation by internal initiation. Oncogene. 2000 Jun 1; 19 (24): 2836-45.

Awards

2003 Best Graduate Student Poster Presentation, EVMS Research Day
2003 Minority Scholar in Cancer Research Travel Award, American Association for Cancer Research
2002 Best Graduate Student Poster Presentation, EVMS Research Day
2002 Minority Scholar in Cancer Research Travel Award, American Association for Cancer Research
2001 Best Graduate Student Poster Presentation, EVMS Research Day
2000 Best Cancer Research Poster Presentation, EVMS Research Day

Student Activities

2000-2002 President, Biomedical Science Graduate Student Organization (BSSO)
1999-2000 Treasurer, Biomedical Science Graduate Student Organization (BSSO)